The Abdus Salam International Centre for Theoretical Physics

IAEA International Atomic Energy Agency

unesco United Nations Educational, Scientific and Cultural Organization

International Conference on Photophysics and Photochemistry | (SMR 4189)

26 Mar 2026 - 28 Mar 2026
Outside, Mumbai, India

P01 - ABDELNAEIM Mostafa

Novel synthesized V2O5-doped PMMA nanocomposite films for effective photocatalytic removal of methylene blue from water

P02 - ACHARYA Dinesh

Understanding Excited States in Magic Series Au8n+4(SR)4n+8 Nanoclusters: Role of Size, Ligands, and Theory Level

P03 - ACQUAH Isaac Kwesi

Wavelength-Dependent Optical Activity in Aqueous Chiral Solutions: A Polarimetric Study Using Monochromatic and Filtered Light Sources

P04 - ADANE Tsigie Getie

A Comprehensive Review of 2D Heterostructures for Energy Materials: Classification, Computational Design, and Tunable Properties

P05 - MOHAMMAD AYAZ AHMAD -

Electrochemical Performance of Lanthanum Ferrite (LaFeO 3) Nanomaterials for Enhanced Supercapacitor and Photocatalysis Applications

P06 - AIT OUFAKIR Mohamed

Next-Gen Solar: Revealing the Promise of CsPbI3/CsSnI3 Tandem Cells

P07 - ALEMU Mekuria Tsegaye

Enhancing the photovoltaic potential of lead-free CsSnCl3 perovskite via Al/In doping: A combined DFT and SCAPS-1D study

P08 - ARCHISHA -

Cobalt-Engineered Infrared Absorptivity in Erbium Aluminium Garnet for Advanced Photonic Devices

P09 - AROKIASAMY Susaiammal

Electronic, magnetic, and topological properties of ferromagnetic 2D perovskite-type oxides

P10 - BAISHYA Himangshu

Bulk Doping-Driven In-Situ Simultaneous Modulation of Dual Interfaces Improves Charge Transport Dynamics and Reduces Recombination Loss enabling > 26% Efficient Perovskite Solar Cells

P11 - BALAKRISHNAN Hemanth

Color Tunability in NaYF4: Er3+ Phosphor

P12 - BAMBAL Ashitosh Rambhau

MORPHOLOGY-DRIVEN ENHANCEMENT OF WATER OXIDATION PERFORMANCE IN HEMATITE (Î±-FeâOâ) PHOTOANODE

P13 - BANDYOPADHYAY Rajdip

Impact of external strain on electron–phonon coupling strength in SnTe pseudo-monolayer

P14 - BASAK Krishnanshu

Unraveling anisotropic mechanical and electronic attributes of MN4 (M= Be, Mg, Zn, Cd) monolayers and their excellent supercapacitive performances

P15 - BASAVARAJAPPA Manasa Gattavadi

Interplay of Dynamic Defects and Ultrafast Carrier Dynamics in Lead Free Double Perovskites Toward Stable, High-Performance Photovoltaics

P16 - BASU Meghasree

Intrinsic Bulk Photovoltaic Effect in Symmetry-Broken CVD-Grown Spiral WS_2

P17 - BISOI Swapneswar

Functional Engineering and Defect Passivation in Monolayer MoS2 for High-Performance Optoelectronics

P18 - CHAKRAVORTY Ayan

First-Principles Insights into Electronic, Excitonic, and Polaronic Properties of Lead-Free X_3BI_3 Halide Antiperovskite Derivatives for Optoelectronic Applications

P19 - CHAWKI Najwa

Simulation and analysis of high-performance HTL- SrZrS3 based perovskite solar cells using SCAPS-1D: Comparative study

P20 - CHHIPA Mayur Kumar

All-Optical Pseudo-Spin Waveguide and Directional Coupling in Nonlinear Photonic Crystals

P21 - CHITARA Rajeshkumar

Tuning Photocatalytic CO_2 Conversion Efficiency via Single and Double Vacancy Engineering in 2D o-B_2N_2 Monolayer

P22 - CHOUDHURY Shouvik

Investigations on upconversion nanophosphors for temperature sensing

P23 - C Keerthana

Development of a Cost-Effective In-House Circular Dichroism Spectroscopy Setup

P24 - DAS Bishal

Testing Abstract Upload :)

P25 - DASGUPTA Diganta

Microscopic Origins of O-H Stretching Raman Features in Aqueous LiCl Solutions

P26 - DASHORA Alpa

Superior OER selectivity in bifunctional amorphous cobalt phospho-boride for electrocatalytic seawater splitting

P27 - DAS Indranil

"Impact of external strain on electron–phonon coupling strength in SnTe pseudo-monolayer " - co-author with Rajdip Bandyopadhyay .

P28 - DAS Mandira

Decoding Aerosol Surface Chemistry: Insights from XPS Spectra via DFT and Machine Learning

P29 - DESHPANDE Siddhant Naresh

Dual modifications of graphitic carbon nitride nanostructures for enhanced photoelectrochemical performance

P30 - DESTA Mulu Berhe

Molecular Engineering of Mono and Di-Anchoring Metal Free Organic Sensitizers Containing Electron Deficient Entity for Dye Sensitized Solar Cells (DSSCs)

P31 - DEVI Nisha

Porous Fe-MOF as an Advanced Energy Material for High-Performance Supercapacitors Electrode

P32 - DEY Amrita

Cu2+ Driven Localized Band Formation and Photoluminescence Excitation Splitting in Low Symmetry Cs2NaBiCl6 Double Perovskite

P33 - DEY Tuya

Double transition metal MXenes as anode materials for high-capacity multivalent metal-ion batteries: a computational study

P34 - DHOBI Saddam Husain

Photon-Assisted Hydrogen Evolution using Cu-Fe Composite Photoelectrode

P35 - ELAYAPERUMAL Manikandan

Fingerprint Raman spectroscopy diagnosis for Gamma Radiolysis Synthesized Noble Metal Nanoparticles: A Green Synthesis Approach

P36 - EL BASHAR Ramy Ramadan Mostafa

Enhancement of Nanowire Solar Cells via Innovative Reinforcement Learning Optimization

P37 - EMETERE Moses Eterigho

Proton irradiation effects on perovskite solar cells: A critical review and future modifications

P38 - ESSAH Bruce Kwaku Offei

The effect of co-sensitization between N719 dye and 1-phenylazo-2-naphthol on dye sensitized solar cell performance

P39 - FARAJPOUR Maryam

Dynamic Modeling of Charge Carrier Transport and Recombination in Energy Conversion Materials: A System-Level Perspecti

P40 - FATMA Nisha

Probing Structural Dynamics of 6 -Methoxyflavone in Different Environments

P41 - FWALO Chewe

Investigating the adsorption mechanisms of CO2 and N2 on monolayer Nb2Se2C for efficient reduction reaction: A DFT study

P42 - GAJJAR Niyati Bhupendra

DFT Analysis of CO_2 Dissociation and Reduction Pathways to CO and HCOOH on a ZrN Cluster

P43 - GEBREHIWOT Elias Assayehegn

Ageing-driven formation of ternary phase N/TiO2 nanocrystals for sustainable visible-light catalysis

P44 - GEBREMARIAM Kidan Gebreegziabher

Synergistic Effect of 2D Self-Assembled Monolayer and ZnO Nanoparticles on the Passivation of Sol-gel ZnO Electron Transport Layer to Enhance the Performance and Stability of Non-Fullerene Organic Solar Cells.

P45 - GHOSH Animesh

f - f like d -d transition of Mo(III) for near infrared (NIR) emisison

P46 - GITTY Pooja

Luminescent europium doped hydroxyapatite nanoparticles as fluorescent labels for cell imaging

P47 - GOPAL Ramalingam

Taming Light with Carbon dots

P48 - GUPTA Mayank

Development and Photoluminescence Spectroscopy study of Luminescent Solar Concentrator for Building Integrated Photovoltaics

P49 - GUPTA Neelam

Interpretable Machine-Learning-Assisted Discovery of Novel Double Perovskite Compounds for Energy Harvesting Applications

P50 - GURAV Nalini Dattatraya

Hydrogen-Bond-Mediated Modulation of Tyrosine Photophysics under External Electric Fields

P51 - HUZORTEY Andrew Atiogbe

Laser-Induced Fluorescence Spectroscopic Study of Water from Mosquito Breeding Habitats

P52 - JATOLIYA Mohit

Bi2S3 nanoparticulate thin-film growth for photocatalytic applications using the SILAR method.

P53 - JHA Minakshi Satish

I want to do oral presentation. As no option was there so I selected a poster.

P54 - KACHHAP Santosh

The sharp Blue Emission of Eu2+ in Eu-doped CsPbBr3

P55 - KHALIL Dina Mohamed Mohamed Atwa

"Pulsed Laser Ablation Derived MoS_2 Nanosheets with Strong Third-Order Nonlinearities for Ultrafast Photonics"

P56 - KHOSROSHAHI Negin

Steel Mesh-Supported SNW-1/CsPbBr3 Nanocomposite: Photocatalyst for Sustainable Ammonia Production

P57 - KHUNTE Janhavi Jayawant

Defect Engineering in Silicon Nitride Micro-disk Cavities for Quantum Photonic Applications

P58 - DHIRENDRA KUMAR -

Impact of strain on excitonic radiative lifetime in a polar Hf3ZrS8 monolayer: Theoretical insight based on many-body perturbation theory

P59 - KUMAR Vipin

Phosphorus-Doped BP_xN_{1-x} Monolayer as an Efficient Photocatalyst for Solar Water Splitting: A First-Principles Study

P60 - SARA KURIYAN Navya

Structure-Luminescence Correlation Studies in Eu3+ Doped Silicate Phosphors for Bioimaging Applications

P61 - LAHON Doulat

Designing a bio-inspired electrocatalyst based on V2C-MXene for nitrogen reduction

P62 - MAHAR Aishwarya

Theoretical Investigation of Electronic Structure and Photophysical Properties of Salicylic Acid Derivatives.

P63 - MAHEPAL Nisha

Photophysical and Optical Characterization of Nitride-Based Perovskite $SrReN_3$ from First-Principles Calculations

P64 - MAJUMDER Amrita

Deterministic Engineering of Single-Photon Emitter Arrays in Hexagonal Boron Nitride at Room Temperature

P65 - MAJUMDER Sudipta

Emergent Excitonic Physics and Interlayer Coupling in Bubble-Free hBN Encapsulated TMDC Heterostructures

P66 - MALIK Saqlain Mushtaq

Self-Powered broadband and polarisation-sensitive photodetection in $CrSBr/WSe_2$ van der waals heterostructure.

P67 - MALLIKA Parvathy

Host-dependent Photoluminescence Properties of Lanthanide Doped A2P2O7 (A= Ca and Ba) Phosphors

P68 - MIDDYA Asif Iqubal

Electronic Restructuring and Conformational Inversion in Sulfur- and Oxygen-Based Heterocycles: Insights from Hydrated Cluster Analysis

P69 - MOHAMED Fayrouz Sayed Ahmed Abdelhady

Zn-Doped BiOBr Embedded in PVDF Sponge as a Recyclable Dip-Photocatalyst for Wastewater Treatment

P70 - MOHANTY Kalyani

Molecular Insights into Electric Double Layer Formation at $Ti_3C_2T_x$ MXene–Ionic Liquid Interfaces

P71 - MUDOI Riya

Investigating the effect of metal and non-metal dual doping on the electrocatalytic performance of VSe2 for water splitting

P72 - MULMI Deependra Das

Bi2WO6-ZnO heterostructures for photocatalytic degradation of organic dyes

P73 - NAIN Sushmita

Design and Analysis of Gold Nanoparticle-Based PCF for Cancer Cells Detections

P74 - NA Yadav Rohit Umashankar

Probing Spectral and Dynamical Aspects of Photoluminescence–Plasmon Coupling in PPV–Silver Systems

P75 - NEMATALLAH Omnia Hamdy Abdelrahman

Integrating Diffuse Optics and Laser-Induced Spectrochemical Techniques for Reliable Biological Tissue Screening, Classification, and Characterization

P76 - NEZA HOZANA Germaine

Data-Driven Discovery of the Origins of UV Absorption in Alpha-3C Protein

P77 - NITIKA Nitika

TCAD-Based Performance Analysis of MFMIS FeFET for Energy Efficient Electronics

P78 - PAMBUNGAL Adhithya Pramod

First Principles Study of Structural and Electronic Properties of Cubic $Ca_{3-x}Mg_xPN$ Anti-Perovskites: Promising Lead-Free Photovoltaic Materials

P79 - PANDEY Nupur

Solvation-Driven Dual-Mode Fluorescence Response of Aminoquinoline Derivative for Water Detection

P80 - PANDEY Satish

Layer-Dependent Study of Exfoliated MoS2 for Photodetector Operation

P81 - PARVEEN SINGH -

HARNESSING ARTIFICIAL INTELLIGENCE FOR ENHANCED PHOTOPHYSICAL AND PHOTOCHEMICAL SYSTEMS: PATHWAYS TO SOLAR ENERGY CONVERSION AND PHOTOELECTROCHEMICAL CO_2 REDUCTION

P82 - PARVIN Mousumi

Unlocking Vanadium Dichalcogenide Monolayers (V2Se2 and V2Te2) for High-Performing Sodium-Ion Batteries: From Experiment to First-Principles

P83 - PAWAR Kanchan Jagannath

Z scheme charge transfer study using $BiVO_4$/boron-doped g-C_3N_4 for photoelectrocatalytic (PEC) water splitting.

P84 - PILLAI Anandavadivel Annamalai

Band Alignment and Optical Response in BN- and BP-Based MX2 (M = Mo, W; X = S, Se) Heterostructures Toward Photocatalytic Water Splitting

P85 - PONKIYA Zarnaben Dileepbhai

Accelerating Photocatalyst Discovery in Halide Double Perovskites via Machine Learning Driven High-Throughput Screening

P86 - POOBALAN Vijayalakshmi.P

From Hydrothermal Crystals to Thin-Film-Compatible Growth of $Cs_2(Na/Ag)FeCl_6$ Double Perovskites.

P87 - RAHAMAN Towhidur

Explainable Machine Learning for Data-Driven Discovery of Single Perovskites for Photovoltaic Applications

P88 - RAJABI Yasser

Enhanced nonlinear optical and photothermal properties of Sr/Bi-doped LaMnO3 and LaCoO3 nano-perovskites: Towards optoelectronic and biomedical applications

P89 - RAWAT Abhay

A First-Principles Study of Rashba-Driven Hydrogen Evolution Activity in 2D BiSb and BiAs Monolayers

P90 - DEBOJYOTI RAY CHAWDHURY -

Fluorescence enhancement in hexagonal boron nitride quantum dots coupled microcavity

P91 - ROY Anirban

Chirality-Driven Second Harmonic Generation and Distinctive Modal Raman Optical Activity in SiC–GeC Quantum Nanodots

P92 - SAFARIFARD Vahid

Engineering Ce-MOF/$CoFeO_3$ Heterostructures for Enhanced Piezo-Photocatalytic Chromium Reduction and Nitrogen Fixation

P93 - SANGHAVI Bhavya

Convoluted nested square split ring resonator for multiband and chiral response in THz range

P94 - SARKAR Akram Hossain

Spin-Orbit Driven Dark Excitons in Low Dimensional Systems from First Principles Calculations .

P95 - SARKAR Ranjini

CO2 Activation in B- and N-doped C20 Fullerene-supported Single-Atom Catalysts - A DFT Study

P96 - ANJALI -

Polarons additive enhanced saturable absorption in MoS2/PANI nanocomposite films.

P97 - SHAW Swati

Visible-Light-Driven CO$_2$ Conversion on Group-10 Metal–Supported Janus Sc$_2$COS MXene with Enhanced Solar-to-Hydrogen Efficiency

P98 - SHYAM Ikshvaku

Quantum Emitters in Two-Dimensional Materials via Ion Implantation

P99 - SIMIYU Emmanuel Karungani

Solvatochromic Photophysics of Benzanthrone Derivatives for Next-Generation Optoelectronic and Photovoltaic Applications

P100 - SINGLA Akshat

Composition-Driven Luminescence Tuning in Silicate Nanophosphors

P101 - POOJA Kumari

Enhancement of Solar Cell Performance with Layered Filler Graphite for Natural Dye Sensitized Solar Cell

P102 - SOLANKI Miteshkumar Balavantbhai

G0W0 Many-Body Perturbation Theory for Ground and Excited States in CsSrF3 Perovskite First-Principles Study with Yambo

P103 - SRIVASTAVA Pradhi

Electron-phonon coupling induced renormalization of electronic properties in a ternary chalcogenide, FeBi4S7

P104 - THEKKE PARAYIL Reshmi

Up/down conversion luminescence properties of Ca2Ga2GeO7: Er, Yb for versatile applications.

P105 - TRIAPTHI Ayushi

Cationic Interplay for the Halide Ion Migration: Implication to Neuromorphic Computing

P106 - TUKADIYA Namrataben Arjan

Improved Power Conversion Efficiency of RbAX3 (A= Ge, Sn; X=Cl, Br) Absorber Based Solar Cell Through the Variation of ETL

P107 - VERMA Rahul

Quantized spin Hall effect in bottom-up designed synthetic 2D materials

P108 - VIKRAM -

Atomic-Scale Insights into Passivation and Halide Mixing in 3D and 2D Halide Perovskites

P109 - VORA Aditya Mahabhai

Prediction of the Thermoelectric Properties of Lead Telluride under Applied Strain Using Advanced Computational Methods

P110 - VANNADIL PUTHIYAVEETIL -

Solvent Driven Crystallisation in $CsPbBr_3$ Perovskites for High Structural Quality and Luminescence Stability

P111 - VUTUKURI V N Ravi Kishore

Rational Design of Electron-Deficient Tricyanofuran HTMs for Stable Perovskite Solar Cells: A DFT-Based Approach

P112 - WADHWA Arshiya

Photophysical Optimization of CdS/CdSe Co-sensitized Quantum Dots for Enhanced Quantum Dot Sensitized Solar Cells

P113 - WAKOLI Franklyne Wekesa

Comparative investigation of fullerene and non-fullerene acceptors blended with polymer donor P3HT for solar cell applications

P114 - YADAV Sukrit Kumar

Mechanical, Dynamical, Thermal, Electronic, Magnetic, and Optical Properties of Ti_2InC and Ta_2InC MAX Phases: Potential for Thermoelectric and Optoelectronic Applications

P115 - ZEDAN Mostafa Fathy Abdelnaeim

Visible-light Active Metal Nanoparticles@Carbon Nitride for Photocatalytic Degradation of Organic Water Pollutants and Photoelectrochemical Properties

P01

Novel synthesized V_2O_5-doped PMMA nanocomposite films for effective photocatalytic removal of methylene blue from water

Redha A. Elkhadry , Souad A. Elfeky , Walid Tawfik and Mostafa Fathy Zedan *

Cairo University, National Institute of Laser Enhanced Sciences, Giza, Egypt

The synergistic effects of population growth, industrialization, and urbanization drive an increase in environmental crises, such as water pollution. Polymeric nanocomposites (PNCs) offer a promising trend for large-scale applications in environmental remediation including photocatalytic water pollutants. In this work, V_2O_5 nanoparticles were synthesized using the sol-gel method and successfully incorporated into PMMA using the casting method. A series of V_2O_5/PMMA photocatalyst films have been fabricated with various loading content of V_2O_5 NPs. The morphological, crystal structure, and optical properties of the prepared V2O5/PMMA photocatalysts were characterized using SEM, XRD, FTIR, and UV-Vis spectrophotometry, respectively. The SEM images indicate that there are mainly physical interactions between PMMA and V_2O_5 NPs. Moreover, the prepared V_2O_5/PMMA films before and after treatment with H_2O_2+UV were evaluated toward MB photodegradation under UV irradiation. The results obtained showed that doping V_2O_5 NPs into PMMA could inhibit the recombination rate of the photogenerated charge carriers. Among all prepared catalysts, the highest photocatalytic performance toward MB degradation under UV irradiation was obtained using the treated P-VPO1 nanocomposite film (0.033% V_2O_5/PMMA) compared to other formulations. Approximately 80% of MB was degraded after 60 min of UV irradiation in the presence of the treated P-VPO1. The enhanced photocatalytic activity was ascribed to the promoting effect of the H_2O_2+UV treatment for the prepared V_2O_5 doped PMMA films and with an appropriate loading amount of V_2O_5 NPs. Moreover, the P-VPO1 shows good reusability and stability for MB dye photodegradation after five consecutive runs under UV irradiation. This study reported a straightforward, and rapid approach to fabricate an improved V_2O_5/PMMA nanocomposite films with excellent reusability and attractive photocatalytic properties for diverse environmental applications, including water treatment.

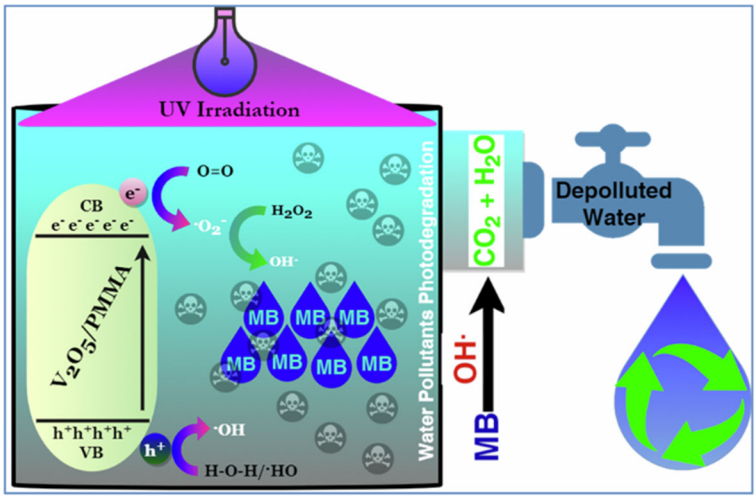

The suggested photocatalytic mechanism of MB degradation over the treated PNC films under UV light irradiation

P02

Understanding Excited States in Magic Series $Au_{8n+4}(SR)_{4n+8}$ Nanoclusters: Role of Size, Ligands, and Theory Level

Dinesh Acharya,[†] Baoliang Han,[†] Hao Liang,[†] Rakesh Kumar Gupta,[†] Zhi Wang,[†] Fahri Alkan,[#*] Zhi-Yong Gao,[§] Mohammad Azam,[¶] and Di Sun[†*]

[†]*School of Chemistry and Chemical Engineering, State Key Laboratory of Crystal Materials, Shandong University, Ji'nan, 250100, People's Republic of China*

[#]*Department of Chemistry, Bilkent University, Ankara, 06800, Turkey*

[§]*School of Chemistry and Chemical Engineering, Henan Normal University, Henan Xinxiang 453007, People's Republic of China.*

[¶]*Department of Chemistry, College of Science, King Saud University, PO Box 2455, Riyadh 11451, Saudi Arabia.*

ABSTRACT

The excited-state properties of metal nanoclusters have attracted considerable attention for potential applications in optoelectronics and biomedicine. However, the theoretical exploration of these properties, particularly emission mechanisms, remains challenging due to the high computational cost of excited-state structure optimization.[1] Herein, we investigate the geometric and electronic structural changes upon photoexcitation in the magic series gold nanocluster $Au_{8n+4}(SR)_{4n+8}$ (R=H or phenyl, n = 3–6) using time-dependent density functional theory (TDDFT) and its approximate variant, DFT plus tight binding (TD-DFT+TB).[2,3] Our results demonstrate that approximate methods, which combine full DFT-ground-state descriptions with the tight-binding approximation in linear response calculations, offer a cost-effective and reliable approach for predicting size and ligand effects on excited-state properties of gold nanoclusters. Key parameters such as Stokes shift, charge-transfer character, and the energy gap between the first singlet (S_1) and triplet (T_1) states show strong dependence on cluster size and the nature of the ligand shell, and these trends are well captured by the approximate methods. These results emphasize their potential for efficient design of gold nanoclusters with tailored optical functionalities.

(1) Jin, R.; Zeng, C.; Zhou, M.; Chen, Y. Atomically Precise Colloidal Metal Nanoclusters and Nanoparticles: Fundamentals and Opportunities. *Chem. Rev.* **2016**, *116* (18), 10346–10413.

(2) Jin, R.; Li, G.; Sharma, S.; Li, Y.; Du, X. Toward Active-Site Tailoring in Heterogeneous Catalysis by Atomically Precise Metal Nanoclusters with Crystallographic Structures. *Chem. Rev.* **2021**, *121* (2), 567–648.

(3) Liu, X.; Xu, W. W.; Huang, X.; Wang, E.; Cai, X.; Zhao, Y.; Li, J.; Xiao, M.; Zhang, C.; Gao, Y.; Ding, W.; Zhu, Y. De Novo Design of $Au_{36}(SR)_{24}$ Nanoclusters. *Nat. Commun.* **2020**, *11* (1), 3349.

P03

Wavelength-Dependent Optical Activity in Aqueous Chiral Solutions: A Polarimetric Study Using Monochromatic and Filtered Light Sources

Isaac Kwesi Acquah [1], Desmond Appiah [1], and Michael Gyan [1]

[1]*Department of physics Education, University of Education, Winneba, Ghana*

Abstract

Understanding how polarized light interacts with chiral aqueous media is essential for several photophysical and sensing applications. In this study, we investigate the wavelength-dependent optical activity of brown sugar, white sugar, and salt solutions using a sodium D-lamp, laser source, and a set of optical filters (red, yellow, green, and cyan). Optical rotation was measured as a function of solute concentration and incident wavelength using a controlled polarimetric setup. The results show a strong linear dependence between concentration and rotation angle for both white and brown sugar, with cyan light (shortest wavelength) producing the highest rotation. Brown sugar exhibited higher optical activity than white sugar, attributed to compositional differences such as potassium and magnesium content. Salt solutions showed no measurable optical activity due to the absence of chirality. These findings provide insight into wavelength-selective light–matter interactions in simple chiral media and highlight the potential of low-cost polarimetric methods for optical sensing and analytical photochemistry.

P04

A Comprehensive Review of 2D Heterostructures for Energy Materials: Classification, Computational Design, and Tunable Properties

P05

Electrochemical Performance of Lanthanum Ferrite ($LaFeO_3$) Nanomaterials for Enhanced Supercapacitor and Photocatalysis Applications

Mohammad Ayaz Ahmad[1,2], Shahnaz Kossar[3], Shawn Jagnandan[1], Antalov Jagnandan[1], Nasharath Mapjan[4], Fazal Um Min Allah[5], [1,2] , and Third C. Author [2]

[1]Department of Mathematics, Physics & Statistics, Faculty of Natural Sciences, University of Guyana, Greater Georgetown, South America

[2]Department of Physics, Maryam Abacha American University of Nigeria, Kano State, Nigeria

[3]School of Natural Sciences, GNA University, Sri Hargobindgarh, Phagwara-Hoshiarpur Road, Phagwara, Punjab 144401, India

[4]Department of Chemistry, Faculty of Natural Sciences, University of Guyana, Greater Georgetown, South America

[5]Department of Mechanical Engineering., Faculty of Engineering & Techchonology, University of Guyana, Greater Georgetown, South America

Lanthanum Ferrite ($LaFeO_3$) nanoparticles have received interest for their potential in energy storage and photocatalytic applications. $LaFeO_3$ powder was prepared through a novel sol-gel hydrothermal method and its electrochemical, morphological, structural and photocatalytic properties were investigated. The structural characterization confirmed that the orthorhombic perovskite structure is followed by synthesized $LaFeO_3$ material. The electrochemical performance of $LaFeO_3$ electrode materials was evaluated using a 2.0 M KOH electrolyte in a potential window of - 0.3 to 0.4 V. The Cyclic voltammetry (CV) measurements were carried out at scan rates ranging from 10 to 50 mVs^{-1}, and specific capacitance values were calculated from these curves. The specific capacitance of LFO electrode material was found to be 89, 81, 73, 68, and 58 F g^{-1} for scan rates of 10, 20, 30, 40, and 50 mVs^{-1}, respectively, indicating excellent rate capability and efficient charge storage. Photocatalysis analysis revealed that the 84.2% of the dye was degraded after 180 minutes of exposure to visible light. The above findings confirm that the resultant $LaFeO_3$ material exhibits better electrochemical performance and photocatalysis activity. The combination of the material's high capacitance values and stable performance at varying scan rates signifies the potential of $LaFeO_3$ as a highly efficient and reliable electrode material for energy storage devices. Further optimization of the synthesis process and exploration of composite materials could enhance the performance and scalability of $LaFeO_3$ based electrodes for commercial applications.

[1] Garima Srivastava, Ravina, M. Ayaz Ahmad, A.M. Quraishi, Virat Khanna, P.A. Alvi, Nano Trends. **9(3)**, 100067 (2025).

[2] Wahid Ali, A. M. Quraishi, Mohammad E. Khan, Syed Kashif Ali, Wakeel Ahmad, Anwar Ulla Khan, Waleed Zakri, M. Ayaz Ahmad, Sandhya Kattayat, and P. A. Alvi, Int. J. of Mod. Phys. B. **255**, 2550191-1-15 (2025).

[3] Neha Sharma, Aakansha, M. G. Siddiqui, Saurabh Dalela, Shalendra Kumar, S. Z. Hashmi, M. Ayaz Ahmad, A. M. Quraishi, P. A. Alvi, J. of Appl. Poly. Sci. **142(12)**, (1-18):e56835 (2025).

P06

Next-Gen Solar: Revealing the Promise of $CsPbI_3/CsSnI_3$ Tandem Cells

[1*]Mohamed Ait oufakir, [2]Rubayyi T.Alqahtani, [1]Younes Chrafih, [2]Abdelhamid Ajbar

*Mohamed ait oufakir
[1]moufakirmohemad@gmail.com, faculty of scences rabat, morocco
[2] faculty of sciences of rabat, morocco

Tandem solar cells offer a wider photon absorption range, enabling greater efficiency compared to single junction counterparts. The upper cell efficiently captures high-energy photons, while the lower cell absorbs low-energy photons filtered through the top layer. Achieving efficient, cost-effective, and durable solar cells requires the integration of absorber layers with optimal band gaps. This study presents a computational exploration of tandem perovskite solar cells using SCAPS-1D simulations to improve device performance. The proposed dual-layer configuration features a top cell composed of ITO/ZnSe/CsPbI3 and a bottom cell of ITO/ZnSe/CsSnI3. The thickness of the perovskite CsPbI3 layer in the top cell was optimized for peak performance, maximizing light absorption and enhancing charge carrier dynamics. Emission spectra from the first cell were utilized to guide the SCAPS-1D simulations for the second cell. The results reveal a notable fill factor (FF) and an impressive power conversion efficiency (PCE) of 29.38%, underscoring the superiority of this tandem configuration over single-junction designs. These findings demonstrate the potential of tandem perovskite solar cells to drive next-generation photovoltaic technologies, fostering advancements in high-efficiency and cost-effective solar energy solutions

[1]M.Ait Oufakir, M, Alqahtani, solar energy 12.298.(2025)

BIOGRAPHY (preferable but not mandatory)

Mohamed Ait Oufakir is currently a PhD student in Mathematical Physics and Materials Science at the Faculty of Sciences, Mohammed V University in Rabat, Morocco, affiliated with the High Energy Physics Laboratory (LPHE). He holds a Master's degree in Mathematical Physics through the national PM program supported by CPM-Maroc and ICTP, and a Bachelor's degree in Modern Physics. His research focuses on the numerical and experimental study of perovskite materials for hydrogen storage and solar cells, including tandem and HIT configurations. He has experience with advanced simulation tools such as SCAPS-1D, Quantum ESPRESSO, and WIEN2k, and recently integrated machine learning methods for solar cell optimization. He is the lead author of an article on tandem perovskite solar cells achieving over 29% PCE through SCAPS simulations, and currently co-authors further publications on energy materials. He is also a member of the International Association of Physics Students (IAPS) and contributed to organizing the Pre-Planck Morocco competition and participating in the ICPS community. Mohamed is passionate about fundamental physics and applied energy science, open to interdisciplinary collaborations, and dedicated to advancing materials research for renewable energy technologies.

P07

Enhancing the Photovoltaic Potential of Lead-Free $CsSnCl_3$ Perovskite via Al/In Doping: A Combined DFT and SCAPS-1D Study

Mekuria Tsegaye Alemu[1,2], **Derje Fufa Hirpa**[2], **Kingsley Onyebuchi Obodo**[3] and **Chernet Amente Gefe**[2]

[1] *(Department of Physics, College of Natural and Computational Science, Kebri Dehar University, P.O. Box 250, Kebri Dehar, Ethiopia)*

[2] *Physics Department,College of Natural and Computational Science, Addis Ababa University, P.O. Box 1176, Addis Ababa, Ethiopia*

[3] *School of Chemistry & Physics, University of KwaZulu-Natal, Pietermaritzburg, Scottsville 3209, South Africa*

Abstract

The pursuit of high-efficiency, environmentally friendly photovoltaics has intensified the search for lead-free perovskite solar cells (PSCs). This study comprehensively investigates the potential of inorganic cesium tin chloride ($CsSnCl_3$) as a stable, non-toxic absorber material via a combined computational approach. To address the inherent instability of Sn^{2+}, we propose strategic doping with aluminum (Al) and indium (In). First-principles density functional theory (DFT) calculations reveal that doping successfully widens the band gap from 0.95 eV to 1.63 eV (Al) and 1.95 eV (In), induces beneficial p-type conductivity, enhances optical absorption, and improves structural stability. Subsequently, device-level performance is evaluated through SCAPS-1D simulations of pristine $CsSnCl_3$ in three novel heterojunction architectures: FTO/ZnO/CsSnCl3/Spiro-OMeTAD/Au, FTO/C60/$CsSnCl_3$/CuSCN/Au, and FTO/WS_2/$CsSnCl_3$/P3HT/Au. These configurations yield high power conversion efficiencies (PCEs) of 24.89%, 24.53%, and 23.03%, respectively, at an 800 nm absorber thickness. The ZnO/Spiro-OMeTAD structure achieves superior performance due to optimal band alignment and minimized recombination losses. Further optimization of the absorber thickness boosts the PCE to 25.00% for the leading device. All configurations exhibit exceptional quantum efficiency, exceeding 99%. Our findings not only validate doped $CsSnCl_3$ as a highly promising lead-free absorber but also underscore the critical importance of synergistic materials engineering and device architecture optimization in developing efficient and sustainable PSCs.

P08

Cobalt-Engineered Infrared Absorptivity in Erbium Aluminium Garnet for Advanced Photonic Devices

Archisha[1], Y. Dwivedi*

Department of Physics, National Institute of Technology Kurukshetra, Haryana, 136119, India

**yashjidwivedi@nitkkr.ac.in*

Cobalt-doped erbium aluminium garnet (Co:$Er_3Al_5O_{12}$) has been examined as a promising photonic material for infrared absorption[1] and photophysical applications. $Er_3Al_5O_{12}$ (ErAG) provides a thermally stable, low-phonon-energy garnet host that supports sharp f–f transitions of Er^{3+}, while the incorporation of Co^{2+} introduces broad d–d absorption bands arising from crystal-field-driven electronic transitions. In this work, $Er_3Al_5O_{12}$:Co nanophosphors were synthesized through a combustion synthesis method. X-ray diffraction confirmed the successful formation of a single-phase ErAG structure with cobalt incorporated into the lattice, while SEM–EDS analyses revealed a porous network of interconnected grains and agglomerated nanoparticles, a morphology conducive to enhanced optical interaction.

UV–visible–NIR absorption spectra exhibited enhanced broadband absorption in the infrared region, attributed to Co^{2+} electronic transitions and their interaction with Er^{3+} energy levels between 900–1200 nm and distinct Stark-split peaks near 1450 nm and 1550 nm, attributable to the $^4I_{15/2} \rightarrow {}^4I_{13/2}$ intra-4f transitions of Er^{3+} ions, responsible for the characteristic 1.54 μm emission. Cobalt doping modified the local crystal field environment around Er^{3+} ions, inducing spectral shifts and variations in emission intensity, indicating strong Er–O–Co interactions. This establishes the material's potential as an effective infrared absorber and functional nanophosphor for photonic devices including optical amplifiers, lasers, and IR sensing technologies.

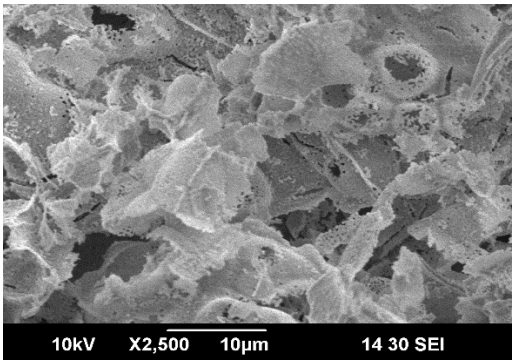

Figure 1. SEM images of Co:$Er_3Al_5O_{12}$ sample annealed at 1100 °C.

[1] I. L. H. Kwak, pp. 631–638, 2010, doi: 10.1007/s00340-010-4199-z.

P09

Electronic, magnetic, and topological properties of ferromagnetic 2D perovskite-type oxides

Susaiammal Arokiasamy[1,2,3], Gennevieve M. Macam[4], Sreeparvathy P. C.[1,5], Rovi Angelo B. Villaos[1], Zhi-Quan Huang[1], Chia-Hsiu Hsu[6], Yoshinori Okada[6], Hsin Lin[7], and Feng-Chuan Chuang[1,5,8,9]

[1] (Presenting author underlined) Department of Physics, National Sun Yat-sen University, Taiwan

[2] Department of Physics, St. Bede's College, India

[3] Department of Physics, School of Physical Science, St Aloysius (Deemed to be University), India.

[4] National Institute of Physics, University of the Philippines Diliman, Philippines

[5] Physics Division, National Center for Theoretical Sciences, Taiwan

[6] Quantum Materials Science Unit, Okinawa Institute of Science and Technology, Japan

[7] Institute of Physics, Academia Sinica, Taiwan

[8] Center for Theoretical and Computational Physics, NSYSU, Taiwan

[9] Department of Physics, National Tsing Hua University, Taiwan

Two-dimensional (2D) materials within the hematene-type binary oxides and perovskites family have recently gathered huge research interest for nanoelectronic devices. However, the exploration of their fascinating topological properties remains limited. Herein, through first-principles calculations, we systematically examine the electronic, magnetic, and topological properties of substitutionally doped 2D ABO_3 (A = As, Sb, or Bi, and B = V, Nb, or Ta) perovskite structures at the B site of a B_2O_3 system. Interestingly, the atomic substitution makes the 2D ABO3 structures dynamically stable. Our detailed calculations show the ferromagnetic (FM) and antiferromagnetic phases of these materials. The calculated Chern number (C) for the FM 2D ABO_3 (A = As, Sb, or Bi, B = Nb or Ta) suggests their topologically non-trivial phases. Furthermore, the computed nontrivial Berry curvature highlights the topological properties in $AsNbO_3$. These findings highlight opportunities in 2D-ABO_3 materials for applications in spintronics.

References:

[1] S. Arokiasamy *et al.*, New J. Phys. 26, 123031 (2024).

P10

Bulk Doping–Driven In-Situ Simultaneous Modulation of Dual Interfaces Improves Charge Transport Dynamics and Reduces Recombination Loss enabling > 26% Efficient Perovskite Solar Cells

***H. Baishya*,[1] *R. Das Adhikari,* [1] *S. Laha,*[2] *K. Bhattacharyya,*[2] *and P. K. Iyer* [1,2]**

[1]*Centre for Nanotechnology*

[2]*Department of Chemistry*

Indian Institute of Technology, Guwahati

Guwahati-781039, Assam, INDIA

Abstract

The buried interface plays a crucial role in governing perovskite film crystallization and morphology, while both the buried and top interfaces strongly influence defect formation, non-radiative recombination pathways, and charge-transport dynamics. Consequently, these interfacial processes directly impact device performance and long-term operational stability. In this work, we propose a **simultaneous dual-interface engineering strategy** by incorporating a molecular additive, *maleimido propionic acid hydrazide hydrochloride* (MPAH), into the perovskite precursor solution. Upon film formation, MPAH exhibits **bidirectional segregation**, wherein the **$MPAH^+$ cations migrate toward the top surface**, while the **Cl^- anions preferentially accumulate at the buried interface**. The Cl^- ions at the buried interface promote improved perovskite crystallization, regulate film morphology, passivate deep trap states, and modulate the interfacial energetic landscape. Meanwhile, the $MPAH^+$ cations effectively passivate dominant vacancy (V_I, V_{Pb}) and antisite (Pb_I, I_{Pb}) defects at the top surface. As a result, the morphological and photophysical properties of both interfaces are simultaneously enhanced, leading to suppressed non-radiative recombination loss and efficient charge extraction and transport. Benefiting from these synergistic interfacial improvements, the optimized device delivers a substantially enhanced fill factor (FF), increasing from **80.6%** in the control to **86.6%**, thereby boosting the power conversion efficiency (PCE) from **23.02%** to **26.10%**. The improved crystallinity and stabilized surface morphology also yield markedly superior operational stability under ambient storage, continuous illumination, and thermal stress. This integrated approach highlights the effectiveness of **bidirectional additive segregation** in simultaneously tuning the buried and top perovskite interfaces to achieve high device performance and long-term stability.

References

[1] Z. Xiong, Q. Zhang, K. Cai, H. Zhou, Q. Song, Z. Han, S. Kang, Y. Li, Q. Jiang, X. Zhang and J. You, *Science*, 2025, **390**, 638–642.

[2] H. Zhu, B. Shao, Z. Shen, S. You, J. Yin, N. Wehbe, L. Wang, X. Song, M. Abulikemu, A. Basaheeh, A. Jamal, I. Gereige, M. Freitag, O. F. Mohammed, K. Zhu and O. M. Bakr, *Nat. Photonics*, 2025, **19**, 28–35.

[3] X. Li, Z. Ying, S. Li, L. Chen, M. Zhang, L. Liu, X. Guo, J. Wu, Y. Sun, C. Xiao, Y. Zeng, J. Wu, X. Yang and J. Ye, *Nanomicro Lett.*, 2025, **17**, 141.

P11

Color Tunability in $NaYF_4$: Er^{3+} Phosphor

Hemanth B[1], Sabeena M[1]

[1]*Department of Physics, Cochin University of Science and Technology, Kochi, Kerala, India, 682022*

Corresponding author: sabeena@cusat.ac.in

Over the years, an increasing demand is noticed for the development of energy efficient phosphors, particularly in the field of solid-state lighting, displays, biosensors, bio-imaging and optical sensors. Among the different rare earth doped phosphors, $NaYF_4$: Er^{3+} have advantages such as low autofluorescence, high signal to noise ratio, large antistocks shift, possibility of colour tunability due to the existance of ladder like energy levels and high conversion efficiency due to low phonon energy. $NaYF_4$: Er^{3+} phosphor produce *f-f* transitions upon NIR excitation, whose intensity depends on the nature of the host matrix and symmetry of the lattice site. These characteristics make $NaYF_4$: Er^{3+} suitable candidate for various applications including bio-imaging, optical sensors, among others and hence understanding the photoluminescence mechanism of these materials has relevance. The present study focussed on the upconversion studies of hexagonal phase of $NaYF_4$: *x* mol% (*x*= 2,4,5,6) Er^{3+} phosphors prepared via sol-gel method to explore the possibility of colour tuning and intensity modification of all emission transitions of Er^{3+} by concentration variations. From structural and morphological analysis, both pristine and doped phosphors showed hexagonal crystal structure with agglomerated morphology, irrespective of doping concentration. Photoluminescence studies confirmed the characteristic sharp and narrow 4*f*-4*f* transitions of Er^{3+}, such as $^2H_{11/2} \rightarrow {}^4I_{15/2}$ (520-530 nm), $^4S_{3/2} \rightarrow {}^4I_{15/2}$ (540-550 nm), and $^4F_{9/2} \rightarrow {}^4I_{15/2}$ (650-665 nm) upon 980 nm excitation. Based on the analysis of emission transitions, Jablonski diagram has been drawn to understand the energy transition mechanism during upconversion. The CIE color coordinates of (0.274,0.706) and color purity of ~ 97% confirms the highly monochromatic intense green emission from the phosphor.

[1] G. Chen, H. Qiu, Paras N. Prasad, X. Chen, Chem. Rev. 114, 5161 (2014).

[2] J. Chen, J. X. Zhao, J. Sens, 12, 2414 (2012).

[3] G. Liu, Chem. Sov. Rev, 44, 1635 (2015).

P12

MORPHOLOGY-DRIVEN ENHANCEMENT OF WATER OXIDATION PERFORMANCE IN HEMATITE (α-Fe_2O_3) PHOTOANODE

Ashitosh Bambal[1], Somnath Ladhane[1], and Sandesh Jadkar[1*]

[1]Department of Physics, Savitribai Phule Pune University, Pune 411007

[*]Corresponding authors: sandesh@physics.unipune.ac.in

Hematite (α-Fe_2O_3) is a promising photoanode material due to its advantageous features, such as visible light absorption, adequate band gap energy, earth abundance, chemical stability and inexpensive cost. However, its performance has been limited by short hole diffusion length (2-4 nm), poor absorption and a low electrical conductivity [1, 2]. Herein, to resolve this issue α-Fe_2O_3 nanoparticles have been successfully grown on FTO using a chemical approach via the hydrothermal method by varying reaction time and reaction temperature. On varying these two parameters the morphology of α-Fe_2O_3 has been tuned, which enhances photoelectrochemical (PEC) water oxidation performance. X-ray diffraction (XRD), field emission scanning electron microscopy (FESEM), UV-visible spectroscopy, and photoelectrochemical activity were used to study the structural, morphological, optical, and photoelectrochemical properties. X-ray diffraction pattern confirms the formation of polycrystalline α-Fe_2O_3 and crystallite size varies from ~220 Å to ~234 Å. FESEM analysis confirms the formation of α-Fe_2O_3 nanoparticles (as displayed in **Figure**) further the optical absorption study gives the variation in bandgap from 1.77 eV to 1.90 eV. The maximum photocurrent density (~ 0.35 mA/cm² at 0.7 V vs. SCE) was observed for 6 hr reaction time and 150 ^{0}C reaction temperature. Electrochemical impedance spectroscopy (EIS) was carried out to study the charge transfer dynamics at the electrode–electrolyte interface of pristine α-Fe_2O_3 nanoparticles. The minimum charge transfer resistance recorded for pristine α-Fe_2O_3 at same reaction time and temperature was approximately 17.5 kΩ that leads to enhancement in PEC performance.

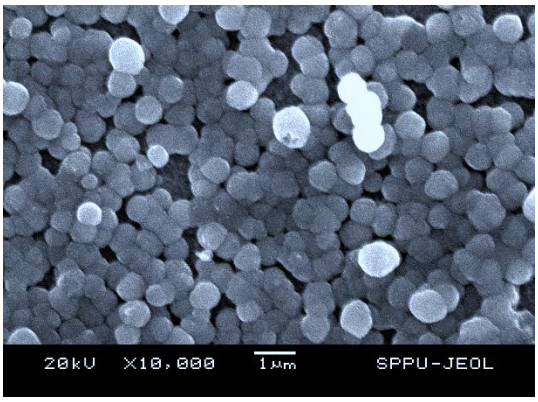

Figure: Displays FESEM micrographs of α-Fe_2O_3 nanoparticles

References

[1] P. Sharma, J-W. Jang, J. L. Lee, ChemCatChem, **11**, 157–179, (2019)
[2] G. C. Behera, B. Biswal, J. K. Bidika, B. R. K. Nanda, S. Alwarappan, J. K Rath, and Somnath C. Roy, Small, **21**, 2406715, (2025)

P13

Impact of external strain on electron–phonon coupling strength in SnTe pseudo-monolayer

Rajdip Bandyopadhyay[1], Indranil Das[1], Sudip Chakraborty[1]

[1]Materials Theory for Energy Scavenging (MATES) Lab, Condensed Matter Physics, Harish-Chandra Research Institute(HRI) Prayagraj, Chhatnag Road, Jhunsi, U.P. 211019, India

Two-dimensional SnTe has emerged as an important lower dimensional condensed matter system due to the corresponding lattice dynamics and strong electron–phonon interactions. In this work, we present a first-principles investigation of the effect of external biaxial strain on the structural, vibrational, and electron–phonon coupling properties of a SnTe pseudo-monolayer. External strain is employed as an effective control parameter to tune lattice geometry and phonon characteristics, thereby influencing phonon-assisted optical processes. To further quantify electron–phonon coupling, we com- pute the Huang–Rhys factor using a dedicated analysis workflow. Our results show a pronounced sensitivity of the Huang–Rhys factor to applied strain, indicating that both tensile and compressive strain significantly modify the coupling strength. This behaviour highlights the strong interplay between mechanical deformation and vibrational properties in two-dimensional SnTe. The present study demonstrates that strain engineering offers a viable route to control electron–phonon interactions in SnTe pseudo-monolayers, with potential implications for optoelectronic and phonon-mediated device applications. Our aim is to envisage a more quantitative understanding of carrier–phonon interactions, as well as their impact on transport and optical response in strained two-dimensional pseudo-monolayer systems.

References

[1] F. Giustino, "Electron–phonon interactions from first principles," *Reviews of Modern Physics*, vol. 89, p. 015003, 2017. Erratum: *Rev. Mod. Phys.* 91, 019901 (2019). DOI: 10.1103/RevModPhys.89.015003.

[2] Computational 2D Materials Database (C2DB), DTU Physics. Available: `https://c2db.fysik.dtu.dk`. Accessed: 20 Dec 2025.

P14

Unravelling anisotropic mechanical and electronic attributes of MN_4 (M= Be, Mg, Zn, Cd) monolayers and their excellent supercapacitive performances

Krishnanshu Basak[1*], Arka Bandyopadhyay[2], Debnarayan Jana[1]

[1]*Department of Physics, University of Calcutta, 92 A. P. C. Road, Kolkata 700009, India*

[2]*Institute for Theoretical Physics und Astrophysics, University of Würzburg, D-97074 Würzburg, Germany*

*Presenting Author E-mail: kbasakbu@gmail.com

The recent experimental realization of BeN_4 monolayer, Berylllonitrelene (Phys. Rev. Lett. 126(2021), 175501), has unveiled a novel group of nitrogen-rich 2D materials, namely MN_4 (M = Be, Mg, Zn, Cd). In this present work, we systematically investigate the direction dependent mechanical and electronic features of all systems based on the first principles calculation. The geometrical stability of all structures is confirmed by evaluating phonon dispersion relation and molecular dynamics simulation results. Among these, BeN_4 and MgN_4 sheets are brittle while ZnN_4 and CdN_4 are ductile in response to external strain, exhibit strong mechanical anisotropy along [01] and [10] directions. Electronic band structure analysis infers that all the structures exhibit anisotropic Dirac cone like features in their respective band diagram. We further investigate the occurrence and robustness of such Dirac cone by considering a simple coupled-chain model, validating our numerical results. In addition, the capacitive responses of all systems are elucidated by computing quantum capacitance (QC) across different potential ranges, attributed to good electrical and thermal conductivity, high specific surface area, impressive thermodynamical stability. It is noteworthy that maximum value of QC is reported for CdN_4 monolayers at relatively higher electrode (positive) potential. On contrary, capacitive responses for other MN_4 monolayers are nearly comparable for lower electrochemical potential ranges, applicable for aqueous electrolytes. The adaptability of a particular electrode as cathode or anode is confirmed by evaluating surface charge density i.e. Q_a/Q_c. The results indicate that CdN_4 is preferable for anode material, whereas other MN_4 structures emerge as promising candidates for designing symmetric supercapacitors. Moreover, significant improvement in QC values is evidenced for metal atom adsorbed BeN_4 structure at positive electrode potential. These findings are expected to encourage future research in developing nanoelectronics and energy storage applications.

Keywords: Band structure, quantum capacitance, surface charge density

References:

1. B. Mortazavi, F. Shojaei, X. Zhuang, *Mater. Today Nano* 15 (2021) 100125.
2. X. Yang, R. Ahuja, W. Luo, *Nano Energy* 113 (2023) 108557.
3. K. Basak, A. Bandyopadhyay, Debnarayan Jana, *Appl. Surf. Sci* 702 (2025) 163250.

P15

Interplay of Dynamic Defects and Ultrafast Carrier Dynamics in Lead Free Double Perovskites Toward Stable, High-Performance Photovoltaics

Manasa G. Basavarajappa and Sudip Chakraborty*

Materials Theory for Energy Scavenging Lab, Harish-Chandra Research Institute (HRI), CI of Homi Bhabha National Institute, Chhatnag Road, Jhunsi, Prayagraj - 211019, India

Oxide-based double perovskites are gaining increasing attention as stable and environmentally benign alternatives to halide perovskites in photovoltaic and optoelectronic devices. Their structural versatility and chemical flexibility open pathways for fine-tuning both electronic and lattice properties, yet their carrier dynamics and defect behavior remain less understood. In this work, we investigate these aspects using a combination of first-principles calculations and advanced simulation techniques.

Nonadiabatic molecular dynamics is employed to capture ultrafast carrier relaxation and to quantify the role of electron–phonon coupling in determining charge transport and recombination lifetimes. The results highlight efficient charge separation and suppressed nonradiative recombination channels, which are essential for high photovoltaic efficiency. To establish the dynamical stability of the materials, we carry out a phonon-based symmetry analysis that confirms the absence of imaginary modes and reveals the interplay between structural distortions and vibrational spectra. In parallel, we explore the formation and dynamic evolution of intrinsic point defects through defect-mediated molecular dynamics simulations. These studies shed light on migration pathways, possible defect-assisted recombination channels, and their impact on overall carrier dynamics. The comparative analysis reveals how compositional variations influence defect tolerance, lattice anharmonicity, and the balance between radiative and nonradiative processes.

Together, these insights provide a comprehensive understanding of the interplay between electronic excitations, lattice vibrations, and defect physics in oxide-based double perovskites. The findings point toward design strategies for engineering defect-resilient, dynamically stable photovoltaic absorbers with long carrier lifetimes, thereby advancing the development of robust next-generation solar materials.

P16

Intrinsic Bulk Photovoltaic Effect in Symmetry-Broken CVD-Grown Spiral WS_2

Meghasree Basu,[1] Sagnik Chatterjee,[1] Mainak Mondal,[2] Kartick Biswas, [3] Tomasz Kazimierczuk, [4] Adam Babiński,[4] Pavan Nukala, [3] Akshay Singh, [2] Maciej R Molas,[4] Arka Karmakar,[4] and Atikur Rahman [1]

[1] Department of Physics, Indian Institute for Science Education and Research - Pune, Dr. Homi Bhabha Road, Pune -411008, India
[2] Department of Physics, Indian Institute of Science, Bangalore 560012, India
560012, India
[3] Centre for Nanoscience and Engineering, Indian Institute of Science, Bangalore 560012, India
[4] University of Warsaw, Faculty of Physics, 02-093 Warsaw, Poland

Materials exhibiting the bulk photovoltaic effect (BPVE) can generate electrical current under illumination purely due to the absence of inversion symmetry, without relying on p–n junctions, built-in electric fields, or external bias, making them attractive for self-powered optoelectronic technologies [1] In two-dimensional transition metal dichalcogenides, however, BPVE has largely been achieved by imposing external symmetry breaking, such as strain or substrate engineering, which complicates device fabrication and limits scalability. In this work, we demonstrate that CVD-grown spiral WS_2, formed through a screw-dislocation-driven growth process, naturally hosts broken inversion symmetry and supports a pronounced BPVE. Structural and optical probes, including low-temperature Raman spectroscopy, polarisation-resolved second-harmonic generation, and cross-sectional transmission electron microscopy, reveal intrinsic anisotropic strain and non-centrosymmetric stacking across the spiral architecture. Devices fabricated on these spiral WS_2 flakes exhibit a clear zero-bias photovoltaic response, with measurable open-circuit voltage and short-circuit current that increase systematically with illumination intensity. The photocurrent shows strong polarisation dependence and nonlinear power scaling, identifying shift current as the dominant photoresponse mechanism.[2],[3] Our results highlight spiral WS_2 as an intrinsically asymmetric, scalable material platform for BPVE-based energy harvesting and photodetection.

[1] Y. Li *et al.*, *Nat. Commun.*, vol. 12, no. 1, p. 5896 (2021).
[2] Y. J. Zhang *et al.*, *Nature*, vol. 570, no. 7761, pp. 349–353 (2019).
[3] D. Yang *et al.*, *Nat. Photonics*, vol. 16, no. 6, pp. 469–474 (2022).

P17

Functional Engineering and Defect Passivation in Monolayer MoS_2 for High-Performance Optoelectronics

Swapneswar Bisoi, Manisha Rajput, Meghashree Basu, Atikur Rahman

Department of Physics and IHUB Quantum Technology Foundation, Indian Institute of Science Education and Research, Pune-411008, India

Sulfur vacancies (V_S) in monolayer molybdenum disulfide (MoS_2) are a critical impediment to the realization of high-performance optoelectronic devices. These point defects introduce mid-gap trap states that result in significant persistent photoconductivity (PPC), high dark currents, and restricted response speeds. Herein, we found a facile, near-room-temperature chemical functionalization strategy using copper thiocyanate (CuSCN) to overcome these limitations. This approach utilizes a synergistic dual-function mechanism: copper cations (Cu^+) act as effective electron acceptors, inducing p-type doping via interfacial charge transfer, while thiocyanate anions (SCN^-) facilitate the passivation of electronically active V_S sites.

Spectroscopic and microscopic analyses, including X-ray Photoelectron Spectroscopy (XPS) and Kelvin Probe Force Microscopy (KPFM), confirm the charge transfer and defect controlling, showing a significant downward shift of the Fermi level consistent with p-type doping. An intense transition in the photoluminescence (PL) spectrum from trion-dominated to exciton-dominated emission is observed, with the trion spectral weight decreasing by more than one order of magnitude following treatment. These material-level modifications translate directly to superior photodetector performance. The functionalized devices exhibit a four-order-of-magnitude reduction in dark current, yielding an on/off ratio of 10^4. Furthermore, PPC is drastically reduced, and the photoresponse speed is improved by more than three orders of magnitude, reaching the microsecond regime. Consequently, the photodetector achieves an excellent specific detectivity of $\sim 10^{12}$ Jones and a noise equivalent power of $\sim 10^{-14}$ W/$\sqrt{\text{Hz}}$. This work demonstrates a practical and scalable route to harness the full potential of functionalized MoS_2 for next-generation optoelectronic applications.

P18

Decoding optoelectronic behaviour in X_3BI_3 antiperovskite derivatives through many-body perturbation theory

Ayan Chakravorty, Surajit Adhikari, and Priya Johari
Department of Physics, School of Natural Sciences, Shiv Nadar Institution of Eminence, Greater Noida, Gautam Buddha Nagar, Uttar Pradesh 201314, India
Contact Email: ac900@snu.edu.in

Abstract:
Sustainable, lead-free perovskites that combine thermal robustness with strong visible absorption are in high demand for next-generation optoelectronics. In this context, halide antiperovskite derivatives present chemical tunability and structural flexibility, yet their excitonic and polaronic responses-key to light–matter interactions and carrier dynamics—are not well understood. Using state-of-the-art first-principles calculations (DFT, DFPT, GW and the Bethe-Salpeter equation) [1-5] together with the Feynman polaron model, we investigate structural, electronic, optical, excitonic and polaronic properties of a series of halide antiperovskite derivatives, X_3BI_3 (X = Ca, Sr; B = P, As, Sb, Bi). All compositions satisfy structural and mechanical stability criteria; phonon spectra show five of eight compounds are dynamically stable at 0 K. G_0W_0@PBE method yields direct bandgaps of 2.42-3.02 eV, appropriate for visible-near-UV absorption. BSE calculations give exciton binding energies of 0.258–0.318 eV, indicating moderate electron–hole attraction that still permits efficient exciton dissociation under ambient conditions. Polaron analysis reveals weak-to-intermediate carrier-phonon coupling (Fröhlich $\alpha \approx$ 2-5) with polaron mobilities reaching up to 37.19 $cm^2 V^{-1} s^{-1}$, signalling competitive charge transport. These findings identify X_3BI_3 antiperovskites as mechanically robust, wide-bandgap, lead-free candidates meriting experimental validation for stable optoelectronic devices.

[1] L. Hedin, Phys. Rev. **139**, A796 (1965).

[2] M. S. Hybertsen and S. G. Louie, Phys. Rev. Lett. **55**, 1418 (1985).

[3] S. Albrecht, L. Reining, R. Del Sole, and G. Onida, Phys. Rev. Lett. **80**, 4510 (1998).

[4] M. Rohlfing and S. G. Louie, Phys. Rev. Lett. **81**, 2312 (1998).

[5] M. Gajdoš, K. Hummer, G. Kresse, J. Furthmüller, and F. Bechstedt, Phys. Rev. B **73**, 045112 (2006).

P19

like phase of $SrZrS_3$ is the one subje
at the lowest temperature, 550 °C bu
appear stable in air with an oxidation
to 600 °C. Parera et al, [5] also
characterized different chalcogeni
Among them, $SrZrS_3$ by hig
sulfurization of their oxide cou
identified their crystal structure and
EDX, as well as they confirmed tha
gap semiconductors from 1.73 eV to
UV-vis and photoluminescence measu

Contact Informat

Najwa Chawki
Faculty of Science, Mohammed V U
chawli.najwa@gmail.co

P20

All-Optical Pseudo-Spin Waveguide and Directional Coupling in Nonlinear Photonic Crystals

Mayur Kumar Chhipa [1], John Semakula [2], and Kabedi Masanka Emmanuella [3]

[1,2,3] *Department of Electronics and Communication Engineering, Faculty of Engineering, ISBAT University, Kampala, Uganda, East Africa*

Guiding light forms the backbone of numerous photonic circuits that allow complex, robust, and miniaturized light control [1-2]. Commonly, guiding is achieved by modifying linear permittivity, resulting in a non-homogeneous linear medium. Here, we propose and realize photonic circuits in a homogeneous refractive index medium, where the guiding is driven entirely by nonlinear interaction, enabling dual-wavelength light beam guidance and optical control [3-4]. This mechanism is analogous to spin current transport in sharp magnetic domain walls, where magnetization texture constitutes a spin-dependent potential. Using narrow custom-poled nonlinear photonic crystals, we guide frequency superposition beams that act as pseudo-spins over more than four Rayleigh lengths [5]. We show that guiding properties depend on the relative phase between participating wavelengths, which can be optically switched on and off with an optical pump. Additionally, using two parallel-poled structures, we realize a pseudo-spin directional coupler, paving the way for numerous waveguiding hallmarks in a single nonlinear crystal and offering robust control over frequency superposition states of light. Finally, our findings show that it is possible to experimentally emulate complex, precise 2D magnetization domain wall structures, opening avenues for exploration that remain challenging in magnetic materials [6].

We further show that the PS waveguide attributes can be all-optically controlled by varying the relative phases of the participating wavelengths. The on-chip nonlinear guiding and manipulation allow exact spatial control over frequency superposition states of light, which are key in many classical and quantum information protocols, in a robust and compact manner, all-optically controlled by the optical pump beam [7]. Furthermore, the presented results open an experimental testbed for new magnetic domain walls spintronic devices, in 2D or 3D configurations.

[1] Saleh, B. E. A. & Teich, M. C. Fundamentals of Photonics 3rd Edition. 5, 447–469 (2013).
[2] Joannopoulos, J. D., Villeneuve, P. R. & Fan, S. Photonic crystals: putting a new twist on light. Nature 386, 143–149 (1997).
[3] Chen, Z., Segev, M. & Christodoulides, D. N. Optical spatial solitons: historical overview and recent advances. Rep. Prog. Phys. Rep. Prog. Phys. 75, 086401 (2012).
[4] Yesharim, O. et al. Observation of the all-optical Stern-Gerlach effect in nonlinear optics. Nat. Photonics 16, 582–587 (2022).
[5] Karnieli, A., Tsesses, S., Bartal, G. & Arie, A. Emulating spin transport with nonlinear optics, from high-order skyrmions to the topological Hall effect. Nat. Commun. 12, 1092 (2021).
[6] Izhak, S., Karnieli, A., Yesharim, O., Tsesses, S. & Arie, A. All-optical spin valve effect in nonlinear optics. Opt. Lett. 49, 1025 (2024).
[7] Zhang, Y., Sheng, Y., Zhu, S., Xiao, M. & Krolikowski, W. Nonlinear photonic crystals: from 2D to 3D. Optica 8, 372 (2021).

`

P21

International Conference on Photophysics and Photochemistry

Tuning Photocatalytic CO_2 Conversion Efficiency via Single and Double Vacancy Engineering in 2D o-B_2N_2 Monolayer

Rajesh Chitara [1,2], **P N Gajjar** [1], **and Sanjeev K Gupta** [2]

[1] *Department of Physics, University School of Sciences, Gujarat University, Ahmedabad 380009, India*

[2] *Computational Materials and Nanoscience Group, Department of Physics, St. Xavier's College, Ahmedabad 380009, India*

The efficient conversion of carbon dioxide (CO_2) into renewable fuels and value-added chemicals offers a sustainable approach to mitigating greenhouse gas emissions while promoting clean energy development. Among various strategies, photocatalytic CO_2 reduction has attracted significant attention due to its potential to directly utilize solar energy. In this work, we explore the recently proposed orthorhombic boron nitride (o-B_2N_2) monolayer a two-dimensional van der Waals effect of boron nitride as a metal-free photocatalyst for CO_2 reduction reactions (CO_2RR). Using first-principles density functional theory (DFT) calculations, both pristine and vacancy-engineered o-B_2N_2 systems are systematically investigated to understand the influence of single and double defect states on catalytic activity. The pristine o-B_2N_2 monolayer exhibits a direct band gap of 0.78 eV, enabling visible-light absorption but showing weak CO_2 adsorption, which limits its photocatalytic performance. In contrast, defect engineering significantly enhances surface reactivity. The introduction of single and double atomic vacancies strengthens CO_2 adsorption (up to –3.75 eV) and facilitates its activation toward multi-step reduction. Reaction pathway analysis reveals that the formate (∗OCOH) mechanism is more favourable than the carboxylic (∗COOH) route for methanol (CH_3OH) production. The rate-determining step corresponds to the conversion of ∗OCOH into ∗HCOOH, with a low limiting potential (U_l) of 1.10 V, indicating high catalytic efficiency under moderate conditions.

Overall, this study demonstrates that vacancy engineering effectively tunes the electronic structure, adsorption properties, and reaction energetics of o-B_2N_2, transforming it from an inert surface into a highly active photocatalyst. The findings provide valuable insights into defect-driven photocatalytic mechanisms and establish defective o-B_2N_2 as a promising, stable, and metal-free platform for CO_2-to-fuel conversion in sustainable energy applications.

[1] R. Chitara, H. Kolavada, M. Menon, P. N. Gajjar & S. K. Gupta, *J. Mater. Chem. A*, 2024, **12**, 32204–32216. RSC Publishing

[2] R. N. Somaiya, M. Sajjad, N. Singh & A. Alam, "Efficient Electrochemical CO_2 Reduction Reaction over Cu-decorated Biphenylene," *arXiv*, 2024, arXiv:2404.10409v2.

P22

Investigations on upconversion nanophosphors for temperature sensing

Shouvik Choudhury[1]*, Shruti Narayanan[1], Debojyoti Ray Chawdhury[1], Prem B. Bisht[1,2]

[1] Department of Physics, Indian Institute of Technology Madras, Chennai, Tamil Nadu, India
[2] Centre of Excellence in Biochemical Sensing and Imaging Technologies (CenBioSIm), Indian Institute of Technology Madras, Chennai, Tamil Nadu, India

**e-mail: ph19d201@smail.iitm.ac.in*

ABSTRACT

Fluoride-based materials with trivalent yttrium cations doped with rare earth ions are the most widely studied upconversion systems. Their convenient lattice structure and high photoluminescence (PL) quantum yield are suitable for optical and optoelectronic applications [1,2]. In this work, we have synthesized Cr^{3+} doped $NaYF_4:Er^{3+}/Yb^{3+}$ upconversion nanophosphors using a hydrothermal method. Structural and optical characterizations were conducted on the samples to study the effects of Cr^{3+} doping. Upconversion PL study conducted under 980 nm laser excitation showed a drastic increase in green luminescence. Temperature dependent PL study revealed the high sensitivity of PL making it a promising candidate for temperature sensing application.

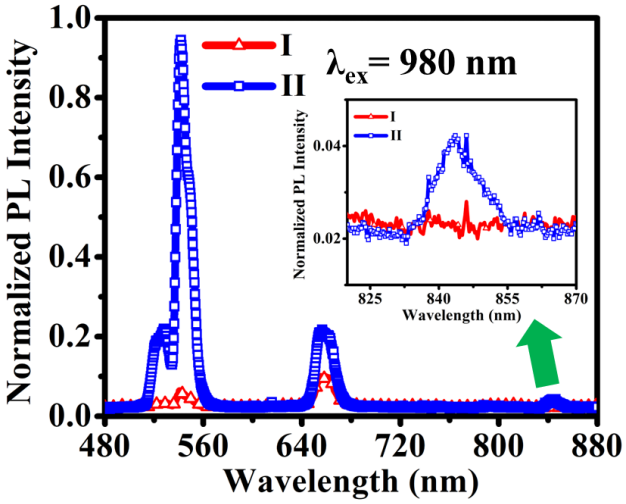

Figure 1: : Upconversion photoluminescence of (I)$NaYF_4:Er^{3+}/Yb^{3+}$ and (II) $NaYF_4:Er^{3+}/Yb^{3+}/Cr^{3+}$(15%) nanophosphors under fs laser excitation at 980 nm. Inset shows an expanded representation between 820 nm to 870 nm.

References:

[1] P. Huang et al., Angewandte Chemie International Edition, vol. 53, no. 5, pp. 1252–1257, Jan. 2014, doi: https://doi.org/10.1002/anie.201309503.

[2] C. Wang and X. Cheng, J Alloys Compd, vol. 649, pp. 196–203, 2015, doi: https://doi.org/10.1016/j.jallcom.2015.07.024.

P23

Development of a Cost-Effective In-House Circular Dichroism Spectroscopy Setup

Keerthana C, Anandajith T S, Khashiya Khalid and Amrita Dey*
Department of Physics, School of Advanced Sciences, Vellore Institute of Technology (VIT)
Vellore, 632014, TN, India
*Email: amritadey@vit.ac.in

Circular dichroism (CD) spectroscopy is used to study the chiral optical responses in materials by comparing their interaction with left- and right-circularly polarized light. CD spectroscopy is mostly known for its application in protein and biomolecular studies [1]. Nowadays growing interest in chiral-semiconductor research has driven its use in understanding and controlling chirality in materials such as chiral-perovskites [2][3]. Probing chirality in these systems is important for the development of advanced polarization sensing, and spin-photonic devices [4]. CD measurements provide insights into optical controls of spin-states in chiral semiconductor. Nevertheless, the available CD spectrometers are often costly and offer limited flexibility for customization, which can restrict their use in laboratory-scale chiral-semiconductor characterizations. In this work, we develop a cost-effective, home-built circular dichroism spectroscopy setup using waveplates, polarizer combination with lock-in amplifier. The CD spectroscopy measures the difference between absorbance of left and right circularly polarized light ($\Delta A = A_L - A_R$) when it passes through the sample. To create a circularly polarized light our optical arrangement setup has a xenon lamp coupled with a monochromator, objective lenses, a linear polarizer, and a quarter-wave plate to generate left- and right-circularly polarized light. Now the circularly polarized light transmitted through the sample is detected using a photodetector and processed with lock-in amplification to improve the signal-to-noise ratio. The CD response is obtained from the differential absorbance calculated from the measured transmittance spectra. This simple and flexible in-house CD spectrometer provides an accessible platform for studying chiral optical properties in optoelectronic and chiral-materials research.

References

[1] A. S. Ladokhin, M. Fernández-Vidal, S. H. White, J. Membr. Biol. 236, 247 (2010).

[2] Y. Dong, Y. Zhang, X. Li, Y. Feng, H. Zhang, J. Xu, Small 15, 1902237 (2019).

[3] G. Long, R. Sabatini, M. I. Saidaminov, G. Lakhwani, A. Rasmita, X. Liu, E. H. Sargent, W. Gao, Nat. Rev. Mater. 5, 423 (2020).

[4] Q. Wei, Z. Ning, ACS Mater. Lett. 3, 1266 (2021).

P24

Abstract template for … Activity Title …

First A. Author [1] , Second B. Author [1,2] , and Third C. Author [2]

[1](Presenting author underlined) Affiliation 1
[2] Affiliation 2

This document is the template for contributed abstracts (posters and/or talks) and gives the guidelines for preparing and submitting abstracts for the *Activity Title* to be held online from *start_date* to *end_date*.
The maximum length of the abstract is one page, including references. When preparing the abstract in a Word processor, please use the standard A4 document with the size definitions as in this template. Please follow the template for the structure of the abstract, formatting its elements including capitalizing the title, spacing between the elements, etc. Use superscripts for relating authors to multiple affiliations. Format references [1, 2] as shown below.
Convert your abstract to **PDF format** for submission. The PDF file should be uploaded in the "Upload Abstract" field with the on-line application form.

[1] A. Author, B. Coauthor, J. Sci. Res. **13**, 1357 (2012).
[2] A. Author, B. Coauthor, J. Sci. Res. **17**, 7531 (2013).

P25

Microscopic Origins of O–H Stretching Raman Features in Aqueous LiCl Solutions

Diganta Dasgupta[1,2], **Cesare Malosso**[3], **Chun-Ting Lin**[4], **Ali Hassanali**[1], **Giovanni Bussi**[2], **Paul Cremer**[4]

[1]*The Abdus Salam International Centre for Theoretical Physics (ICTP)*
[2]*Scuola Internazionale Superiore di Studi Avanzati (SISSA)*
[3] *École Polytechnique Fédérale de Lausanne (EPFL)*
[4] *The Pennsylvania State University (PennState)*

Raman spectroscopy in the O–H stretching region (3000–4000 cm^{-1}) provides a sensitive probe of hydrogen-bonding heterogeneity and ion-induced perturbations of water structure in concentrated electrolyte solutions, yet its interpretation is hindered by strongly overlapping vibrational features. While spectroscopic mapping frameworks linking local hydrogen-bonding environments to vibrational frequencies have been established for neat water and ice, most notably by the Corcelli and Skinner groups[1], an analogous, quantitatively validated map for electrolyte solutions remains absent, underscoring a key gap in the molecular-level description of ion–water interactions.

Raman spectra were experimentally measured for aqueous LiCl solutions over a broad concentration range spanning 0.5 to 9.5 M and analyzed via Multivariate curve resolution (MCR) to separate bulk-like water contributions from solute-correlated hydration environments[2]. The solute-correlated component exhibits structural heterogeneity and may further be decomposed using a Gaussian mixture model comprising multiple spectral features associated with distinct hydrogen-bonding motifs. To elucidate the molecular origins of these features and construct a structure–spectra map, theoretical Raman spectra were computed via harmonic normal mode analysis[3] of representative ion–water clusters spanning contact ion pairs, solvent-shared ion pairs, and solvent-separated ion pairs. Comparison between cluster-based spectra and the deconvoluted Raman components establishes a direct correspondence between specific spectral features and progressively weakened hydrogen-bonding environments driven by increasing ion proximity and coordination complexity.

[1] Baiz et al., Chem. Rev. **2020**, 120, 15, 7152–7218.
[2] Perera et al., J. Phys Chem B. **2009** Feb 19;113(7):1805-9.
[3] Neugebauer et al., J. Comput. Chem., **2002**, 23, 895–910.

P26

Superior OER selectivity in bifunctional amorphous cobalt phospho-boride for electrocatalytic seawater splitting

Kishan H. Mali[1], **B.R. Bhagat**[1], **and Alpa Dashora**[*1]

[1] *Department of Physics, Faculty of Science, The M.S. University of Baroda, Vadodara, 390002, India*

[*] *e-mail: dashoralpa@gmail.com*

Utilization of seawater for electrocatalytic water splitting to produce hydrogen and oxygen is a promising yet challenging pathway toward sustainable energy. Conventional water splitting is limited by the scarcity of freshwater resources at large scale, making seawater electrolysis a highly desirable alternative. However, this process requires robust, cost-effective catalysts capable of withstanding the harsh, corrosive environment of seawater—particularly at the anode, where high selectivity for the oxygen evolution reaction (OER) is essential. A significant challenge is the competing oxidation of chloride (Cl^-) ions into various chlorine species, which varies with pH. In this work, we investigated the catalytically active sites of amorphous cobalt phospho-boride, modelled using Car-Parrinello molecular dynamics (CPMD)[1, 2] simulations within the QUANTUM ESPRESSO[3] code. Furthermore, we studied the modulation of active sites through phosphorus incorporation. DFT calculations reveal that phosphorus plays a critical role in optimizing the binding of reaction intermediates by enriching the electron density at the active sites. This mechanism was confirmed through charge transfer and electron localization function (ELF) analyses. These electronic modifications facilitate the OER with high selectivity, providing a sufficient thermodynamic window to suppress the evolution of chlorine-based species. Experimental validation demonstrated low overpotentials of ≈270 mV for the hydrogen evolution reaction (HER) and ≈410 mV for OER, achieving a current density of 2 $A.cm^{-2}$ at an overall voltage of 2.5 V in highly alkaline natural seawater. These results demonstrate the catalyst's potential for practical, large-scale seawater splitting[4].

[1] R. Car, M. Parrinello, Phys. Rev. Lett. 55, 2471 (1985).

[2] K. Laasonen, A. Pasquarello, R. Car, C. Lee, D. Vanderbilt, Phys. Rev.B 47, 10142 (1993).

[3] P. Giannozzi, S. Baroni, N. Bonini, M. Calandra, R. Car, C. Cavazzoni,D. Ceresoli, G. L. Chiarotti, M. Cococcioni, I. Dabo, A. Dal Corso,S. de Gironcoli, S. Fabris, G. Fratesi, R. Gebauer, U. Gerstmann,C. Gougoussis, A. Kokalj, M. Lazzeri, L. Martin-Samos, N. Marzari,F. Mauri, R. Mazzarello, S. Paolini, A. Pasquarello, L. Paulatto, C.Sbraccia, S. Scandolo, G. Sclauzero, A. P. Seitsonen, J. Phys. Condens.Matter 21, 395502 (2009).

[4] R. Silviya, A. Bhide, S. Gupta, R. Bhabal, K.H. Mali, B.R. Bhagat, M. Spreitzer, A. Dashora, N. Patel and R. Fernandes, Small Methods 8(8), 2301395 (2024).

P27

"Impact of external strain on electron–phonon coupling strength in SnTe pseudo-monolayer " - co-author with Rajdip Bandyopadhyay .

P28

Decoding Aerosol Surface Chemistry: Insights from XPS Spectra via DFT and Machine Learning

Mandira Das[1*], Abdurrahman Adhyatma[1], Jack Lin[2], Nønne Prisle[2], Milica Todorović[1]
[1]Materials Informatics Laboratory, University of Turku, Vesilinnantie 5, Turku 20500, Finland
[2]Center for Atmospheric Research (ATMOS), University of Oulu, Pentti Kaiteran katu 1, 90570 Oulu, Finland

Aerosols, which are nano- to microscale particles suspended in the air, have a significant influence on climate, weather, health, and ecology. The size and composition of aerosol particles determine their interactions with atmospheric compounds. Among these, Sodium Chloride (NaCl) is the most abundant aerosol particle. Surface-sensitive Ambient Pressure X-ray Photoelectron Spectroscopy (APXPS) has revealed that NaCl aerosol particles undergo structural transformations depending on atmospheric humidity levels [1]. However, understanding the surface atomic arrangement that governs the interaction of NaCl aerosols with the atmosphere under humid conditions remains an ongoing challenge.

To address this challenge, we employ Bayesian Optimization Structure Search (BOSS) [2] code combined with DFT to model the adsorption geometry of atmospheric water on the NaCl aerosol surface. BOSS code samples various configurations of atmospheric water on aerosol surfaces, enabling the learning of adsorption energy landscapes. Once the adsorption geometry is optimized, we apply the Δ self-consistent field (ΔSCF) [3] approach to compute the core electron binding energy of the Na 1s electron in NaCl aerosol particles. By comparing the Na 1s binding energy before and after atmospheric water adsorption, we can interpret changes in experimental XPS spectra under humid conditions.

This study leverages ML-driven DFT to reveal atomic-scale interactions between aerosols and atmospheric water, providing insights into APXPS data. Additionally, it serves as a framework for exploring interactions between aerosols and more complex atmospheric compounds.

References

1. Lin, J. J *et. al.,* Pre - deliquescent water uptake in deposited nanoparticles observed with in situ ambient pressure X-ray photoelectron spectroscopy, Atmos. Chem. Phys., 21, 4709–4727
2. Järvi, J. *et. al.*, Detecting stable adsorbates of (1*S*)-camphor on Cu (111) with Bayesian optimization, Beilstein J. Nanotechnol. **2020,** 11, 1577–1589
3. Kahk, J. M. *et. al.*, Core Electron Binding Energies in Solids from Periodic All-Electron Δ- Self-Consistent-Field Calculations, J. Phys. Chem. Lett. 2021, 12, 9353−9359

Dual modifications of graphitic carbon nitride nanostructures for enhanced photoelectrochemical performance

Siddhant Deshpande , Mohit Jatoliya , Vijay Kumar , and Rajendra C. Pawar

Central University of Rajasthan, Ajmer, India-305817.

Graphitic Carbon Nitride (g-CN) materials have been utilized in a wide range of photocatalytic and photoelectrocatalytic applications due to tuneable bandgap, high surface area and excellent chemical stability [1]. Along with strong photo-response in the visible light region, these features position g-CN as an effective and versatile photocatalytic material.

In this work, g-CN was synthesized using facile wet-chemical routes, specifically reflux and hydrothermal methods, followed by thermal polycondensation through sintering, to obtain the final sample. Scanning electron microscopy (SEM) was utilized to study the morphology of the as-synthesized g-CN, wherein predominantly a bulk-like structure was observed.

Chemical and surface modifications were performed with the addition of surfactants like polyvinylpyrrolidone (PVP) and Ascorbic Acid (AA) in the reaction solution, to overcome the limitations of bulk morphology [2]. The successful modifications of g-CN surface were confirmed with the help of Fourier transform infrared spectroscopy (FTIR), where the presence of added functional groups was demonstrated.

These surface modifications led to superior photo-response of the material when compared to the unmodified bulk material. To further enhance the photoresponsivity and photocatalytic performance, several heterojunction strategies like S-scheme were also employed, with the aim of reducing charge carrier recombination and enhancing light absorption range. With these surface modifications and strategies to improve interfacial charge transfer, the as-synthesized materials are suitable for several applications like photocatalytic dye degradation, photoelectrocatalytic water splitting and photodetection.

[1] Michael Volokh et. al., Angew. Chem. Int. Ed. **58**, 6138 (2019).

[2] Xiaonan Yang et. al., International Journal of Hydrogen Energy **46**, 38310 (2021).

P30

The Abdus Salam International Centre for Theoretical Physics

IAEA International Atomic Energy Agency

unesco United Nations Educational, Scientific and Cultural Organization

Solar Cells

Molecular Engineering of Mono and Di -Anchoring Metal Free Organic Sensitizers Containing Electron Deficient Entity for Dye Sensitized Solar Cells (DSSCs)

Mulu Berhe Desta,[a,b] *Sumit Chaurasia,*[a] *Jiann T. Lin*[a]

[a]Institute of Chemistry, Academia Sinica, Nankang, Taipei

[b]Department of Chemistry, Mekelle University, Mekelle

Email: muller.desta@yahoo.com

Introduction

Solar Cells

Dyes for possible application in Dye Sensitized Solar Cells

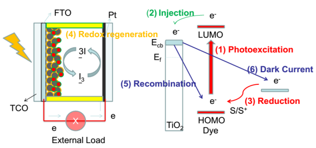

$$S + h\nu \longrightarrow S^* \quad (1)$$

$$S^* \longrightarrow S^+ + e^- \quad (2)$$

$$2S^+ + 3I^- \longrightarrow 2S + I_3^- \quad (3)$$

$$I_3^- + 2e^- (Pt) \longrightarrow 3I^- \quad (4)$$

$$S^+ + e^- \longrightarrow S \quad (5)$$

$$I_3^- + 2e^- (TiO_2) \longrightarrow 3I^- \quad (6)$$

Scheme 1. Electron transformation mechanism in DSSCs

Revised Y-shaped Di-anchoring Sensitizers for Dye Sensitized Solar Cells based on Benzimidazole Core

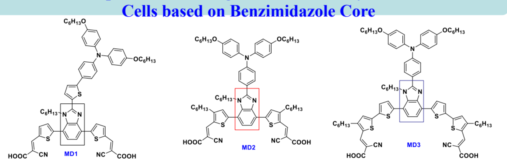

Scheme 2. Molecular structure of **MD** dyes

Photophysical and Electrochemical properties

Table 1. Photophysical and electrochemical of the dyes)

Dye	λ_{abs} (ε M^{-1} cm^{-1})[a] [nm]	λ_{abs}[b] [nm]	E_{ox} ($\triangle E_p$)[c] [mV]	HOMO/LUMO[d] [eV]	E_{ox} (V) [vs. NHE][e]	E^*_{ox}(V) [vs NHE][f]	E_{0-0}[g] [eV] λ (nm)
MD1	417 (37847)	443	272 (114)	5.07/3.23	1.04	−1.02	2.06 (602)
MD2	451 (34330), 344 (23970)	438	348 (116)	5.15/2.93	1.12	−1.10	2.22 (558)
MD3	488 (48100), 345 (33677)	448	352 (121)	5.15/3.05	1.12	−0.98	2.10 (590)

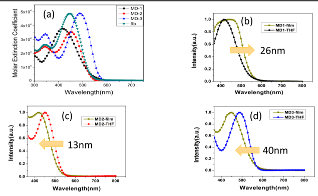

Fig.1. Absorption spectra of **MD1** –**MD3** dyes dissolved in THF (a) and on mesoporous TiO_2 film (b, c,d)

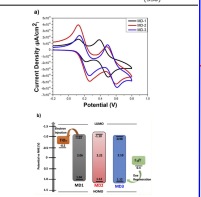

Fig.2. Cyclic voltammograms (a) and energy level diagram (b) of **MD1-MD3**

Photovoltaic Properties

Table 2: Photovoltaic parameters of **MD1 – MD3** dyes with and without CDCA co-adsorbent

Dye	CDCA	J_{SC} (mA cm^{-2})	V_{OC} (V)	FF	η (%)	Dye loading (~10^{-7} mol cm^{-2})
MD1	0	9.68 ± 0.12	0.733 ± 0.004	0.65 ± 0.01	4.74 ± 0.03	10.0
	3	11.73 ± 0.11	0.764 ± 0.001	0.54 ± 0.01	4.81 ± 0.01	
MD2	0	9.11 ± 0.09	0.711 ± 0.002	0.66 ± 0.01	4.49 ± 0.03	6.0
	3	9.82 ± 0.07	0.721 ± 0.001	0.67 ± 0.01	4.57 ± 0.02	
MD3	0	12.53 ± 0.13	0.752 ± 0.005	0.66 ± 0.01	6.45 ± 0.06	15.0
	3	14.21 ± 0.11	0.774 ± 0.003	0.65 ± 0.01	6.69 ± 0.03	
9b	0	11.32 ± 0.12	0.755 ± 0.005	0.69 ± 0.01	6.02 ± 0.07	13.0
	3	11.54 ± 0.10	0.743 ± 0.003	0.70 ± 0.01	6.11 ± 0.03	
N719		15.53 ± 0.15	0.740 ± 0.003	0.68 ± 0.01	7.76 ± 0.04	

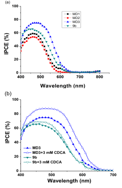

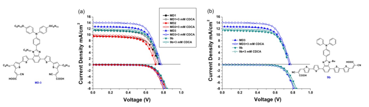

Fig. 3. Current density-voltage and IPCE curves measured at 100 mW cm^{-2} of the DSSCs based on dyes **MD1** – **MD3**

Electrochemical impedance spectra (Nyquist plots)

Dye	PCE [%]	V_{oc}[mv]	R_{rec} [Ω]	J_{sc}[mA cm^2]	FF	Dye loading
MD3	6.45±0.06	752	327	12.53±0.13	0.66±0.01	15.0
9b	6.02±0.07	750	292	11.32±0.12	0.69±0.01	13.0
MD1	4.74±0.03	733	243	9.68±0.12	0.65±0.01	10.0
MD2	4.49±0.03	711	157	9.11±0.09	0.66±0.01	6.0

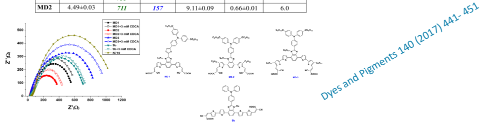

Fig. 4. Nyquist plots of DSSCs based on dyes **MD1** – **MD3** measured in the dark

Pyrazine-Incorporating Panchromatic Sensitizers for Dye-Sensitized Solar Cells under One Sun and Dim Light

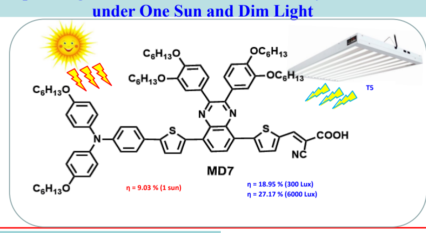

Photophysical and Electrochemical properties

Table 3. Electro-optical parameters of **MD** dyes

Dye	λ_{abs} [nm]	ε [M^{-1} cm^{-1}]	λ^{film}_{abs} [nm]	λ^{film}_{onset} [nm]	E_{ox}(V) [vs. NHE]	E_{ox}*(V) [vs. NHE]	E_{0-0}[eV] (λ nm)
MD4	427, 633	33832, 32231	613	800	1.03	-0.73	1.76 (705)
MD5	356, 513	41667, 37998	498	630	1.13	-0.97	2.10 (590)
MD6	420, 642	40188, 26210	629	815	1.00	-0.74	1.74 (713)
MD7	365, 532	47545, 39360	524	660	1.02	-0.99	2.01 (615)

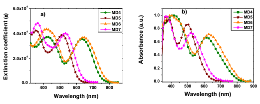

Fig.5. Absorption spectra of **MD** dyes dissolved in THF (a) and on mesoporous TiO_2 film (b)

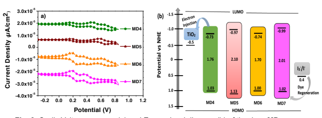

Fig. 6. Cyclic Voltammograms (a) and Energy-level diagram (b) of the dyes **MD**

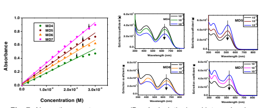

Fig. 7. Absorption spectra vs conc. (Beer's deviation) and intermolecular interaction at different conc. of **MD** dyes in THF solution

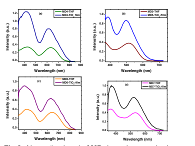

Fig.8. Absorption band of **MD** dyes chemosorbed onto the surface of TiO_2 films vs **THF**

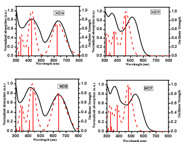

Fig. 9. Comparison between experimental (black) and calculated (red) absorption spectra of the **MD** dyes in THF

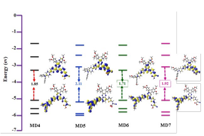

Fig. 10. Calculated HOMO-LUMO gaps and respective HOMO-LUMO orbitals of the **MD** dyes in THF

Photovoltaic Properties

Table 4: Photovoltaic parameters of **MD** dyes under one sun (100 mW cm^{-2})

dye	η %	V_{OC} V	J_{SC} mA cm^{-2}	FF	R_{rec} Ω	τ_{rec} ms	DL 10^{-7}mol cm^{-2}
MD4	3.92	0.631	9.56 (8.13)	0.65	112		1.29
MD4*	4.58	0.687	10.11 (8.65)	0.66			1.01
MD6	5.08	0.695	11.25 (9.85)	0.65	136	12.75	2.81
MD6*	5.26	0.700	11.58 (10.16)	0.65			2.02
MD5	7.88		16.50 (15.05)	0.67	163	19.41	3.10
MD5*	8.39	0.727	**17.16** (15.67)	0.67			2.12
MD7	8.22	0.719	17.12 (15.78)	0.67	172	37.91	5.03
MD7*	9.03	0.753	17.65 (16.28)	0.68			4.51
N719	8.87	0.745	17.50	0.68	204		

Table 5: Photovoltaic parameters of **MD** dyes under room light (0.1960 $mWcm^{-2}$)

dye	illuminance Lux	irradiance mW cm^{-2}	Voc mV	Jsc µA cm^{-2}	FF %	η %
MD5	300	0.09	543.26	33.47	77.24	15.10
	600	0.18	568.20	67.95	77.73	16.49
	900	0.27	586.23	104.61	78.04	17.38
	6000	1.7	651.16	762.13	79.01	23.17
MD7	300	0.09	572.67	40.92	75.85	18.95
	600	0.18	596.77	81.80	76.59	20.16
	900	0.27	611.89	124.33	76.83	21.10
	6000	1.7	676.32	913.69	76.42	27.17
N719	300	0.09	550.53	41.48	75.34	19.02
	600	0.18	582.94	82.17	75.72	20.23
	900	0.27	597.55	126.06	75.72	20.94
	6000	1.7	676.37	923.38	75.85	27.64

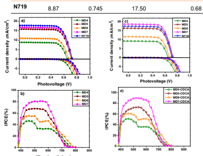

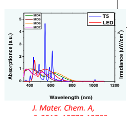

J. Mater. Chem. A, 6, 2018, 13778-13789

Fig. 11. Current density-voltage (a, c) and IPCE spectra (b, d) for the DSSCs based on the dyes **MD**

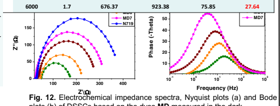

Fig. 12. Electrochemical impedance spectra, Nyquist plots (a) and Bode plots (b) of DSSCs based on the dyes **MD** measured in the dark

Conclusions

In our first project we started working on Benzimidazole based di-anchoring (D-(π-A)$_2$) dyes. Since these dyes showed a blue shifted absorption, another interesting electron deficient entity D−π−A'−π−A framework mono-anchoring pyrazine based organic dyes were chosen as a building block. The new **MD** sensitizers showed a red-shifted absorption band ranging over 600 nm to the NIR region and a maximum PCE using CDCA co-adsorbent (9.03 %) which surpassed **N719**-based standard DSSC (8.92 %) under 1.0 sun and that of dim light reaches 18.95% under 300 lux and 27.17% under 6000 lux irradiance.

References

1. Velusamy, M.; Thomas, K. R. J.; Lin, J. T.; Hsu, Y.-C.; Ho, K.-C. *Org. Lett.*, **2005**, *7*, 1899–1902.

2. Chaurasia, S.; Hung, W.I.; Chou, H.-H.; Lin, J. T. *Org. Lett.*, **2014**, *16*, 3052−3055.

3. Chaurasia, S.; Hsu, C.Y.; Chou, H.-H.; Lin, J. T. *Org. Electron..*, **2014**, *15*, 378−390.

4. Mulu, B.D; Chaurasia, S.; Lin, J. T. Dyes and pigments, **2017**, *140*, 441−451.

Acknowledgment

We thank the Academia Sinica and Ministry of Science and Technology (MOST), Taiwan (MOST 104-2113-M-001-009-MY3), for financial support, and the Instrumental Center of Institute of Chemistry (IoC)

P31

Porous Fe-MOF as an Advanced Energy Material for High-Performance Supercapacitors Electrode

Nisha Devi [1], Prakash Chand[1]

[1]Department of Physics, National Institute of Technology, Kurukshetra-136119 Haryana, India

The escalating global energy crisis, coupled with environmental challenges arising from the extensive use of fossil fuels, has created an urgent need for sustainable and efficient energy storage systems. In this context, supercapacitors have emerged as a promising device. The choice of electrode material largely dictates the performance of supercapacitors. Metal-organic frameworks (MOFs) have emerged as promising electrode materials for next-generation energy storage devices due to their high porosity, large surface area, and abundant electrochemically active sites. These features facilitate efficient charge storage and rapid ion transport, which are essential for high-performance supercapacitors. In this study, we report the synthesis of an iron-based metal-organic framework (Fe-MOF) via a controlled hydrothermal approach, utilising DMF solvent to achieve a highly crystalline and porous structure. Structural and morphological characterisation by X-ray diffraction (XRD) and scanning electron microscopy (SEM) analysis confirmed the successful formation of the Fe-MOF with a well-defined porous network. Electrochemical evaluation in a three-electrode configuration demonstrates that the Fe-MOF electrode exhibits good specific capacitance and pseudocapacitive behaviour, indicative of effective charge storage facilitated by the redox-active framework and high surface area. The electrode also shows excellent rate capability and stable cycling performance, reflecting its suitability for long-term supercapacitor operation. The enhanced performance is attributed to the synergistic combination of redox-active Fe centres and the extended porous structure, which promotes rapid ion diffusion and efficient charge storage. These findings suggest that the synthesised Fe-MOF holds great potential as a high-performance electrode material for supercapacitor applications, contributing to the development of sustainable and efficient energy storage devices.

[1] Darabi, R., Karimi-Maleh, H., Zhong, N., & Karimi-Harandi, M. H. *Electrochimica Acta*, *480*, 143871 (2024).

[2] Zaka, A., Iqbal, M. W., Afzal, A. M., Hassan, H., Rafique, H., Wabaidur, S. M., ... & Elahi, E. *RSC Advances*, *13*(38), 26528-26543 (2023).

[3] Ramasubramanian, B., Chinglenthoiba, C., Huiqing, X., Xiping, N., Hui, H. K., Valiyaveettil, S., ... & Chellappan, V. *Surfaces and Interfaces*, *34*, 102397 (2022).

P32

Cu^{2+} Driven Localized Band Formation and Photoluminescence Excitation Splitting in Low Symmetry $Cs_2NaBiCl_6$ Double Perovskite

Anandajith T S [1], Vijayalakshmi P.[1] and Amrita Dey [1*]

Email ID: amritadey@vit.ac.in

Department of Physics, School of Advance Sciences, Vellore Institute of Technology (VIT) Vellore, 632014

Lead-free halide double perovskite (HDP) have attracted great attention as a non-toxic alternative of lead halide perovskites, targeted towards solar energy conversion devices. [1,2] Nevertheless, the major challenge with HDP remains its wide bandgap and low photoluminescence quantum yield which limits their applications.[3] Here, we report Cu^{2+} induced electronic modulation in low symmetry $Cs_2NaBiCl_6$ nanocrystals, synthesized using ligand assisted reprecipitation method. These crystals exhibit orthorhombic Pmmm phase, as compared to the commonly observed Fm-3m phase for $Cs_2NaBiCl_6$.

All our nanocrystals exhibit a pronounced optical absorption peak around 330 nm, corresponding to partially allowed $^1s_0 \rightarrow {}^3p_1$ transition. Upon Cu^{2+} incorporations, we observe a broad optical absorption shoulder emerges at ~390 nm, attributed to dipole forbidden $^1s_0 \rightarrow {}^3p_0$, transition. Though, electronically forbidden ($^1s_0 \rightarrow {}^3p_0$), excitation at 400 nm results into a broad green emission band centred around 515 nm. The emission spectra from both doped and undoped samples have two gaussian contribution in the emission spectra. Their photoluminescence excitation origin is attributed to $^1s_0 \rightarrow {}^3p_1$ and $^1s_0 \rightarrow {}^3p_0$ transitions. Both these, the photoluminescence excitation bands reveal pronounced splitting upon Cu^{2+} doping while the intrinsic $Cs_2NaBiCl_6$ exhibit broad excitation bands. In the intrinsic $Cs_2NaBiCl_6$ host lattice, strong Bi-centred spin-orbit coupling renders the $^1s_0 \rightarrow {}^3p_1$ transition weakly allowed and strongly coupled to lattice vibrations, leading to vibronically broadened excitation and subsequent self-trapped exciton (STE) formation. Upon Cu^{2+} incorporation, localized Jahn-Teller-active Cu-3d states introduce additional ligand-to-metal charge-transfer pathways and impose static and dynamic local symmetry breaking. These effects lift the degeneracy of the excited-state manifold and enhance electron–phonon coupling, resulting in a resolvable multi-component PLE profile.

References:

1. Abhoy Karmakar,† Mya S. Dodd,† Satyam Agnihotri,† Enrico Ravera,‡,§ and Vladimir K. Michaelis*,†,American Chemical Society (2018).

2. Tamilselvan Appadurai, ‡ Sanket Chaure,‡ Maruthi Mala, and Aravind Kumar Chandiran* Energy Fuels 2021,35,11479−11487.

3.Neelu Neelu 1 , Nivedita Pandey 1 , Subhananda Chakrabarti*, Optical Materials,143 (2023) 114250.

P33

Double transition metal MXenes as anode materials for high-capacity multivalent metal-ion batteries: a computational study

Tuya Dey[1], Bikash Chandra Gupta[1], and Jagadish Chandra Mahato[1]

[1]Department of Physics, Visva-Bharati, Santiniketan 731235, West Bengal, India

The growing global energy crisis and increasing demand for sustainable energy storage solutions have intensified the search for the efficient and high-capacity battery technologies. Conventional lithium-ion batteries, although widely used, face challenges of resource scarcity, limited energy density, and environmental concerns. As a promising alternative, multivalent metal-ion (Mg^{2+}, Zn^{2+}, and Al^{3+}) batteries offer higher charge storage capabilities and improved cost-effectiveness compared to monovalent (Li^{+}, Na^{+}, and K^{+}) metal-ion batteries [1, 2]. Here, we explore the potential of double transition metal (DTM) MXenes, namely, VNbC, VtaC, and NbTaC, as electrode materials for multivalent metal-ion batteries using density functional theory (DFT). Geometrical stability, electronic property, ion adsorption behavior, and electrolyte compatibility with popular electrolytes (ethylene carbonate ($C_3H_4O_3$), dimethyl carbonate ($C_3H_6O_3$), diethyl carbonate ($C_5H_{10}O_3$), and propylene carbonate ($C_4H_6O_3$)) are systematically analyzed to evaluate their electrochemical performance. Our results reveal that these MXenes exhibit excellent specific capacities of 3096.64, 2064.42, and 688.14 $mAhg^{-1}$ (VNbC); 1978.76, 1319.17, and 439.72 $mAhg^{-1}$ (VTaC); and 844.14, 1125.52, and 375.17 $mAhg^{-1}$ (NbTaC) for Al, Mg, and Zn, respectively. The estimated average open circuit voltage (OCV) values are 0.39, 0.37, 0.44 V for Al; 0.48, 0.47, 0.53 V for Mg; and 0.54, 0.54, 0.58 V for Zn on VNbC, VTaC, and NbTaC nanosheets, respectively. Additionally, we obtained low diffusion barriers of 0.26, 0.13, and 0.19 eV (on VNbC); 0.25, 0.10, and 0.16 eV (on VTaC); and 0.18, 0.06, and 0.16 eV (on NbTaC) for Al, Mg, and Zn, respectively using CI-NEB method. This study shows that the VNbC monolayer provides a much higher Al^{3+}-ion storage capacity than that of widely commercialized graphite in lithium-ion batteries. This investigation unearths key insights into the fundamental mechanisms governing ion intercalation in DTM MXene-based anodes, which is encouraging for their application in advanced rechargeable battery technologies.

[1] M. Zhou, Y. Shen et al., Vacuum **213**, 112150 (2023).
[2] T. Dey. B. C. Gupta, and J. C. Mahato, J. Mat. Chem. A **13**, 42101 (2025).

P34

Photon-Assisted Hydrogen Evolution using Cu-Fe Composite Photoelectrode

Saddam H. Dhobi[1*], Susmita Kafle[1], Santosh Kumar Das[1], Surendra Hangsarumba[1]
[1]*Department of Physics, Patan Multiple Campus, Tribhuvan University, Patandhoka, Nepal*
*Corresponding Authors: saddam@ran.edu.np

Abstract: Hydrogen gas has recently emerged as a promising alternative to conventional fossil fuels because it possesses many of the properties required for next-generation energy systems, including sustainability, environmental compatibility, economic feasibility, and high energy efficiency[1]. Global climate targets and increasing commitments to achieve net-zero emissions by as early as 2045/50s, hydrogen is widely recognized as a climate-neutral energy [2]. Among various hydrogen production pathways, photoelectrochemical water splitting using solar energy is considered one of the most environmentally friendly methods, requiring a minimum thermodynamic potential[3]. Electrodeposition and related synthesis routes are widely employed for photoelectrode preparation due to their low cost, simplicity, versatility, and scalability [5]. A $CuFeO_2$/CuO delafossite composite was synthesized on a copper substrate via a combustion reaction, and comprehensive characterization was performed to verify the formation and quality of the $CuFeO_2$/CuO/Cu photoelectrode [4].

The aim of this work is to preparation, characterization, and performance evaluation of the $CuFeO_2$/CuO/Cu composite photoelectrode for green hydrogen production using normal tap water as the electrolyte, with a pure Cu electrode. Hydrogen generation experiments were carried out at a constant applied voltage of 5 V under dark, normal room condition, sunlight (atmospheric condition), and filament bulb (40 W) illumination conditions. Under dark conditions, the composite photoelectrode exhibited hydrogen production approximately 9.6% lower than that of pure Cu, indicating that both electrodes show similar baseline electrochemical behavior in the absence of light. However, under room-light conditions, hydrogen production from the $CuFeO_2$/CuO/Cu electrode increased by approximately 11% compared to pure Cu, demonstrating its ability to utilize low-intensity ambient illumination. A more pronounced enhancement was observed under sunlight, where hydrogen production increased by approximately 28.4%, highlighting effective light absorption and improved charge separation within the $CuFeO_2$/CuO heterostructure. The highest improvement was achieved under filament bulb illumination, with a significant 35.5% increase in hydrogen production relative to the pure Cu electrode. The enhanced photoelectrochemical performance of the $CuFeO_2$/CuO/Cu electrode is attributed to improved light harvesting, efficient separation of photogenerated charge carriers, increased active reaction sites, and reduced recombination losses resulting from the $CuFeO_2$/CuO heterojunction. Hydrogen evolution was measured using the downward displacement of water method. This demonstrate that photon-assisted voltage stimulation can significantly enhance hydrogen generation efficiency while reducing energy consumption. This study highlights the strong potential of low-cost Cu/Fe-based photoelectrodes for sustainable, hydrogen production without storage requirements, offering a viable pathway toward green and pollution-free energy technologies.

Reference

[1] R. Solmaz, H. Yüksel, *Int. J. Hydrogen Energy* **44**, 14108 (2019).

[2] M. Wappler, D. Unguder, X. Lu, H. Ohlmeyer, H. Teschke, W. Lueke, *Int. J. Hydrogen Energy* **47**, 33551 (2022).

[3] Y. Bicer, G. Chehade, I. Dincer, *Int. J. Hydrogen Energy* **42**, 6490 (2017).

[4] A. Gondolini, N. Sangiorgi, A. Sangiorgi, A. Sanson, *Energies* **14**, 2942 (2021).

[5] N. M. A. Hadia *et al.*, *Catalysts* **13**, 456 (2023).

P35

Fingerprint Raman spectroscopy diagnosis for Gamma Radiolysis Synthesized Noble Metal Nanoparticles: A Green Synthesis Approach

E. Manikandan[1*], S. Balamurugan[1], M. Manikandan[1], K. Tharanikkarasu[2], and Siva Umapathy[3]

[1] Centre for Nanoscience & Technology, Pondicherry University, Puducherry–605014, India.
[2] Department of Chemistry, Pondicherry University, Puducherry–605014, India.
[3] Inorganic & Physical Chemistry, Indian Institute of Science, Bengaluru–560012, India.

The synthesis of noble metal nanoparticles with uniform size and morphology is critical for achieving reproducible surface plasmon resonance (SPR) properties, which underpin advanced sensing and diagnostic applications. In this study, gamma radiolysis is employed as a clean, controllable, and reagent-free method to synthesize uniform nanoparticles of gold (Au), silver (Ag), copper (Cu), and palladium (Pd). This radiolysis approach enables precise control over nucleation and growth, minimizes contamination, and ensures reproducibility. The resulting nanoparticles are systematically characterized using UV-visible spectroscopy, TEM, XRD, and Raman spectroscopy, with particular emphasis on correlating SPR absorption features with Raman diagnostic signatures, including surface-enhanced Raman scattering (SERS) effects. A comparative analysis of Au, Ag, Cu, and Pd nanoparticles reveals the influence of particle size, crystallinity, and defect structures on Plasmonic coupling and vibrational responses. This work establishes a direct link between gamma radiolysis-driven nanoparticle uniformity and Raman diagnostic performance, offering new insights into defect analysis, plasmonic enhancement, and biosensor design. The outcomes contribute to the development of next-generation diagnostic platforms that exploit SPR-active nanoparticles for sensitive, reproducible, and scalable biomedical applications.

[1] R. Gaur, E. Manikandan, et al. Plasmonics **16(5)**, 1461–1493 (2021).
[2] E. Manikandan, et al. Journal of Raman Spectroscopy. **52(11)**, 1838–1846, (2021).
[3] E. Manikandan, et al. Spectrochimica Acta Part A: Mol. Biomol. Spect. 124, 203–207, (2014).
[4] E. Manikandan, et al. Plasmonics. 2014, 9(3), pp. 637–643.

P36

Enhancement of Nanowire Solar Cells via Innovative Reinforcement Learning Optimization

R. El-Bashar[1,2], Mohamed Farhat. O. Hameed[2], Hamdy Abdelhamid[3], S. S. A. Obayya[2]

[1]National Institute of Laser Enhanced Sciences (NILES), Cairo University, Giza 12613, Egypt
[2]Nanotechnology and Nanoelectronics Engineering Program, Zewail City of Science and Technology, October Gardens, 6th of October City, Giza 12578, Egypt
[3]Electrical Engineering Department, College of Engineering and Information Technology, Ajman University, UAE

As technology has advanced, the number of parameters involved in system design has grown, making it increasingly difficult to identify optimal solutions. Optimization, a long-standing challenge, aims to find the best solution among many possibilities to maximize system efficiency, performance, and cost-effectiveness. Techniques have evolved from simple parametric sweeps to more sophisticated methods like genetic algorithms and Neuroevolution of Augmenting Topologies (NEAT) [1,2], as well as Particle Swarm Optimization (PSO), which has seen continued refinement over time [3,4]. In recent years, artificial intelligence—especially reinforcement learning (RL)—has emerged as a powerful optimization tool, capable of handling complex, multi-variable problems through continuous learning and adaptation to diverse operational environments [5,6]. This paper introduces a reinforcement learning (RL) optimization framework utilizing a neural network to design high-efficiency nanowire (NW) solar cells (SCs) with modified elliptical geometries. The proposed methodology features a 2×2 array of elliptical NWs with varying shapes to enhance design versatility and degrees of freedom. Initial validation through Finite Difference Time Domain (FDTD) simulations in Ansys/Lumerical achieved a short-circuit current density (Jsc) of 17.6 mA/cm² for a single NW with a 40 nm diameter. Integrating cylindrical NWs with varying diameters in a 2×2 array disrupted mirror symmetry, broadening guided resonances and increasing Jsc by 7.1% to 18.9 mA/cm². Further optimization introduced asymmetrical elliptical-shaped NWs within the 2×2 unit cell, resulting in Jsc improvements of 15.3% and 7% compared to single cylindrical NWs and varied cylindrical NWs, respectively. These findings highlight the RL-driven approach's capability to optimize NW geometries and achieve significant advancements in light absorption and SC efficiency.

References

[1] D. C. Fabry, E. Sugiono, and M. Rueping, "Self-optimizing reactor systems: algorithms, on-line analytics, setups, and strategies for accelerating continuous flow process optimization," Isr. J. Chem. **54**, 341–350 (2014).
[2] R. K. Mishra and R. Agarwal, "Impact of digital evolution on various facets of computer science and information technology," Digit. Evol. Adv. Comput. Sci. Inf. Technol. **17**, (2024).
[3] E. Garcia-Gonzalo and J. L. Fernandez-Martinez, "A brief historical review of particle swarm optimization (PSO)," J. Bioinforma. Intell. Control **1**, 3–16 (2012).
[4] El-Bashar, R., Hussein, M., Hegazy, S. F., Badr, Y., Hameed, M. F. O., "Efficient Silicon Nanowires Solar Cell," in *ACES2021OL-1263* (IEEE, 2021).
[5] M. Gautam, "Deep Reinforcement learning for resilient power and energy systems: Progress, prospects, and future avenues," Electricity **4**, 336–380 (2023).
[6] S. Stavrev and D. Ginchev, "Reinforcement Learning Techniques in Optimizing Energy Systems," Electronics **13**, 1459 (2024).

P37

Proton irradiation effects on perovskite solar cells: A critical review and future modifications

M.E. Emetere

[1] *Bowen University*
Iwo, Nigeria
Email: emetere@yahoo.com

Extended Abstract

Perovskite solar cells (PSCs) have emerged as promising alternatives for next-generation photovoltaic technologies due to their high efficiency, lightweight nature, and tunable bandgap. Their potential for space applications, however, raises critical concerns about resilience under proton irradiation. Most of the experimental proton irradiation effects on perovskite solar cells (PSCs) are intended for space applications and high-radiation environments. The chemistry of PSCs is complex depending on their stoichiometry. In the context of simulating perovskite performance for space applications and high-radiation environments, they are highly efficient and lightweight. However, when exposed to proton irradiation, they are faced with several unresolved challenges, such as soft ionic lattices, complex multilayer interfaces, and sensitivity to defect formation. Some of the challenges include lack of fundamental data on how proton energy/fluence alters perovskite defect structure, diffusion length, and carrier lifetime. This review critically examines experimental and theoretical studies on proton irradiation effects across various perovskite architectures, including single-junction, tandem (perovskite/Si and perovskite/CIGS), and all-inorganic compositions. The methodologies of the examined papers are shown in Table 1 below.

Table 1: Methodology of proton irradiation effect on perovskites

Proton energy	Cell type	Diagnostics	References
68 MeV	Perovskite; Silicon; CIGS	EL; EPR; EQE; IV; J-V; PL; SEM; TEM	[1]
1 MeV	Perovskite	EDS; EL; ELECTROLUMINESC; EPR; I-V; IV; JV; PL; SEM; SPECTROSC; TEM; XRD	[2]
4.5 MeV	Perovskite; Silicon; CIGS	EDS; EL; EPR; I-V; IV; MICROSCOP; PHOTOLUMINESC; PL; SEM; SPECTROSC; TEM	[3]
10 MeV	Perovskite; Silicon; GaAs/III-V; Triple-junction	EDS; EL; EPR; EQE; IPCE; IV; PHOTOLUMINESC; PL; SEM; SPECTROSC; TEM; TRPL; XPS; XRD	[4]
68 MeV	Perovskite; Silicon; GaAs/III-V; CIGS; Triple-junction	EDS; EL; ELECTROLUMINESC; EPR; EQE; I-V; IV; JV; MICROSCOP; PHOTOLUMINESC; PL; SEM; TEM; TRPL	[5]

1 MeV	Perovskite; Silicon; GaAs/III-V; CIGS; Triple-junction	EDS; EL; EPR; IV; PL; SEM; TEM	[6]
68 MeV	Perovskite; Silicon; GaAs/III-V	EL; EPR; I-V; IV; PL; SEM; TEM	[7]
1 MeV	Perovskite; Silicon	EDS; EL; EPR; I-V; IV; J-V; MICROSCOP; PHOTOLUMINESC; PL; SEM; SPECTROSC; TEM; TRPL	[8]
2.80 MeV	Silicon; GaAs/III-V; Triple-junction	DLTS; EDS; EL; ELECTROLUMINESC; EPR; EQE; I-V; IV; PL; SEM; SPECTROSC; TEM	[9]
30 MeV	Silicon	EDS; EL; EPR; I-V; IV; PL; SEM; TEM	[10]

Figure 1 shows that while PSCs demonstrate remarkable intrinsic tolerance to moderate proton fluences (up to ~10^{12} cm^{-2}), their long-term performance is limited by ion migration, interfacial degradation, and defect generation within soft ionic lattices. Comparative studies reveal that compositional engineering—such as partial substitution with cesium (Cs) and formamidinium (FA)—enhances lattice stability and reduces defect susceptibility. Moreover, in tandem architectures, degradation is often dominated by the more radiation-sensitive silicon or CIGS subcells, not the perovskite layer itself. Operando experiments further highlight dynamic processes of trap formation, partial recovery, and defect passivation. Collectively, these studies underline the need for interface engineering, standardized test protocols, and integrated radiation modeling to fully harness perovskites for high-radiation and space-based photovoltaic applications.

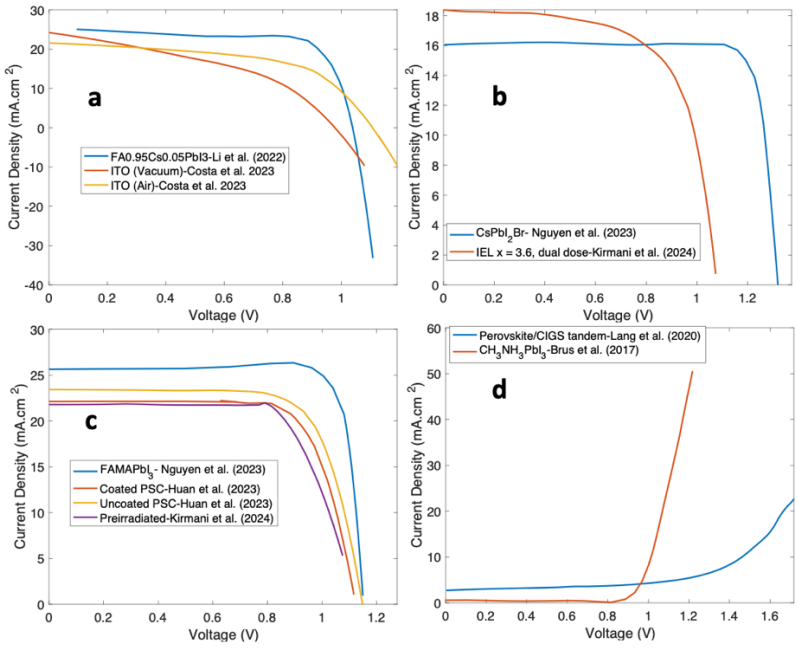

Figure 1: J-V curve for different proton irradiation effect on solar cell

This review establishes that perovskite solar cells possess significant radiation tolerance compared to conventional silicon or III–V solar cells, especially when optimized through compositional and interfacial engineering. Proton irradiation studies across energies from 1 MeV to 68 MeV consistently indicate that the perovskite absorber itself is not the weakest link; rather, device failure originates from charge-transport and recombination layers. Compositional strategies—such as employing $CsPbBr_3$ or $FAPbI_3$—have proven effective in mitigating defect formation and maintaining structural integrity under high fluence. In tandem configurations, the asymmetric degradation between perovskite and silicon subcells underscores the importance of designing radiation-hardened interfaces and passivation layers. Despite advances, the field still lacks standardized damage-dose frameworks and unified testing conditions, which hampers cross-comparison of results. Future research must integrate operando diagnostics, multi-energy proton exposures, and defect spectroscopy to provide a comprehensive understanding of radiation-induced processes. Through these coordinated efforts, PSCs can evolve from laboratory prototypes into reliable power sources for satellites and deep-space missions, combining low cost, high efficiency, and superior radiation resilience.

[1]. Brus Viktor V., Felix Lang, Jürgen Bundesmann, Sophie Seidel, Andrea Denker, Bernd Rech, Giovanni Landi, Heinrich C Neitzert, Jörg Rappich and Norbert H. Nickel, (2017). Defect Dynamics in Proton Irradiated CH3NH3PbI3 Perovskite Solar Cells, Advanced Electronic Materials, 3(2), 1600438, https://doi.org/10.1002/aelm.201600438

[2]. Costa Carla, Matthieu Manceau, Sophie Duzellier, Thierry Nuns, Romain Cariou. Perovskite solar cells under protons irradiation: From in-situ IV-monitoring to root cause degradation elucidation. Solar Energy Materials and Solar Cells, 2023, 257, pp.112388. 10.1016/j.solmat.2023.112388 . hal- 04113919

[3]. Erickson Samuel , Calista Lum, Katie Stephens, Mritunjaya Parashar, Darshpreet Kaur Saini, Bibhudutta Rout, Cheol Park, Timothy J. Peshek, Lyndsey McMillon-Brown, Sayantani Ghosh, (2025). Elucidating early proton irradiation effects in metal halide perovskites via photoluminescence spectroscopy,iScience, 28, 111586, https://doi.org/10.1016/j.isci.2024.111586.

[4]. Huan Zhenghao, Yifan Zheng, Kangpeng Wang, Zicai Shen, Wang Ni, Jifeng Zua and Yuchuan Shao (2024). Advancements in radiation resistance and reinforcement strategies of perovskite solar cells in space applications, J. Mater. Chem. A, 2024, 12, 1910

[5]. Lang, F., Jošt, M., Frohna, K., Köhnen, E., Al-Ashouri, A., Bowman, A. R., Bertram, T., Morales-Vilches, A. B., Koushik, D., Tennyson, E. M., Galkowski, K., Landi, G., Creatore, M., Stannowski, B., Kaufmann, C. A., Bundesmann, J., Rappich, J., Rech, B., Denker, A., Albrecht, S., … Stranks, S. D. (2020). Proton Radiation Hardness of Perovskite Tandem Photovoltaics. Joule, 4(5), 1054–1069. https://doi.org/10.1016/j.joule.2020.03.006

[6]. Nguyen Dang-Thuan, Daniel Walter, Klaus J. Weber, The Duong, Thomas P. White (2023). Simulating Proton Radiation Tolerance of Perovskite Solar Cells for Space Applications, Advanced Energy and Sustainability Research, 4(12), 2300085, https://doi.org/10.1002/aesr.202300085

[7]. Li, P.; Dong, H.; Lan, J.; Bai, Y.; He, C.; Ma, L.; Li, Y.; Liu, J. Tolerance of Perovskite Solar Cells under Proton and Electron Irradiation. Materials 2022, 15, 1393. https://doi.org/10.3390/ ma15041393

[8]. Kirmani, A.R., Byers, T.A., Ni, Z. et al. Unraveling radiation damage and healing mechanisms in halide perovskites using energy-tuned dual irradiation dosing. Nat Commun 15, 696 (2024). https://doi.org/10.1038/s41467-024-44876-1

[9]. Raya-Armenta, J. M., Bazmohammadi, N., Vasquez, J. C., & Guerrero, J. M. (2021). A Short Review of Radiation-Induced Degradation of III-V Photovoltaic Cells for Space Applications. Solar Energy Materials & Solar Cells, 233, Article 111379. https://doi.org/10.1016/j.solmat.2021.111379

[10]. Barrett M. J. and Stroud R. H. (1968). Proton-induced damage to silicon solar cell assemblies a state- of- the-art survey, JPL Contract 9.52246 pages 1-35

P38

The effect of co-sensitization between N719 dye and 1-phenylazo-2-naphthol on dye sensitized solar cell performance

Bruce Offei Kwaku Essah [1], Robert Kingsford-Adaboh [2], and Benjamin Agyei-Tuffour [3]

[1,2,3]*University of Ghana*

The quest for sustainable and affordable energy solutions has spurred extensive research into third-generation photovoltaic technologies, particularly Dye-Sensitized Solar Cells (DSSCs). DSSCs offer a promising alternative to traditional silicon-based solar cells, featuring low production costs, ease of fabrication, and relatively high performance under diffuse light conditions. Central to the performance of DSSCs is the dye sensitizer, which governs light absorption, charge injection, and electron transfer processes. Azo dyes, which incorporate azo (-N=N-) functional group present a compelling alternative. These dyes have emerged as attractive candidates due to their high molar extinction coefficients, tunable electronic structures, and the potential to enhance light-harvesting and redox properties. Despite these advantages, their application as DSSC sensitizers remains underexplored. The study advances the creation of sustainable and reasonably priced substitutes for ruthenium-based dyes and the development of next-generation solar systems based on scalable and reasonably priced materials. This research aims to synthesize, purify, and characterize 1-phenylazo-2-naphthol(1P2N). This compound was evaluated for their structural, photophysical, and electrochemical properties to improve light absorption, charge injection efficiency and dye regeneration with N719 dye. The synthesis of 1P2N involves design through diazotization, direct coupling and characterization (Melting point, UV-Vis, FT-IR, ^{1H} and ^{13}C NMR), the electrochemical analysis showing a HOMO value of -5.08eV and a LUMO Value of -3.02eV. Optical absorption of λmax for 1P2N were recorded at 310nm and 477 showing strong absorption in the visible region whilst N719 were 310nm,395nm and 535nm. DFT computational results, using Dmol^3 gave a prediction of a HOMO value of -4.34 and LUMO value of -2.80eV for 1P2N. A lower optical bad gap of 2.14eV and electrochemical band gap of 2.06eV was calculated. Preliminary findings from other studies indicate that the azo-based organic dye, which features DTP as an extended π-conjugated linker, has a power conversion efficiency of 6.91%, this suggest that 1P2N compound may be a useful co-sensitizer with N719 dye.

P39

Dynamic Modeling of Charge Carrier Transport and Recombination in Energy Conversion Materials: A System-Level Perspective

Maryam Farajpour [1]

Maryam Farajpour, (Ph.D. Candidate)

Abstract

Understanding charge carrier transport and recombination mechanisms is essential for improving the performance and reliability of energy conversion devices such as photovoltaics and photoelectrochemical cells. In this work, we present a dynamic, system-level modeling framework to analyze time-dependent charge carrier behavior under coupled physical processes, including transport, recombination, and external perturbations.

The approach integrates physics-based modeling with probabilistic and dynamic simulation techniques to capture transient phenomena and uncertainties that are often neglected in steady-state analyses. By resolving the temporal evolution of carrier populations and recombination pathways, the framework provides insights into performance degradation mechanisms and operational limits in complex energy materials.

The methodology is general and can be applied to a broad range of photophysical and photoelectrochemical systems, including single-junction and tandem photovoltaic structures. This work highlights the importance of interdisciplinary synergy between photophysics, photochemistry, and system-level modeling, and demonstrates how advanced dynamic analysis can support the design and optimization of next-generation renewable energy devices.

.

Affiliation:

Department of Nuclear Engineering, School of Mechanical Engineering, Shiraz University, Shiraz, Iran.

Email: maryam.farajpour@hafez.shirazu.ac.ir

P40

Probing Structural Dynamics of 6 -Methoxyflavone in Different Environments

Nisha Fatma[1]*, Sanjay Pant[1], M.S. Mehata[2]

[1]*Photophysics Laboratory, Department of Physics, DSB Campus, Kumaun University, Nainital 263002, Uttarakhand, India*

[2]*Laser-Spectroscopy Laboratory, Department of Applied Physics, Delhi Technological University, Delhi 110042, India*

**Email: - noornisha1287@gmail.com*

Abstract

Environment surrounding the probe reflects the changes in its photophysical behavior. The variations that most affect the fluorescence emission of a probe are usually related to changes in polarity, rigidity, or specific reactions with the fluorophore. Dynamics of solvation and specific interaction of the solute with solvent molecules are of utmost importance in context to elucidate the governing excited state process such as CT, hydrogen bonding, protonation etc. [1]. In the present study, an in-depth photophysical analysis of 6-Methoxyflavone (6MF), using steady-state spectroscopy and lifetime measurements across various solvents and polymers have been performed. Findings reveal that key spectral parameters are highly sensitive to both the polarity and hydrogen-bonding characteristics of the solvent. It has been observed that viscosity exerts a measurable influence on both the steady-state and time-resolved properties of 6MF. In aqueous solution, steady-state and transient data indicate the coexistence of hydrogen-bonded and protonated species. Meanwhile, in aprotic solvents, excitation-dependent spectral behavior appears to stem from conformational and geometrical changes in the molecule. These spectral features make 6MF an efficient probe for the detection of halides and acidic strength [2-3].

Furthermore, 6MF proves to be a sensitive sensor for polymer microenvironments: parameters like polarity, proticity, and free volume significantly affect its fluorescence. In synthetic polymers, whose heterogeneous environments serve as simplified models for more complex biological systems-organic molecules interactions, with these hosts often alter photophysical and photochemical behaviours. Such effects are directly tied to micro-environmental factors. These insights carry important implications for the development of advanced polymer-based materials, especially in photonics and electronics. As the demand grows for novel materials: such as organic thin-film transistors, memory devices, and increasingly miniaturized electronics, understanding and development of these micro-environmental effects becomes vital for innovation and integration.

[1]. N. Tiwari, Biologically significant probes in polymers: A photophysical study, Atulya Publications, First edition, **2017.**

[2]. N. Fatma, M. S. Mehata, N. Pandey, S. Pant, J. Photochem. Photobiol. A 404 (**2021**) 112945,

[3]. N. Fatma, S. Pant, N. Pandey, M. S. Mehata, Methods Appl. Fluoresc,11 (**2023**) 045002

P41

Investigating the adsorption mechanisms of CO_2 and N_2 on monolayer Nb2Se2C for efficient reduction reaction: A DFT sudy

C. Fwalo[1,2], A. Kochaev[3], and R. E. Mapasha[1]

[1] *Department of Physics, University of Pretoria, Pretoria, South Africa.*

[2]*Department of Physics, Copperbelt University, Kitwe, Zambia.*

[3]*Department of Silicon and Nanotechnologies, Ulyanovsk State University, Ulyanovsk, Russia.*

Greenhouse gas emissions, such as carbon dioxide and nitrous oxide, released during the combustion of fossil fuels, have been strongly linked to climate change effects, including prolonged droughts and floods. This connection has driven extensive research into carbon dioxide reduction reaction (CO_2RR) [1] and nitrogen reduction reaction (NRR) [2] strategies. These processes aim to convert CO_2 and N_2 into valuable carbon- and nitrogen-based products, such as fuels and chemicals. Consequently, the development of high-performance catalysts to enhance the efficiency of CO_2RR and NRR is very critical. In this regard, monolayers such as Nb_2Se_2C, with its unique and novel properties, is identified as promising candidate for catalytic applications.

In this study, we used density functional theory (DFT) implemented in quantum ESPRESSO code [3, 4] to investigate the adsorption mechanisms of CO_2 and N_2 on monolayer Nb_2Se_2C, aiming to enhance ORR efficiency while assessing the material's thermodynamic and structural stability. The adsorption systems of CO_2 and N_2 on monolayer Nb_2Se_2C were systematically optimized, followed by comprehensive calculations of all ORR-related properties. Our results revealed that monolayer Nb_2Se_2C exhibits excellent adsorption capabilities for both CO_2 and N_2, with relatively low overpotentials of 0.89 V and 0.34 V, respectively. These values indicate that Nb_2Se_2C can significantly accelerate electrochemical reaction rates. Moreover, the low diffusion energy barriers for the adsorbates demonstrate that CO_2 and N_2 can easily migrate to the most stable sites, contributing to system stabilization. Importantly, post-adsorption analyses confirm that the electronic conductivity of monolayer Nb_2Se_2C is maintained, which is highly desirable for efficient ORR activity. Collectively, these findings suggest that Nb_2Se_2C is a promising candidate for facilitating efficient CO_2RR and NRR, offering both high catalytic activity and robust structural properties.

[1] X. Zhu and Y. Li, Wiley Interdiscip. Rev.: Comput. Mol. Sci., 2019, 9, e1416.
[2] 2 X. Guo, H. Du, F. Qu and J. Li, J. Mater. Chem. A, 2019, 7, 3531–3543
[3] P. Giannozzi, O. Andreussi, T. Brumme, et al., J. Con. Mat. **29** (46), 465901, (2017).
[4] J. P. Perdew, K. Burke, and M. Ernzerhof. Phy. Rev. Let. **80** (4), 891 (1998).

Student No: 23907909
Our Ref: Faculty of Natural and Agricultural Sciences
Tel: 012 420 3111

UNIVERSITEIT VAN PRETORIA
UNIVERSITY OF PRETORIA
YUNIBESITHI YA PRETORIA
Denkleiers • Leading Minds • Dikgopolo tša Dihlalefi
Private Bag X20 Hatfield 0028 Republic of South Africa
Tel 012 420 3111 Fax 012 420 4555
http://www.up.ac.za

2025-02-21

Mr Chewe Fwalo
6262
Off Zambezi Way
Riverside
KITWE
Zambia

PROOF OF REGISTRATION AS A STUDENT FOR THE YEAR 2025

This is to certify that **Mr Chewe Fwalo** is a registered student at the University of Pretoria

National ID/ Passport: ZN935669

Field of study: PhD (Physics)

Year of study: Final Year

Commencement of studies: 2023

Registration date: 21/02/2025

Minimum duration of studies (Years): 2

Total years enrolled at UP: 3

Year of NSC examination:

Any changes to information contained in this document must be reported to the Student Administration Office of the Faculty without delay.

Acquaint yourself with the contents of the General Information and Regulations of the University, which is available on the website of the University.

Please keep this document in a safe place. A fee will be levied for issuing an additional proof of registration.

You are personally responsible for the correctness of the information stated in this document. Lectures may only be attended for the courses listed in this document.

COURSES FOR WHICH STUDENT IS REGISTERED

Code	Description	Crdts	Session	Language
FSK 990	Thesis: Physics 990	360	Year	ENG

Dr A.M Mathekga
DIRECTOR:
DEPARTMENT ENROLMENT AND STUDENT ADMINISTRATION

Printed by U23907909 on 2025/02/21 02:03 PM

P42

DFT Analysis of CO_2 Dissociation and Reduction Pathways to CO and HCOOH on a ZrN Cluster

Niyati Gajjar[1], Sanjeev K. Gupta[2,*], P. N. Gajjar [1,*]

[1] Department of Physics, University School of Sciences, Gujarat University, Ahmedabad 380 009, India

[2] Computational Materials and Nanoscience Group, Department of Physics, St. Xavier's College, Ahmedabad 380 009, India

In this study, a ZrN cluster was employed as a model catalyst to investigate the carbon dioxide reduction reaction (CO_2RR) using density functional theory (DFT) [1]. Analysis of the adsorption energies of key reaction intermediates, namely *OCHO and *COOH, indicates that CO_2 reduction proceeds via pathways leading to the formation of CO and HCOOH [2]. Gibbs free energy calculations were further performed to explain the interaction of the ZrN cluster with various hydrocarbon intermediates. This cluster was found to be the self-dissociation agent for carbon dioxide. Comparative pathway analysis reveals that the HCOOH formation route is thermodynamically more favorable than the CO formation pathway. The electrochemical reduction of CO_2 to formic acid and carbon monoxide was evaluated in terms of overpotential, with calculated limiting potentials of −0.44 V and −0.91 V, respectively. In addition, a direct CO_2 dissociation pathway with the study of transition state is investigated using the nudged elastic band (NEB) method.

[1] F. Shirvani, A. Shokri, B.A. Ravan, An ab-initio study of structure and mechanical properties of rocksalt ZrN and its bilayers, Solid State Commun 328 (2021). https://doi.org/10.1016/j.ssc.2021.114218.

[2] Z. Niu, X. Gao, S. Lou, N. Wen, J. Zhao, Z. Zhang, Z. Ding, R. Yuan, W. Dai, J. Long, Theory-Guided S-Defects Boost Selective Conversion of CO2 to HCOOH over In4SnS8 Nanoflowers, ACS Catal 13 (2023) 2998–3006. https://doi.org/10.1021/ACSCATAL.2C05957.

P43

Ageing-driven formation of ternary phase N/TiO_2 nanocrystals for sustainable visible-light catalysis

Elias Assayehegn[1,2,*], Serhii Vorobiov[1], Abraha Tadese Gidey[1], and Vladimir Komanicky[1]

[1]Department of Chemistry, Mekelle University, P.O. Box 231, Mekelle, Ethiopia
[2]Faculty of Science, Pavol Jozef Šafárik University, Košice, Slovakia
**(Presenting author underlined)*

The ever-increasing energy crisis and environmental pollution have threatened humanity in the past several decades; in this regard, advanced oxidation processes have been extensively explored. Particularly, N-doped TiO_2 nanomaterials have received considerable attention; although, their capability of effectively separating the photogenerated charge carriers substantial improvement [1]. Now days rather than preparing mono-phase nanomaterials (of either Anatase (A), Brookite (B) or Rutile (R)), preparing their mixed-phase TiO_2 nanostructures has been widely considered as the most promising strategy for quantum efficiency enhancement [2]. Nevertheless, reports on ABR triphasic N/TiO_2 nanocomposites are extremely rare due to the fact that their preparation techniques are challenging- follows multi-step reaction under high temperature, which damages their structure and texture properties. Furthermore, the formation of oxygen vacancies, low N-dopant level, and usage of toxic hydrazine/ammonium fluoride as dopant source are the other challenges [3]. Thus, developing a facile preparation method for tunable triphase N/TiO_2 at lower energy simultaneously minimizing the impact on the environment remains quite pivotal. In an open literature survey, most investigations focused on the effect of N-dopant, temperature, surfactant, and solvent type/concentration; the obtained nanomaterials were aged mostly for 1-2 days. The effect of aging time on crystal structure, phase composition, morphology, optical response and photocatalytic activity of N/TiO_2 nanomaterials is overlooked.
Guanidinium chloride is a benign amine; despite its huge N-content, it is barely used as N-dopant source. In the present work with a special focus on aging synthesis approach, we report for the first time its usage in preparing various ABR ternary heterojunction N/TiO_2 nanoparticles at low temperature. Systematically varying the aging time (1, 4, 8, and 12 days), its influence on physicochemical properties of as-obtained spherical heterojunction nanomaterials was studied. Detailed characterizations confirmed that a substantial amount of anatase (88% to 50%) was transformed to rutile (2% to 38%) via intermediate brookite phase (9% to 25%) as the function of aging time; not only the ABR phase content of the samples was tuned by sol-gel age of the precursors but also their optical-response and methylene blue photocatalytic properties were profoundly dictated. Notably under visible-light irradiation, the photostable rutile rich mesoporous triphasic N/TiO_2 (50% A, 12% B, 38% R) aged for 12 days demonstrated higher degradation activity (97%) with a faster degradation rate (0.033 min-1) than both lesser aged N/TiO_2 and undoped titania. This enhancement is attributed to the synergistic effect of interstitial-N-doping and optimal ABR interfacial charge transfer that led to higher light absorption, lower band gap energy and well-separated charge carriers. The current work provides a new perspective for designing highly active visible-light heterostructure nanomaterials with controllable phase composition.

[1] M. A. Ahmed and M. Adel, RSC Adv. **13**, 421-439 (2023).
[2] P. Wang, W. Song and W. Li, ChemCatChem. **16**, 1-9 (2024).
[3] Sukarman, B. Kristiawan, E.P.Budiana, Khoirudin, A. Abdulah, Hybrid Advances. **11**, 100523 (2025).

P44

Synergistic Effect of 2D Self-Assembled Monolayer and ZnO Nanoparticles on the Passivation of Sol-gel ZnO Electron Transport Layer to Enhance the Performance and Stability of Non-Fullerene Organic Solar Cells.

Gebremariam G. Kidan*[1], Artur Braun[2,3], Newayemedhin A. Tegegne*[1]

[1]Department of physics, Addis Ababa university 1176 Addis Ababa, Ethiopia;
[2]Laboratory of high-performance ceramics, Empa, Swiss Federal Laboratories for materials science and technology. Uberlandstrasse, 129, CH 8600, Dubendorf Switzerland. ;
[3]Department of Materials, ETH Zurich Swiss Federal institute of technology, CH 8093, Zurich, Switzerland
kidan.ggtabher@aau.edu.et; Artur.Braun@empa.ch; newaye.medhin@aau.edu.et

Organic solar cells (OSCs) have emerged as a promising next generation source of green energy due to some desirable properties such as low-cost fabrication, mechanical flexibility, and tunable opto-electronic properties [1,2]. Although ZnO exhibits excellent optoelectronic properties as an electron transport layer (ETL) in multi-stack organic solar cells (OSCs), the presence of surface defects induces trap-assisted recombination, leading to a reduction in the device's power conversion efficiency (PCE) [3,4]. In this work, a synergistic passivation strategy is implemented to effectively neutralize these defect-induced trap states, thereby mitigating performance degradation and suppressing interfacial deterioration at the inorganic/organic junction, which is a determinant factor for efficient electron extraction. ZnO films were prepared using a sol-gel method and subsequently modified with a ZnO nanoparticle (ZnONP) layer and a silane-based two-dimensional self-assembled monolayer (SAM), forming a bilayer structure on the low-temperature processed sol-gel ZnO ETL. Devices were characterized using current-voltage measurements, Raman spectroscopy, and impedance spectroscopy. Stability tests were measured after one-week of dark storage without encapsulation under ambient condition. Optical and electrical characterization revealed that the synergistic incorporation of ZnO nanoparticles and SAM-based surface passivation enhanced the crystallinity and electrical conductivity of the ZnO layer, while effectively suppressing trap-assisted recombination losses. Consequently, the device exhibited a 14% improvement in power conversion efficiency compared to the pristine ZnO ETL-based organic solar cells. More importantly, devices with modified ZnO ETLs retained over 80% of their initial efficiency whereas the pristine ZnO ETLs based device were degraded significantly. These results highlight the critical role of interfacial engineering in enhancing performance and stabilizing OSCs, providing a practical pathway toward their large-scale application.

Keywords: Organic solar cells, electron transporting layer, Sol-gel ZnO, Surface passivation, Impedance spectroscopy,

References

[1] S. Li, Z. Li, X. Wan, and Y. Chen, eScience **3**, 100085 (2023).
[2] P. Ding, D. Yang, S. Yang, and Z. Ge, Chem. Soc. Rev. **53**, 2350 (2024).
[3] C. Li, J. Song, H. Lai, H. Zhang, R. Zhou, J. Xu *et al.*, Nat. Mater. **24**, 433 (2025)
[4] B. Zhang, Z. Pan, W. Li, Y. Zhao, X. Qin, A. Li *et al.*, Adv. Energy Mater. 2404297 (2025).

P45

f-f–Like *d-d* Transition of Mo(III) for NIR Emission

Animesh Ghosh, Sajid Saikia, Angshuman Nag*
Department of Chemistry, Indian Institute of Science Education and Research (IISER), Pune 411008, India
E-mail: angshuman@iiserpune.ac.in

Sharp near-infrared (NIR) emitters, particularly those operating in the NIR-II window (1000–1700 nm), hold promise for applications in telecommunications, lasers and high-resolution *in vivo* imaging. Such sharp NIR emissions at a few specific wavelengths arise from shielded $f \rightarrow f$ electronic transitions in rare-earth lanthanides like Yb^{3+}, Nd^{3+} and Er^{3+}. In contrast, $d \rightarrow d$ transitions typically yield broad emission, because *d*-electrons strongly interact with the surrounding ligands. In this talk, I will discuss about atomic-scale structure-function link showing how Mo^{3+} doped in $Cs_2NaInCl_6$ double perovskites yield $d \rightarrow d$ electronic transitions emitting ultra-narrow NIR-II radiation, similar to the $f \rightarrow f$ transitions. Recently, we reported the first ambient-stable Mo^{3+}-based ultra-narrow (FWHM < 10 meV) NIR-II emission at 1095 nm.[1,2] The highly symmetric $[MoCl_6]^{3-}$ octahedra with $4d^3$ electrons, result into $t_{2g}^3 e_g^0 \rightarrow t_{2g}^3 e_g^0$ intra-configurational spin-flip (ICSF) $d - d$ transitions. The ICSF $d - d$ transitions behave similar to atomic-like $f - f$ transitions, with ultra-narrow spectral width, violation of Kasha's rule, and upconversion photoluminescence.

Reference:

1. A. Ghosh, S. Saikia, S. Mukherjee, E. Johannesson, H. Rensmo, A. Nag, *Angew. Chem. Int. Ed*. **2025**, *e202415003*.
2. A. Nag, A. Ghosh, S. Saikia, Indian Patent Provisional Application (202521097969), 2025.

P46

Luminescent europium doped hydroxyapatite nanoparticles as fluorescent labels for cell imaging

Pooja Gitty [1] , V. P. N. Nampoori [1] , and M. Kailasnath [1]

[1] *International School of Photonics, Cochin University of Science and Technology, Cochin-682022, Kerala, India*

Europium doped hydroxyapatite (Eu:HAp) nanoparticles was synthesised via a simple co-precipitation method. The structural and optical properties were investigated. Concentration dependent luminescence characteristics of Eu:HAp is discussed. The characteristic red emission of Eu^{3+} ions, corresponding to the $^5D_0 \rightarrow {}^7F_2$ transition (~612 nm), was observed under near-UV excitation (395 nm). The luminescence intensity exhibited a concentration-dependent behaviour, with maximum emission at 3 mol% Eu^{3+}, beyond which concentration quenching occurred. Judd-Ofelt intensity parameters was also obtained for the synthesised particles. In vitro cytocompatibility and fluorescence imaging studies on HeLa cells demonstrated that Eu: HAp nanoparticles were efficiently internalized by the cells without causing morphological changes or cytotoxic effects. These findings establish Eu:HAp nanoparticles as a promising platform for fluorescent labelling, bioimaging, and potential theranostics applications, owing to their combined luminescent efficiency and biocompatibility.

[1] F. Baldassarre, A. Altomare, N. Corriero, E. Mesto, M. Lacalamita, G. Bruno, A. Sacchetti, B. Dida, D. Karaj, G. Della Ventura, F. Capitelli, D. Siliqi, Crystals **10**, 250 (2020)
[2] F. Chen, P. Huang, Y.-J. Zhu, J. Wu, C.-L. Zhang and D.-X. Xiang, Biomaterials **32**, 9031 (2011)

P47

Taming Light with Carbon dots

Arun M [1], Gopal Ramalingam [2]*

[1,2] *Quantum Materials Research Lab (QMRL), Department of Nanoscience and Technology, Alagappa University, Karaikudi, Tamil Nadu, India -630 003*

Corresponding authors: ramalingamg@alagappauniversity.ac.in (G.Ramalingam)

Abstract

The breakthrough of high-power lasers urged the effective light quenching materials for safeguarding eyes, Sensors and Photo detectors. Encountered exploration of Novel carbon dot to manipulate ray of light with a modest price. Nonetheless, a carbon dot suffers a large spectral range detection of a ray of light, so the research has been devoted to exploring the materials to cover different spectral ranges. This article reports a novel multi-photon emissive carbon dot with large spectral emission coverage with an effortless preparation strategy. The rapid fabrication procedure constituted with Multicolour photon emissive carbon dot (MCCD) in a single solvent with utilization of biomass source. We have identified the mono-solvent effect induced Multiple emissive carbon dot observed in fluorescence spectroscopy. The fluorescence carbon particle displays nature of excitation-independent properties, with the granule size ranges 1-15nm result obtained via Transmission Electron Spectroscopy. The carbon structure suffered from the lower carbonization temperature with rapid microwave treatment causing a turbostratic carbon structure. The different colour contains with NIR region bright red emission solution tested against Z-scan non-linear properties, it exposes excited state absorption involved two-photon absorption. It offers an approach for optical limiting behaviour with threshold reaches up to 0.53 x 10^{-10} and 4.54 x 10^{12} W/m^2 was observed for MCCD. These results in a gateway for eco-friendly Carbon dot into an optical limiting appeal.

Keywords : *Carbon dots, Psidium gujava, Non-linear optics, Z-scan technique, Triple emission, Microwave assisted method, , Flexible Optical limiters*

[1] Wang, C.; Xu, Z.; Cheng, H.; Lin, H.; Humphrey, M. G.; Zhang, C. A ,*Carbon* 2015, *82*(C). doi:10.1016/j.carbon.2014.10.035.

[2] Ebrahim Jasim, K. In *Standards, Methods and Solutions of Metrology*; 2019. doi:10.5772/intechopen.84191.

[3] Shalini, M.; Sundararajan, R. S.; Manikandan, E.; Meena, M.; Ebinezer, B. S.; Girisun, T. C. S.; et al. *Optik* 2023, *278*. doi:10.1016/j.ijleo.2023.170705.

[4] Yogeswari, C.; Sabari Girisun, T. C.; Nagalakshmi, R. *J. Electronic Materials* 2021, *50*(8). doi:10.1007/s11664-021-08996-4.

P48

Development and Photoluminescence Spectroscopy study of Luminescent Solar Concentrator for Building Integrated Photovoltaics

Mayank Gupta [1]*, Paramsinh Zala[1], Brijesh Tripathi[1], and Prakash Chandra[2]
[1]*Department of Physics, Pandit Deendayal Energy University, Gandhinagar, Gujarat, 382421, India*
[2]*Department of Chemistry, Pandit Deendayal Energy University, Gandhinagar, Gujarat, 382421, India*

Mayank.G@sot.pdpu.ac.in; *Mayank.g18@gmail.com*

Abstract
Solar energy stands out as a viable renewable source; however, conventional silicon-based photovoltaics exhibit spectral limitations, as they fail to efficiently utilize high-energy UV and low-energy NIR photons, thereby constraining their overall power conversion efficiency. This study aims to enhance solar energy harvesting by integrating upconverting nanoparticles (UCNPs) into luminescent solar concentrators (LSCs) to convert near-infrared (NIR) light into visible light, improving the efficiency of conventional silicon solar cells. Fluoride host matrix $NaYF_4$ co-doped with Er^{3+} and Yb^{3+} was synthesized using the hydrothermal synthesis and characterized structurally and optically. The Upconversion Luminescence (UCL) study based on Photoluminescence (PL), Time Resolved Photoluminescence (TRPL) and Quantum yield measurement is reported. $NaYF_4$: Yb^{3+}, Er^{3+} exhibited the highest UCL efficiency due to its low phonon energy, making it an ideal material for Upconversion. The LSC slabs fabricated with these UCNPs in a resin matrix were evaluated for their optical properties using a custom setup. The findings suggest that $NaYF_4$ based LSCs are particularly promising for enhancing solar energy conversion in building-integrated photovoltaics (BIPV), offering a path toward more sustainable energy solutions.

Keywords: Luminescent Solar Concentrator, Energy harvesting, BIPV,PL,TRPL, Quantum Yield

References

1. P. Zala, B. Tripathi, M. Gupta, M. Kumar, and U. K. Dwivedi, "Measurement of Light Response in Luminescent Solar Concentrators," International Conference on Sustainable Energy Technologies and Computational Intelligence (SETCOM), Gandhinagar, India, pp. 1-6 (2025), doi: 10.1109/SETCOM64758.2025.10932357
2. Li, Y.; Qi, J.; Ma, J. Effect of pH and Yb3+ doping concentration on the structure and upconversion luminescence properties of GdPO4: Er3+, Yb3+. International Journal of Materials Research, **116** (2), 81-90 (2025).
3. Chang, Yulei. "Mechanism in Rare-Earth-Doped Luminescence Nanomaterials." *Photofunctional Nanomaterials for Biomedical Applications*, 77-115 (2025). DOI: 10.1002/9783527845347.ch2

P49

Interpretable Machine-Learning-Assisted Discovery of Novel Double Perovskite Compounds for Energy Harvesting Applications

Neelam Gupta [1], Towhidur Rahaman [1], and Soumya Jyoti Ray [1]

[1]Department of Physics, Indian Institute of Technology Patna, Bihta 801106, India

Lead free double perovskites have emerged as promising candidates for photovoltaic, optoelectronic, thermoelectric, and energy conversion technologies due to their tunable band gaps, improved stability, and reduced toxicity. Efficient discovery of such materials requires accurate and scalable prediction methods. In this work, we develop an interpretable machine-learning (ML) framework integrated with AutoML to accelerate the identification of wide-band-gap halide and oxide double perovskites. Using a curated dataset of 4,800 PBE-calculated band gaps, the AutoML models achieve strong predictive performance ($R^2 = 0.87$, MAE = 0.37 eV). SHAP analysis highlights valence electron count, ionic LUMO energy, and density as the most influential descriptors governing band-gap trends.

Applying the trained models to an extended chemical space under thermodynamic stability constraints yields 1,537 promising and previously unreported lead-free double perovskite compositions. First-principles validation on representative candidates further supports the ML predictions, with typical deviations within ~0.48 eV. Overall, this integrated ML–DFT strategy provides a scalable, interpretable, and efficient pathway for accelerating the discovery of next-generation double perovskite materials.

[1] Talapatra, A., Uberuaga, B.P., Stanek, C.R. et al., Commun Mater 4, 46 (2023).

[2] Siddharth Sradhasagar, Omkar Subhasish Khuntia, Srikanta Biswal, Sougat Purohit, Amritendu Roy, Solar Energy 267, 112209 (2024)

P50

Hydrogen-Bond-Mediated Modulation of Tyrosine Photophysics under External Electric Fields

Nalini D. Gurav

Department of Scientific Computing, Modeling & Simulation
Savitribai Phule Pune University (SPPU) Pune 411 007

The photophysics of aromatic amino acids is strongly influenced by local hydrogen-bonding environments and internal electric fields, yet disentangling these effects remains challenging in complex biological systems. In this work, tyrosine is employed as a minimal chromophore model to systematically investigate how controlled hydration modulates its vibrational and electrostatic properties. Ground-state geometries of isolated tyrosine, tyrosine–water (W1), and tyrosine–water$_2$ (W2) complexes were optimized using density functional theory at wB97X-D/aug-cc-pVTZ level of theory, followed by vibrational and electrostatic potential analyses. The calculated infrared spectra reveal distinct hydrogen-bond-induced shifts and mode-specific signatures that evolve with the number of water molecules, while molecular electrostatic potential maps indicate progressive charge redistribution upon hydration. These results establish a well-defined structural and electrostatic framework for probing electric-field-dependent excited-state behavior, and ongoing time-dependent DFT calculations will elucidate how hydration and external fields cooperatively influence excitation energies, oscillator strengths, and charge-transfer character in tyrosine. Local hydrogen bonding and externally applied purturbative electric fields play a decisive role in shaping the photophysics of biological chromophores, yet their individual and cooperative effects are difficult to isolate experimentally. Here, we present a systematic density functional theory study of tyrosine and its mono- and di-hydrated complexes as a minimal model system to investigate hydration- and field-induced effects. Optimized geometries and infrared spectra reveal pronounced hydrogen-bond-dependent vibrational signatures, particularly in O–H and C=O stretching modes, while molecular electrostatic potential maps show hydration-induced polarization of the electronic density. Preliminary electric-field-aligned calculations indicate enhanced sensitivity of hydrogen-bonded configurations to external fields. Building on these ground-state insights, ongoing time-dependent DFT calculations aim to characterize field-dependent excitation energies, oscillator strengths, and charge-redistribution patterns, providing molecular-level insight into how hydration networks and electric fields jointly govern tyrosine photophysics.

P51

LASER-INDUCED FLUORESCENCE SPECTROSCOPIC STUDY OF WATER FROM MOSQUITO BREEDING HABITATS

Andrew A. Huzortey[1], Andreas A. Kudom[2], Ben A. Mensah[1], Baah Sefa-Ntiri[1], Benjamin Anderson[1], and Angela Akyea[1]

[1] Laser and Fibre Optics Centre, Department of Physics, University of Cape Coast, Ghana; [2] Department of Conservation Biology and Entomology, University of Cape Coast, Ghana

Laser-Induced Fluorescence (LIF) spectroscopy was applied for the first time to investigate the characteristics of water from mosquito breeding habitats of *Anopheles*, *Aedes*, and *Culex* species. Water samples were collected from diverse ecological settings and analyzed to determine the spectral signatures of Dissolved Organic Matter (DOM) and chlorophyll-related constituents. Spectral data were processed using Principal Component Analysis (PCA) and spectral deconvolution techniques to identify variations in fluorescence components across species habitats. The LIF spectra revealed distinct emission features between 450–650 nm (DOM) and 650–750 nm (chlorophyll), with an OH-water Raman band near 520 nm. PCA effectively discriminated between mosquito species based on these spectral variations. The findings indicate that *Anopheles* habitats are characterized by high DOM and low chlorophyll content, while *Aedes* and *Culex* habitats exhibit mixed or higher chlorophyll signatures. This study demonstrates that LIF spectroscopy can be used as a rapid, nondestructive, and sensitive technique for water quality assessment by vector ecologists. It offers a promising analytical tool for understanding breeding site characteristics and can support vector biologists in developing environmentally targeted mosquito control strategies.

References

[1] Monroe et al., *Malaria Journal* **21** (1), 1–5 (2022).
[2] Kudom, *Malaria Journal* **14** (1), 1–13 (2015).
[3] Liu et al., *Applied Optics* **59** (10), C1–C7 (2020).

Bi_2S_3 nanoparticulate thin-film growth for photocatalytic applications using the SILAR method

Mohit Jatoliya , Siddhant Deshpande , Vijay Kumar and Rajendra C. Pawar

Central University of Rajasthan, Ajmer, India, 305817.

Bismuth sulfide (Bi_2S_3) is a material that can effectively interact with visible light, which makes it suitable for photoelectrochemical applications. In this study, Bi_2S_3 thin films were prepared using the successive ionic layer adsorption and reaction (SILAR) method [1]. This method is simple, low-cost, and suitable for large-scale thin film deposition.

The band gap of the Bi_2S_3 thin films was found to be in the range of 1.3–1.7 eV, indicating good sensitivity to visible light [2]. The surface morphology of the films was examined using scanning electron microscopy (SEM). The SEM images revealed a uniform, particle-like nanostructure with particle sizes ranging from 30 to 50 nm.

The photoelectrochemical performance of the Bi_2S_3 films was investigated using cyclic voltammetry and chronoamperometry techniques. The chronoamperometry results showed a stable photo-response. The current was about 100 µA under dark conditions and increased to around 140 µA under light illumination. This enhancement in current confirms effective generation and separation of charge carriers under illumination.

Overall, the results demonstrate that Bi_2S_3 thin films prepared by the SILAR method are promising candidates for photoelectrochemical applications. The simple and economical fabrication process makes these films suitable for future low-cost and scalable energy-related devices.

[1] Duohuan Yu et. al., J. Phys. Chem. C **127**, 2340 (2023).
[2] Shital M. Sonar et. al., J Mater Sci: Mater Electron **35**, 1616 (2024).

P53

Designing all-in-one nanophosphor for thermometry, dosimetry, bioimaging, Anticounterfeiting & X-ray scintillation.

Minakshi Jha

Bharati Vidyapeeth, Chemistry division, Department of Applied Science, DUDET, Kharghar, Navi Mumbai-410210, India
Email: minakshi@bharatividyapeeth.edu

Designing customizable, cost-effective optical material excitable to UV-Vis, X-ray, and β-irradiation ($^{90}Sr/^{90}Y$) is pivotal for technical innovation and a sustainable society. Engineering a single phosphor for multiple applications is challenging and crucial for innovative technology, elevating productivity and flexibility, minimising cost and power intake, etc. The present work focuses on green synthesis of multifunctional nanophosphor exhibiting versatile optical functionalities. The Unique optical behaviour of the material has shown radioluminescence (RL), photoluminescence (PL), thermoluminescence (TL), scintillation and optically stimulated luminescence (OSL), making it indispensable for X-ray to visible light conversion, fit for biological studies, anticounterfeiting and luminescence thermometry. RL study has shown linear intensity dependence on X-ray tube current 1-5 mA at 100 KV and Voltage 40-100 KV at 4mA, demonstrating efficient X-ray to visible light conversion. The fluorescence intensity ratio technique has shown a maximum relative sensitivity of 1.049%K^{-1}. Biological studies using the MTT assay demonstrated selective cytotoxicity towards MCF7 cells rather than A549 cells. The study reveals that materials exhibit thermal stability, customizability, multicolour tunability, and promising optical properties that are significant for dosimetry, lighting, security, theranostics, anticounterfeiting, thermometry, and bioimaging[1].

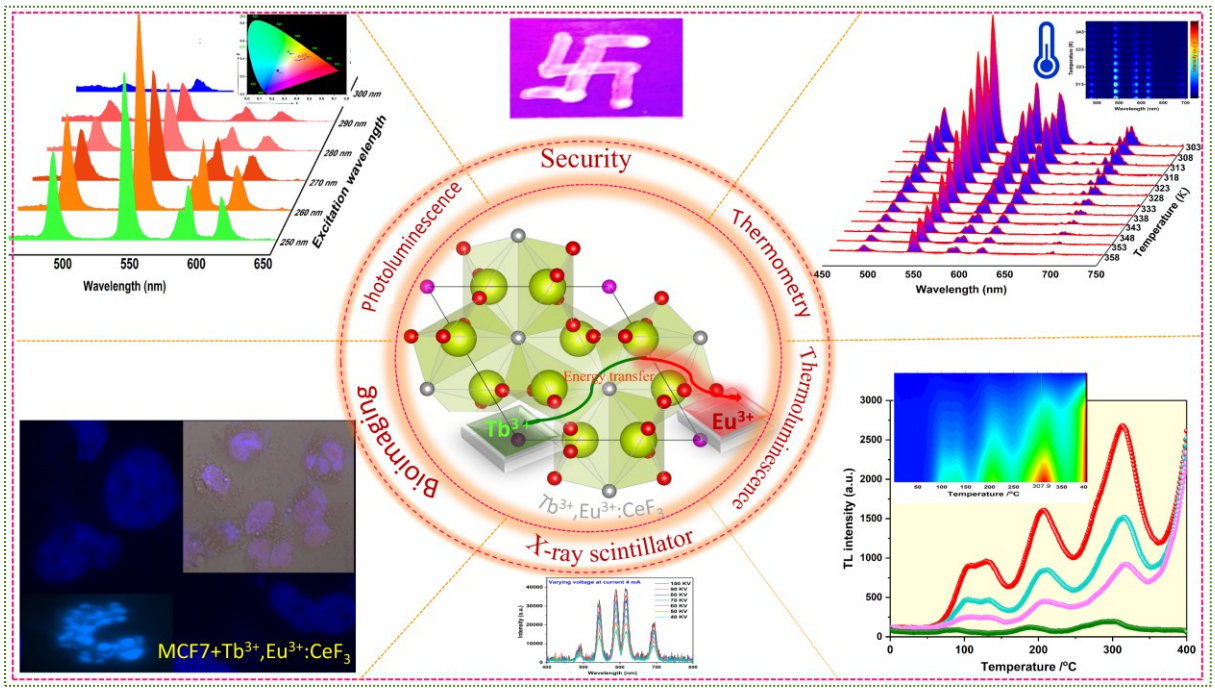

Reference-

1. Jha, M. Insight into Green-Synthesized All-in-One Multifunctional Nanophosphor: Achieving Multicolor Luminescence, Optical Thermometry, Thermoluminescence, Bioimaging, Anticounterfeiting, and X-ray Scintillation Applications. *ACS Appl. Opt. Mater.* 2025, https://doi.org/10.1021/acsaom.5c00486.

P54

The sharp Blue Emission of Eu^{2+} in Eu-doped $CsPbBr_3$

Santosh Kachhap [1,2], Sunil Kumar Singh [1]

[1]*Department of Physics, Indian Institute of Technology (BHU), Varanasi-221005 Uttar Pradesh, INDIA*

[2] *Department of Physics, Chas College Chas, BBMKU-Dhanbad-827013 Jharkhand INDIA*

Abstract: Inorganic halide perovskites (IHPs) have provoked intense research because of their superior stability, excellent optoelectronic properties, cost-effectiveness, and striking optoelectronic applications [1]. Recently, the doping of lanthanide ions in IHPs has opened new avenues, particularly for emerging applications like NIR and white light emitting diodes, NIR emitters, NIR camera, optical temperature sensing, optical data encoding, etc. Besides, lanthanide doping has also improved the stability (thermal, photo, and phase), structure and optical properties of IHPs significantly, which has resulted in improved device performance.

Here we have synthesized the Europium (Eu) doped-$CsPbBr_3$ quantum dots (QDs) using hot-injection method. For the confirmatory text we performed various characterizations such as ultraviolet–visible absorption, photoluminescence, X-ray photoelectron spectroscopy of the sample [2-4]. The photoluminescence spectra of the $CsPbBr_3$ and Eu-doped $CsPbBr_3$ recorded by using 402 nm excitation light are shown in figure 1. The $CsPbBr_3$ QDs shows the emission peak at 521 nm and Eu-doped $CsPbBr_3$ QDs shows emission peaks at 442 and 498 nm. The results are good agreement with previously published reported. In Eu-doped $CsPbBr_3$ QDs, the emission peak at 442 is due to the Eu-ion and 498 nm peak is from the $CsPbBr_3$ host. It is observed that the emission peak due to the host shift towards lower wavelength on doping Eu-ion. At the same time intensity of the emission peaks also increased due to site symmetry breaking upon the Eu-ion doping into the $CsPbBr_3$. The results show that this material can be explored for different optical applications [5].

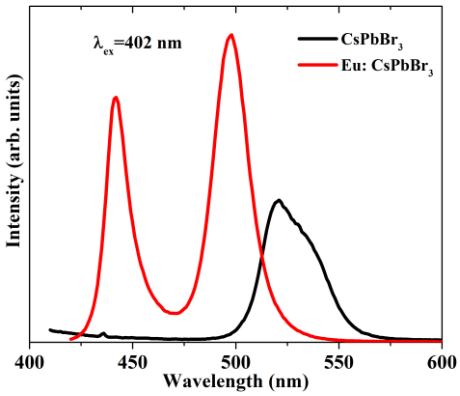

Figure 1. The emission spectra of $CsPbBr_3$ and Eu-doped $CsPbBr_3$ QDs (excitation wavelength is 402 nm).

References

[1] Kachhap, S., Singh, S., Singh, A., & Singh, S. K. *J. Mater. Chem. C*, **2022**, **10**, 3647-3676
[2] Yu, H., Zhou, L., Ye, R., Deng, D., & Xu, S. *Dalton Transactions*, **2022**, *51*(18), 7333-7342.
[3] Chen, H., Li, R., Guo, A., & Xia, Y., *SN Applied Sciences*, **2021**, *3*(6), 1-7
[4] Hu, Q., Li, Z., Tan, Z., Song, H., Ge, C., Niu, G. & Tang, J., Adv. Opt. Mater, **2018**, *6*(2), 1700864.
[5] Song, Y. H., Yoo, J. S., Kang, B. K., Choi, S. H., Ji, E. K., Jung, H. S., & Yoon, D. H., *Nanoscale*, **2016**, *8*(47), 19523-19526.

Keywords: Inorganic halide perovskite, Lanthanide, Quantum dotes, Blue emission, Optical application.

.

P55

"Pulsed Laser Ablation Derived MoS_2 Nanosheets with Strong Third-Order Nonlinearities for Ultrafast Photonics"

Dina M. Atwa

Department of Laser Interaction with Matters, Laser Institute for Research and Applications, Beni-Suef University, PO 62517, Beni-Suef, Egypt, dina.mohamed@lira.bsu.edu.eg

Abstract

Two-dimensional transition metal dichalcogenides (TMDs) such as molybdenum disulfide (MoS_2) are among the most promising nonlinear optical (NLO) materials due to their strong excitonic effects, direct bandgap in the monolayer limit, and inherently large third-order susceptibility. However, scalable synthesis of clean, crystalline nanosheets remains a challenge, as many chemical or solution-based methods introduce surfactant residues and defects that degrade optical performance.

In this work, we report the **green and surfactant-free synthesis of MoS_2 nanosheets** using the **pulsed laser ablation in liquid (PLAL)** technique. A compact MoS_2 target immersed in deionized water was ablated with a Q-switched Nd:YAG laser (λ = 1064 nm, pulse duration ≈ 10 ns, repetition rate 10 Hz, fluence ≈ 1.5 J/cm²), producing colloidal dispersions of few-layer MoS_2 nanosheets. **TEM and SEM** revealed sheet-like morphologies with lateral dimensions of ~200 nm and thicknesses of 3–6 layers, while **XRD** confirmed the preserved hexagonal 2H phase. **FTIR** spectra further validated the integrity of Mo–S bonding, demonstrating that PLAL maintains crystallinity without chemical modification.

Nonlinear optical measurements were performed on the colloidal MoS_2 dispersion of optimized concentration (0.5 mg/mL) using the **open- and closed-aperture femtosecond Z-scan experiments** (800 nm, 120 fs, 1 kHz). The nanosheets exhibited **saturable absorption with ~13% modulation depth and ~0.6 GW/cm² saturation intensity**, alongside a large **nonlinear refractive index ($n_2 \approx 3.4 \times 10^{-13}$ cm²/W)** and **nonlinear absorption coefficient ($\beta \approx 1.1 \times 10^{-9}$ cm/W)**, corresponding to an effective **third-order susceptibility $|\chi(3)| \approx 2.8 \times 10^{-12}$ esu**. These values are **comparable to or exceed previously reported MoS_2 nonlinearities prepared by chemical exfoliation or CVD**, underscoring the efficiency of PLAL as a synthesis route. The combination of **environmentally friendly synthesis, preserved crystalline quality, and strong third-order optical nonlinearities** establishes PLAL-derived MoS_2 nanosheets as **high-performance candidates for saturable absorbers, all-optical modulators, and ultrafast photonic switches**. This work provides both a sustainable fabrication pathway and benchmark NLO parameters for MoS_2, strengthening its position in next-generation integrated photonics.

[1] G. Omar, Mohamed Ashour, Dina. M. Atwa, and Tarek Mohamed, "Experimental exploration of the second order nonlinear optical properties of hexagonal boron nitride nanosheets utilizing femtosecond laser pulses," Appl. Opt. 64, C53-C59 (2025)

[2] Mina Ebrahimzadeh, Azadeh Haghighatzadeh, Joydeep Dutta, Improved third-order optical nonlinearities in Ag/MoS2 Schottky-type nano/hetero-junctions, Optics & Laser Technology Volume 140, August 2021, 107092

P56

Steel Mesh-Supported SNW-1/$CsPbBr_3$ Nanocomposite: Photocatalyst for Sustainable Ammonia Production

Negin Khosroshahi [1], **Vahid Safarifard**[1]

[1] Department of Chemistry, Iran University of Science and Technology, Tehran 16846-13114, Iran

The conversion of solar energy into chemical energy through photocatalysis is an important field of interest in green energy generation and environmental improvement [1]. Nevertheless, its effectiveness currently falls short of expectations, primarily due to the issue of charge recombination. To address this challenge, the photocatalytic effect has become an optimistic approach for enhancing processes [2]. In this research, we have developed a Steel Mesh-Supported SNW-1/$CsPbBr_3$ nanocomposite by combining covalent-organic frameworks with metal halide perovskite. To gauge their effectiveness, the heterostructure was assessed by employing multiple characterization methods including XRD, IR, FESEM, DRS, EDX, VSM, PL, EIS, Zeta, and BET. After the composite's preparation and characterization, we examined its photocatalytic activity in nitrogen reduction. The SNW-1/MHP/Steel mesh nanocomposite exhibited exceptional performance in ammonia generation. These findings suggest that the SNW-1/MHP/Steel mesh nanocomposite holds promise as an environmentally friendly and cost-effective photocatalyst, capable of addressing the challenges of sustainable ammonia production. This study presents a promising method for identifying effective photocatalytic materials using mesh substrates to address environmental concerns.

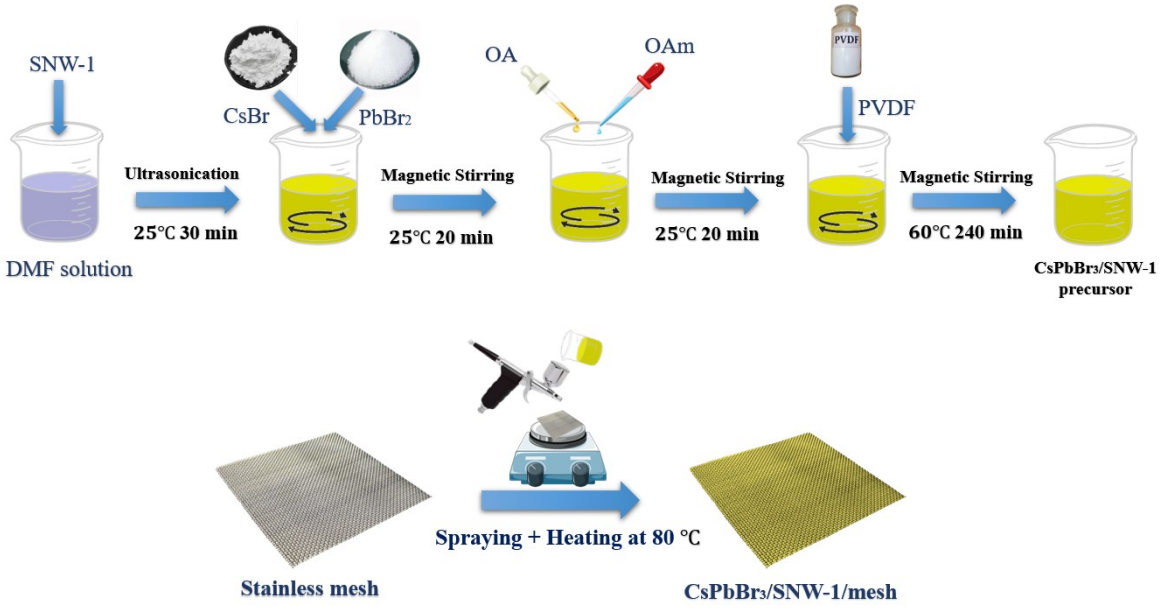

[1] T. Žibert, B. Likozar, M. Huš, Modelling Photocatalytic N2 Reduction: Where We Stand and Where We Are Going, ChemSusChem, (2024) e202301730.
[2] L. Yao, A.M. Pütz, H. Vignolo-González, B.V. Lotsch, Covalent Organic Frameworks as Single-Site Photocatalysts for Solar-to-Fuel Conversion, Journal of the American Chemical Society, (2024).

P57

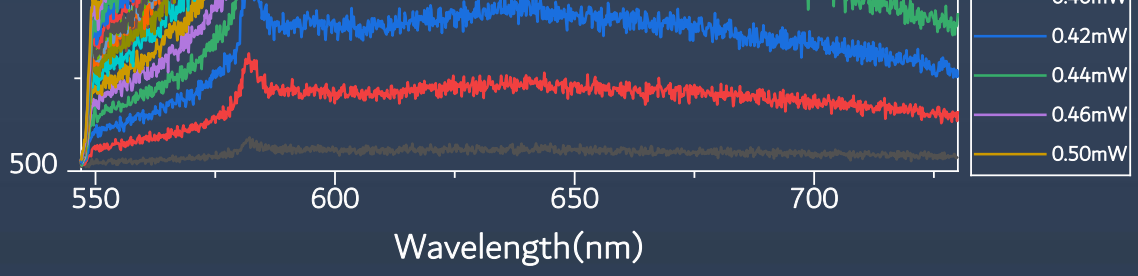

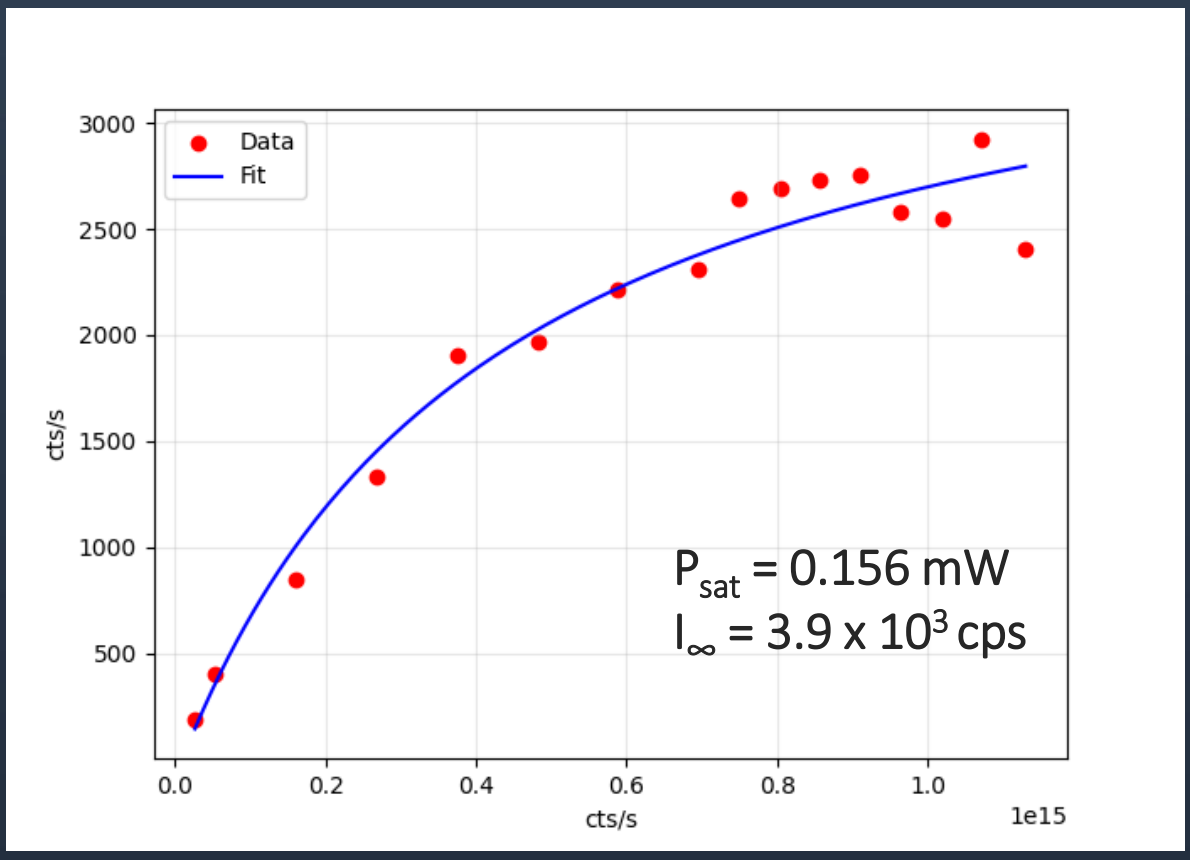

Applic

- On-chip single-photon sources for integ
- Quantum communication using secure,
- Quantum key distribution (QKD) in com
- Quantum information processing with c
- Scalable photonic quantum networks en

P58

Impact of strain on excitonic radiative lifetime in a polar Hf_3ZrS_8 monolayer: Theoretical insight based on many-body perturbation theory

Dhirendra Kumar and Sudip Chakraborty*

Materials Theory for Energy Scavenging Laboratory, Condensed Matter Physics, Harish-Chandra Research Institute, A C.I. of Homi Bhabha National Institute, Chhatnag Road, Jhunsi, Prayagraj 211019, India

An exciton consists of an excited electron and its corresponding hole, where their mutual Coulomb interaction leads to the formation of a bound state with an energy level located between the valence band (VB) and conduction band (CB) [1]. In two-dimensional ultrathin materials, lower dielectric screening enables stronger exciton binding, which plays a crucial role for large excitonic radiative lifetimes [2]. In this work, we have investigated a polar monolayer of Hf_3ZrS_8 from the perspective of many-body perturbation theory and the Bethe-Salpeter equation (BSE) to determine the corresponding excited state properties, particularly the excitonic radiative lifetime. We have envisaged the impact of external biaxial compressive and tensile strain on the excitonic lifetime, optical absorption, and excitonic wave function in the monolayer, based on the GW -BSE formalism, while including relativistic spin-orbit coupling effect. The polar monolayer possesses strong binding energy of the first bright exciton within the quasiparticle band-gap range, while the excitonic radiative lifetime is determined in picoseconds. The optical band gap increases and decreases with tensile and compressive strain, respectively. We have obtained an excitonic radiative lifetime approximately three times larger than the pristine one under biaxial compressive strain. Our finding reveals that the Hf_3ZrS_8 monolayer under the influence of biaxial strain could be useful for miniaturized optoelectronic and photonic devices[3].

[1] J. Frenkel, Phys. Rev. **37**, 17 (1931).
[2] Thomas Mueller and Ermin Malic, npj 2D Materials and Applications **2**, 29 (2018).
[3] D. Kumar and S. Chakraborty, Phys. Rev. B **112**, 125107 (2025).

P59

Phosphorus-Doped BP_xN_{1-x} Monolayer as an Efficient Photocatalyst for Solar Water Splitting: A First-Principles Study

Vipin, Deepak, Neena Jaggi
National Institute of Technology, Kurukshetra, India
Email: neena_jaggi@rediffmail.com

Abstract

The efficient conversion of solar energy into hydrogen fuels via photocatalytic processes is an attractive technology for producing clean and renewable source of energy. Considerable efforts have been made by scientists to search for desirable photocatalyst materials for water splitting. Two-dimensional (2D) materials have shown extraordinary performance in this area. One of the effective option of photocatalyst for water splitting is doped monolayer Boron Nitride (BN) .Hexagonal boron nitride (BN), a typical wide-bandgap semiconductor, exhibits excellent chemical stability but absorbs mainly in the ultraviolet region, limiting its photocatalytic performance. Doping is an effective strategy to enhance the photocatalytic activity of the BN. In this work, the band structure, density of states and refractive index of Phosphorous doped BN are investigated using calculations based on density functional theory (DFT) in its generalized gradient approximation (GGA) as implemented in the Vienna Ab-initio Simulation Package (VASP). Different phosphorus doping concentrations (0–22%) were introduced by substituting P atoms at N sites to systematically analyze the effect of doping level on the photocatalytic behavior. This concentration-dependent approach allows us to identify the optimal doping range for improved performance. The calculated results show that Phosphorus doping lead to band gap narrowing, which enhances the visible light catalytic activity. The calculated conduction band minimum (CBM) and valence band maximum (VBM) positions confirm that the doped BN monolayer satisfies the thermodynamic requirements for overall water splitting. According to our results, the P-doped BN monolayer has a sufficient band gap of 2.8 eV, as well as suitable high visible light absorption which is desirable for photocatalysis. Therefore, phosphorus doping effectively activates BN as a promising 2D photocatalyst for solar-driven water splitting.

References

[1] Liu, Xuecheng, et al., *International Journal of Hydrogen Energy* 48.35, 13181-13188 (2023)

[2] Li, Yunguo, et al., Catalysis Science & Technology 7.3, 545-559 (2017)

P60

Structure-Luminescence Correlation Studies in Eu^{3+} Doped Silicate Phosphors for Bioimaging Applications

Navya Sara Kuriyan [1], and M. Sabeena [1]

[1]*Department of Physics, Cochin University of Science and Technology (CUSAT), Kochi, Kerala, India- 682022.*

Lanthanide doped alkaline earth metal based silicate phosphors have garnered significant attention due to their versatile applications across various fields, including display devices, energy storage systems and biomedical applications such as bioimaging and biosensors. Among the various phosphors,europium (Eu^{3+}) doped calcium magnesium silicate phosphors (CMS: Eu^{3+}) are particularly promising due to their tunable structural, morphological and photophysical properties. Pristine and Eu^{3+} doped CMS are classified within a mineral category characterized by four predominant phases: diopside ($CaMgSi_2O_6$), akermanite ($Ca_2MgSi_2O_7$), merwinite ($Ca_3MgSi_2O_8$) and monticellite ($CaMgSiO_4$). Through the structural modification, we can modify the luminescence properties like excitation, emission, intensity, decay time, quantum yield (QY), color chromaticity and color purity. Hence, the possibility of the integration of the photophysics of four phases of CMS: Eu^{3+} into the biomedical applications, such as bioimaging, is explored [1].

Photophysical studies reveal that the octahedral coordination geometry (coordination number= 6) provides more crystal field effect to the Eu^{3+} ions and hence shows maximum crystal field splitting. This is exhibited by the monticellite phase, which possesses octahedral coordination geometry. In the case of diopside and akermanite phases, the presence of dodecahedral coordination geometry (coordination number= 8) helps to increase the emission peak intensity, decay time and QY since this geometry promotes the intrinsic defects and oxygen vacancies, which serve as electron traps. In merwinite, a combination of 6, 7, 8 and 9 coordination geometries exists and hence the reduction in emission intensity compared to other phases is noticed. Also, the local site preference of Eu^{3+} dopant ions on Ca^{2+} than Mg^{2+} cationic sites enhances the crystal field effect of the host over the Eu^{3+} dopant ions, which makes the phosphor more efficient. The local site symmetry analysis reveals the enhanced induced electric dipole (ED) transition over the magnetic dipole (MD), which suggests the improved red emission due to the presence of non-inversion centers for Eu^{3+} ions. All phases have deep red emission with QY > 50% and color purity > 90% and are found to be suitable for biomedical applications like imaging [2-4].

The intricate relationship between the structure and luminescence reveals that all four phases are potential candidates for bioimaging. The diopside phase with 77% QY and 93% color purity of CMS: Eu^{3+} phosphor is found to be a suitable candidate for in vitro bioimaging applications.

[1] N. S. Kuriyan, M. Sabeena, J. Lumin. **249**, 119038 (2022).

[2] N. S. Kuriyan, P. S. Ghosh, A. Arya, M. Sabeena, J. Lumin. **260**, 119901 (2023).

[3] N. S. Kuriyan, P. S. Ghosh, M. Parvathy, A. Arya, M. Sabeena, J. Lumin. **277**, 120894 (2025).

[4] N. S. Kuriyan, A. Deepti, P. S. B. Chakrapani, M. Sabeena, ACS Appl. Bio Mat. **8**, 1646 (2025).

P61

Designing a bio-inspired electrocatalyst based on V_2C-MXene for nitrogen reduction

Doulat Lahon[1,2], Lakshi Saikia[1,2*]

[1]Materials Sciences and Technology Division, CSIR-North East Institute of Science and Technology, Jorhat, Assam-785006

[2] Academy of Scientific & Innovative Research (AcSIR), Ghaziabad-201002, India

Sustainable ammonia (NH_3) synthesis remains a critical challenge in the transition towards greener and decentralized energy systems. Electrocatalytic nitrogen reduction reaction (eNRR) has gained attention as one of the sustainable ammonia production alternatives to the energy-intensive Haber-Bosch process [1]. However, the development of highly active, selective, and stable electrocatalysts remains the primary bottleneck in eNRR commercialization. This study investigates Mo-doped V_2C MXene as a promising electrocatalyst: a bio-inspired catalyst design for efficient NRR. The design is inspired by nitrogen fixation machinery of nature, where vanadium and molybdenum serve as active metal centers in nitrogenase enzymes of diazotrophic bacteria. Initial characterization reveals that the incorporation of Mo does not affect the sheet-like morphology of V_2C Mxene. First-principles calculation study also reveals anchoring Mo enhances the intrinsic catalytic activity of V_2C Mxene for eNRR [2]. Preliminary electrochemical analysis indicates that Mo doping enhances the surface reactivity and catalytic performance of V_2C MXene. This work highlights the importance of controlled doping strategies in tailoring the properties of MXenes to meet specific catalytic requirements. It promises further advancements in sustainable N_2 reduction for ammonia production.

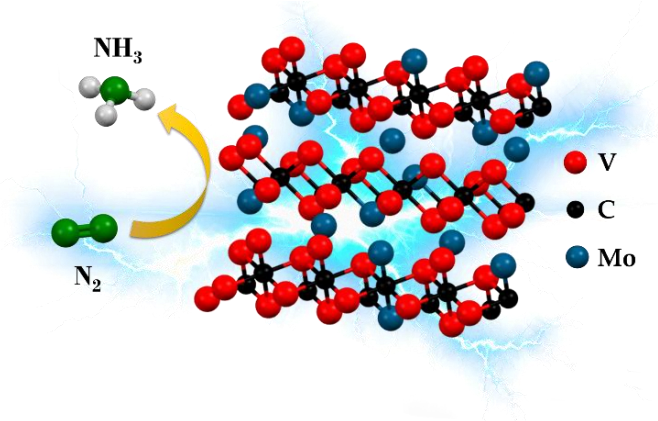

[1] D.R. Macfarlane, P. V. Cherepanov, J. Choi, B. H.R. Suryanto, R. Y. Hodgetts, J. M. Bakker, F. M. F. Vallana, A. N. Simonov, Joule. 4(6) 1186-1205 (2020)

[2] Y. Cao, Y. Tan, X. T. Zhu, H. L. Li, Y. Q. Zhao and Y. Xu, Physica E: Low Dimens. Syst. Nanostruct. **134**, 114875 (2021).

P62

Theoretical Investigation of Electronic Structure and Photophysical Properties of Salicylic Acid Derivatives.

Aishwarya Mahar, N. Pandey and S. Pant

Photophysics Laboratory, DSB Campus, Kumaun University, Nainital

Salicylic acid and its substituted derivatives are well known for their rich intramolecular hydrogen bonding and tunable electronic and photophysical properties, making them promising systems for theoretical and applied studies. These molecules exhibit environment-sensitive photophysical properties such as solvatochromism, pH-responsive fluorescence, charge transfer, and proton transfer, making them attractive for optoelectronics and nonlinear optical (NLO) applications. In this work, a comparative theoretical analysis of 3-methoxy salicylic acid (3-MeOSA) and 6-methoxy salicylic acid (6-MeOSA) is presented to examine the influence of methoxy substitution position on molecular structure and electronic behavior. The quantum-chemical calculations were performed using the Gaussian 16 software package. Ground-state geometries and structural parameters were optimized using Density Functional Theory (DFT) with the B3LYP functional and the 6-311++G(d,p) basis set, while excited-state properties, including electronic absorption and emission characteristics, were investigated using Time-Dependent Density Functional Theory (TD-DFT) at the same level of theory. The electronic structure was explored through frontier molecular orbitals, electronic spectra, and energy gap analysis, revealing noticeable differences in charge distribution and transition nature between the two isomers. Molecular electrostatic potential mapping and molecular surface analysis were employed to identify reactive sites and interaction regions, supported by global reactivity descriptors such as hardness, softness, electronegativity, and electrophilicity. Thermodynamic parameters including total energy, enthalpy, entropy, and Gibbs free energy were also evaluated to assess the relative stability of 3-MeOSA and 6-MeOSA. The results demonstrate that positional methoxy substitution plays a significant role in modulating the structural, electronic, and photophysical responses of salicylic acid derivatives, highlighting their potential relevance in optoelectronic, sensing, and photophysical applications.

[1] F. Lahmani, A. Zehnacker-Rentien, J. Phys. Chem. 101, 6141-6147 (1997).
[2] H.C. Joshi, C. Gooijer, G. Zwan, Journal of Fluorescence 13, 3 (2003).
[3] S. Jang, S. II Jin, C.R. Park, Bull. Korean Chem. Soc. 28, 12 (2007).

P63

Photophysical and Multiphysical Properties of Nitride-Based Perovskite $SrReN_3$: A First-Principles Study

*Nisha Mahepal, Trilok Akhani and Mitesh Solanki
[1]Department of Applied Science and Humanity, Parul Institute of Technology, Parul University, Vadodara, Gujarat, India.
**Corresponding author: Nisha Mahepal (Email – nishamahepal@gmail.com)*

Abstract –

Nitride-based perovskites have recently emerged as promising candidates for optoelectronic and light-driven applications owing to their high thermal stability and tunable electronic structure. In this work, we investigated the photophysical and optical properties of the perovskite $SrReN_3$ using first-principles density functional theory (DFT). The optimized monoclinic structure exhibits a Goldschmidt tolerance factor of 0.98, confirming its structural stability with strong Re–N covalent bonding. The calculated electronic band structure shows a direct band gap of 1.82 eV, suitable for visible-light absorption. The density of states reveals significant Re-5d and N-2p orbital hybridization near the Fermi level, which governs the optical transitions. Optical analyses derived from the complex dielectric function indicate strong UV and visible absorption, high reflectivity in the infrared–visible region, and a pronounced plasmon resonance, highlighting its potential in UV photodetectors, plasmonic devices, and optical coatings. The mechanical and thermoelectric results further confirm $SrReN_3$'s robustness for high-temperature optoelectronic operation.

$$g(2)(\tau) = \frac{< n1(t)n2(t+\tau) >}{< n1(t) >< n2(t+\tau) >}$$

P64

- **indistinguishability *I*, also a loss-independen quantity, captures the degree to which two photons will interfere with each other in a HOM setup.** $I = T_2/2T_1$

Appli

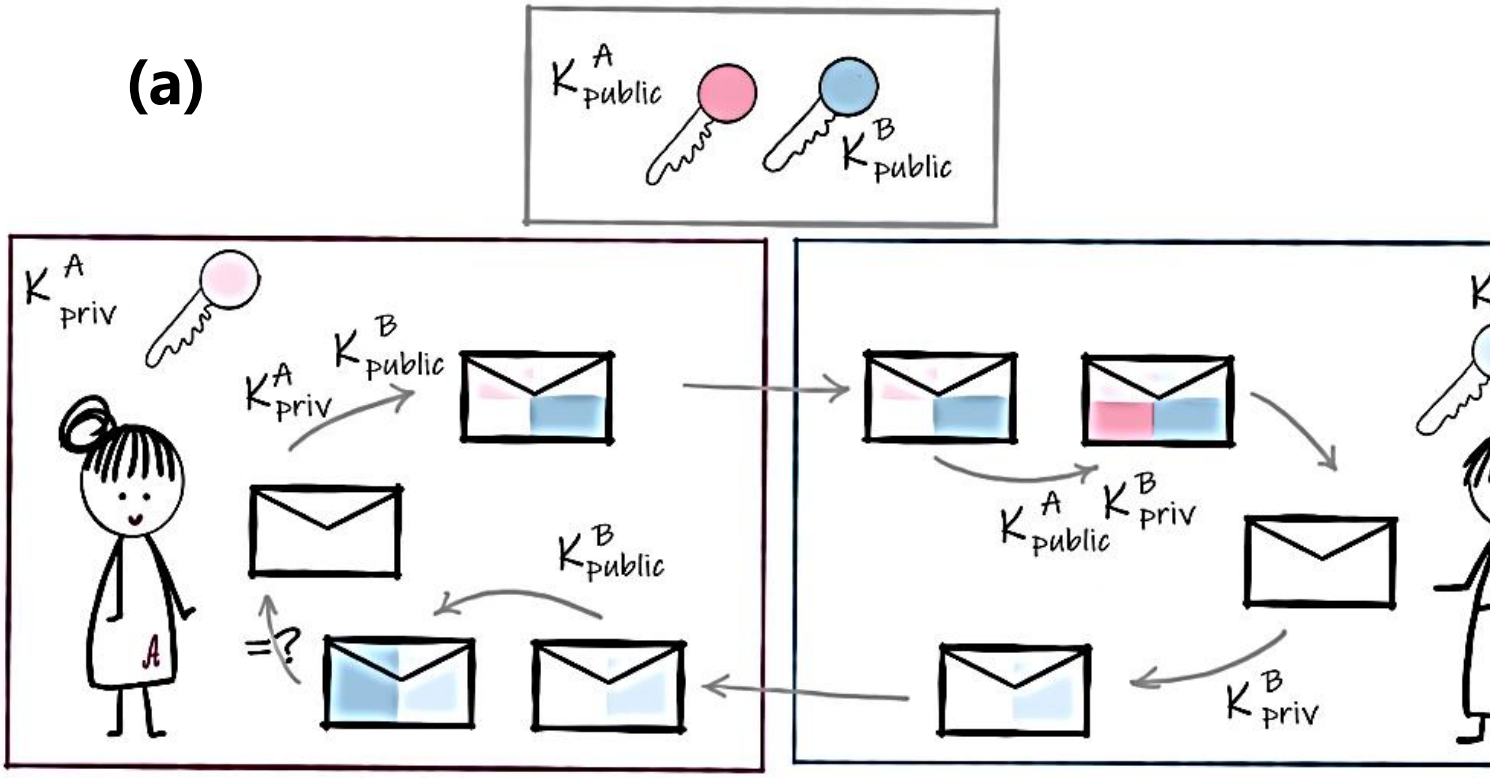

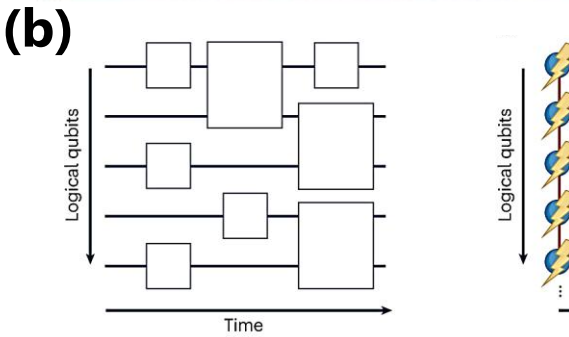

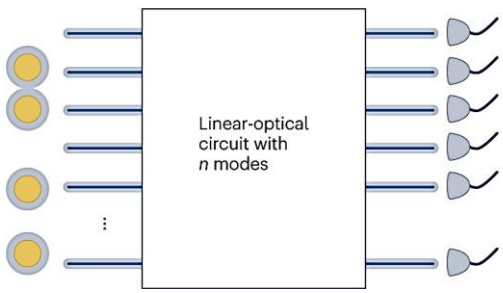

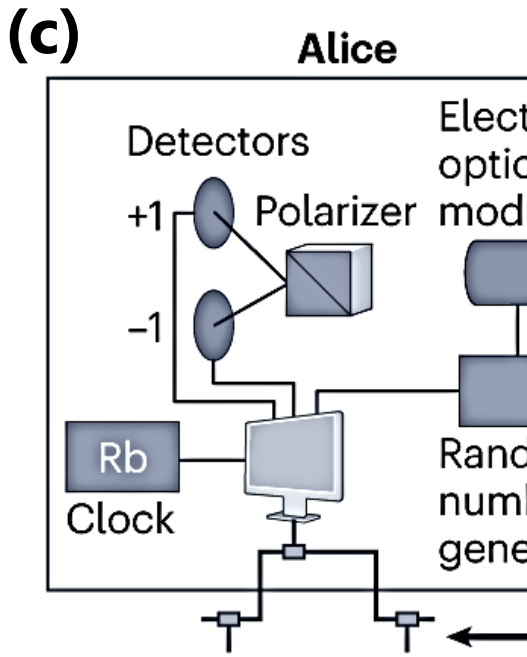

P65

Emergent Excitonic Physics and Interlayer Coupling in Bubble-Free hBN-Encapsulated TMDC Heterostructures

Sudipta Majumder[1], Rahul Chand[1,2], Pradeepa H L[1], Meghasree Basu[1], Avinash Mahapatra[1], Sweta Verma[1], Sagnik Chatterjee[1], Kenji Watanabe[3], Takashi Taniguchi[4], GV Pavan Kumar[1], Atikur Rahman[1]

[1] Department of Physics, Indian Institute of Science Education and Research, Pune, Maharashtra, 411008, India.

[2]Present Address: Faculty of Engineering and Natural Sciences, Tampere University, FI-33014, Tampere, Finland

[3] Research Centre for Functional Materials, National Institute for Material Science, Tsukuba, Ibaraki 305-0044, Japan.

[4] International Centre for Materials Nanoarchitectonics, National Institute for Material Science, Tsukuba, Ibaraki 305-0044, Japan

Two-dimensional (2D) transition metal dichalcogenides (TMDCs) are emerging as a versatile platform for next-generation optoelectronic, photonic, and quantum devices due to their strong excitonic effects, spin–valley coupling, and layer-dependent band structure. However, interfacial contamination, bubbles, and strain in fabricated heterostructures often obscure their intrinsic properties, limiting device performance. Here, we introduce a novel hBN-assisted encapsulation strategy for CVD-grown TMDCs that combines high-temperature processing with an inclined substrate geometry, termed the Hot Inclined Touchdown (HITD) method. This technique leverages the strong adhesion between TMDCs and hBN to achieve clean lift-off from SiO_2 substrates without harsh chemicals, removing interfacial contaminants and minimizing defects. Using this approach, we assemble high-quality homo- and heterobilayers, including MoS_2/MoS_2, WSe_2/WSe_2, and $WSe_2/MoSe_2$, which exhibit narrow excitonic linewidths, enhanced photoluminescence, pronounced interlayer Raman modes, and spatially indirect excitons, demonstrating strong interlayer coupling. Our method provides a scalable route to atomically clean vdW heterostructures, enabling both fundamental excitonic studies and advanced 2D optoelectronic and quantum devices.[1]

[1] Enhanced Excitonic and Interlayer Coupling in Bubble-Free hBN/TMDC Heterostructures, Sudipta Majumder, Rahul Chand, Pradeepa H L, Meghasree Basu, Avinash Mahapatra, Sweta Verma, Sagnik Chatterjee, Kenji Watanabe, Takashi Taniguchi, GV Pavan Kumar, Atikur Rahman. (Under Review)

P66

Self-Powered broadband and polarisation-sensitive photodetection in CrSBr/WSe_2 van der waals heterostructure

Saqlain Mushtaq[1], Meghashree Basu[1], Atikur Rahman[1].

[1] Department of Physics, Indian Institute of Science Education and Research (IISER), Pune, Maharashtra, 411008, India.

Although photodetectors based on 2D materials show better responsivity and gain but suffer in terms of other factors like slow response time, higher recombination rates etc. On the other hand photodetectors based on heterojunction of two or more materials not only help to overcome these anomalies but also synergistically add to the list of tunable parameters. Here we report a high performance photodetector based on CrSBr-WSe_2 van der waals heterostrucure. CrSBr is an anisotropic magnetic semiconductor with bandgap in the NIR region while as WSe_2 is an isotropic p-type semiconductor emitting in the visible region. The two combine to form a p-n junction with a type -III band alignment. Due to the strong built in electric field, the device shows a strong photo response even at zero bias highlighting the efficient charge separation at the interface. The heterojunction shows a broadband photo response extending from 400nm-940nm with ON-OFF ratio of 4 orders of magnitude in the visible region. The device shows a fast photo response with rise time of around 480µs and fall time of 660µs, suitable for high speed electronics. Furthermore, due to the strong in plane anisotropy of the CrSBr, the photodetector shows pronounced polarization dependent photocurrent, with clear modulation as the polarization direction of incident light is rotated, confirming the role of anisotropic absorption of CrSBr in the photo response of the device. These results establish CrSBr-WSe_2 heterostructures as promising building blocks for next-generation low-power, broadband, and polarization-sensitive optoelectronic and sensing applications.

P67

Host-dependent Photoluminescence Properties of Lanthanide Doped $A_2P_2O_7$ (A= Ca and Ba) Phosphors

M. Parvathy [1], P.S. Ghosh [2], A. Arya [2] and M. Sabeena [1]

[1]Materials and Metallurgy Laboratory, Department of Physics, Cochin University of Science and Technology, Cochin, Kerala, 682022, India.

[2] Glass and Advanced Materials Division, Bhabha Atomic Research Centre, Trombay, Mumbai 400085, India

In recent years, rare-earth doped (RE) inorganic phosphors have been established as useful luminescent materials in fabricating optoelectronic devices[1]. Recently, considerable efforts have been devoted to investigating materials with different emission properties that can be used for white LEDs(w-LED) and optical storage devices. Compared to traditional incandescent and fluorescent lamps, w-LEDs have advantages such as high brightness, long lifetime, low power consumption, the absence of toxic mercury, and environmental friendliness. Many methods are currently used to produce w-LED, such as combining blue LEDs with green and red phosphors, using UV-LEDs combined with blue, green, and red phosphors, etc. Among different RE elements, Dysprosium (Dy) doped phosphors are widely explored for w-LED applications due to their intrinsic color tunability. This tunability arises from the ability to modulate the yellow-to-blue (Y/B) emission intensity ratio, which is governed by the electric dipole (ED) transition and the magnetic dipole (MD) transition[1-2]. Similarly, Europium (Eu) in its 3+ oxidation state stands out due to its potential to emit highly monochromatic red emission, which can be used as the red component for the white light generation. Also, Eu^{3+} can be used as a probe to study the structural properties of the host matrix. Pyrophosphate materials are interesting due to the spectroscopic behavior of metal cation polyhedra with well-defined, low-symmetry coordination with multiple 'A' sites, making them highly useful for color tuning[2]. This study investigates the influence of crystal field environments on the luminescence properties of Dy and Eu doped $A_2P_2O_7$ (A= Ca and Ba) host matrices. The present study focuses on the structure and luminescence correlation studies through detailed X-ray diffraction (XRD) and Photoluminescence (PL) spectroscopy, complemented by the detailed DFT+U calculations.

[1] M. Parvathy, P.S. Ghosh, A. Arya, M. Sabeena, Mater.Res.Bull. 178, 112885 (2024).
[2] M. Parvathy, P.S. Ghosh, A. Arya, M. Sabeena, Mater.Res.Bull. 193, 113661 (2026).

P68

Electronic Restructuring and Conformational Inversion in Sulfur- and Oxygen-Based Heterocycles: Insights from Hydrated Cluster Analysis

Asif Iqubal Middya[1], Abhijit Chakraborty[1]

[1]The University Of Burdwan,Physics Department

The structural and electronic properties of heteroaromatic frameworks incorporating oxygen and sulfur exert profound influence on their conformational landscapes and noncovalent interaction profiles. In this work, we deliver an extensive quantum-chemical interrogation of isothiochroman (ITC) and isochroman (IC), both in the gas phase and within monohydrated microenvironments, with particular emphasis on deciphering the hierarchy and cooperative nature of S···H, O···H, N···H, and C···H interactions. A suite of *ab initio* and density-functional methodologies—B3LYP, ωB97X-D, M06-2X, MP2, and CCSD—combined with polarization- and diffuse-augmented basis sets, was employed to describe potential energy surfaces (PES), vibrational manifolds, and electronic delocalization pathways.

The PES topology unequivocally reveals that sulfur substitution leads a remarkable inversion in conformational preference: the bent conformer of ITC consistently manifests as the global minimum, while its twisted analogue resides higher by approximately 60 ± 40 cm^{-1}. Upon hydration, the electronic landscape undergoes substantial reorganization, giving rise to distinct hydrogen-bonding motifs. ITC:H_2O clusters are characterized by an intricate interplay of O–H···S and O–H···π bifurcated interactions, whereas IC:H_2O complexes predominantly feature robust, directionally potent O–H···O hydrogen bonds, thereby conferring superior thermodynamic stabilization.

Infrared spectroscopic signatures, particularly the pronounced red shifts of the ν_3(O–H) stretching mode, confirm that hyperconjugative charge transfer from heteroatom lone pairs into σ*(O–H) antibonding orbitals constitutes the principal stabilizing mechanism. Natural Bond Orbital (NBO) analysis corroborates the subtle competition between hyperconjugation and rehybridization, while Symmetry Adapted Perturbation theory (SAPT) elucidates the relative magnitudes of electrostatic, exchange, dispersion and induction contributions. Furthermore, QTAIM and RDG analyses reveal a rich spectrum of cooperative and weakly attractive interactions that modulate cluster stability.

.

References:

1. Middya I.A : Chakraborty A, Howdoes the conformational landscapechange on replacement in tetralin? Acomputational investigation withoxygen, sulphur and selenium, *Journal of Molecular Modelling*, 31 207(2025). https://doi.org/10.1007/s00894-025-06432-6

2. Bezbaruah J.M, Bezbaruah.B :Quantum mechanical studies on the mode of hydrogen bonding, stability and molecular conformations of phenol-water complexes. *computationalchemistry*, 07(03),5971(2019). https://doi.org/10.4236/cc.2019.73005

P69

Zn-Doped BiOBr Embedded in PVDF Sponge as a Recyclable Dip-Photocatalyst for Wastewater Treatment

Fayrouz S. Mohamed[1], Mohamed Ahmed[1], Alaa Farid[2,3], Hassan Nageh[4], Gehan Safwat[1], and Mohamed Taha[2]

[1]Faculty of Biotechnology, October University for Modern Sciences and Arts (MSA), Giza 12566, Egypt.
[2]Nano Gate Company, 9254 Hoda shaarawy, Al Abageyah, El Mukkatam, Cairo 11571, Egypt.
[3]Central Metallurgical Research and Development Institute (CMRDI),, Cairo 11421, Egypt.
[4]Nanotechnology Research Centre (NTRC), The British University in Egypt (BUE), El-Sherouk City, Cairo 11837, Egypt.

Abstract

Organic dye contamination in wastewater poses serious environmental and health challenges, motivating the development of efficient and reusable photocatalysts [1] . In this work, zinc-doped bismuth oxybromide (Zn–BiOBr) was synthesized via a solvothermal method to enhance photocatalytic performance through the generation of oxygen vacancies [2]. Structural, morphological, and chemical properties were investigated using XRD, FE-SEM/EDAX, FTIR, and XPS, confirming the successful formation of hierarchical BiOBr microspheres and the introduction of oxygen vacancies upon Zn doping. Optical and electrochemical analyses revealed improved charge separation, reduced recombination, and lower charge-transfer resistance in Zn–BiOBr compared to pristine BiOBr. The Zn–BiOBr photocatalyst achieved complete degradation of Rhodamine B within 35 minutes under light irradiation. To overcome the challenge of catalyst recovery from aqueous suspensions, Zn–BiOBr was immobilized into a highly porous polyvinylidene fluoride (PVDF) sponge, forming a three-dimensional dip-photocatalyst [3]. The resulting PVDF–Zn–BiOBr sponge demonstrated excellent photocatalytic efficiency and reusability, maintaining nearly constant performance over five consecutive cycles. This simple and scalable immobilization strategy offers a practical route for photocatalyst reuse, highlighting the potential of PVDF–Zn–BiOBr sponges for sustainable wastewater treatment and environmental remediation applications.

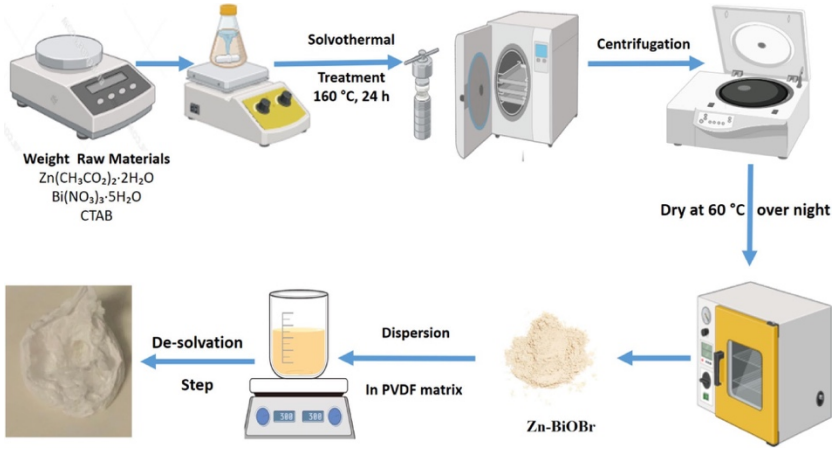

References

[1] M. F. Lanjwani et al., Inorg. Chem. Commun. 159, 111613 (2024).
[2] L. Yu et al., Appl. Surf. Sci. 649, 159169 (2024).
[3] M. Ahmed et al., Sci. Rep. 15, 42544 (2025).

P70

Molecular Insights into Electric Double Layer Formation at $Ti_3C_2T_x$ MXene–Ionic Liquid Interfaces

Kalyani Mohanty [1], **Kartick Tarafder** [1]

[1] *National Institute of Technology, Srinivasnagar, Surathkal, Karnataka – 575025*
E-mail id: kalyanimohantyphysics@gmail.com

Energy storing devices are essential to cater the ever-increasing demand of modern life. The quest for flexible, safe, and high-performance energy storage devices has directed research into next-generation electrochemical capacitors [1-3]. $Ti_3C_2T_x$ MXene has garnered substantial interest as an electrode material for electrochemical energy storage due to its remarkable electronic conductivity, layered structure, and diverse surface terminations (–O, –OH, –F). When combined with ionic liquids such as 1-butyl-3-methylimidazolium hexafluorophosphate (BMIM-PF_6), $Ti_3C_2T_x$ forms a stable electrochemical interface characterized by a well-defined electric double layer (EDL) [4,5].

In this study, we examine the formation of the EDL at the $Ti_3C_2T_x$-BMIM-PF_6 interface by analyzing charge density and electrostatic potential profiles. We observe significant ion layering near the MXene surface, with preferential adsorption of $BMIM^+$ and PF_6^- ions influenced by surface terminations and the applied surface charge. The electrostatic potential reveals strong screening effects within a few nanometers from the interface, leading to enhanced interfacial capacitance [6]. These findings provide valuable molecular-level insights into charge storage mechanisms at $Ti_3C_2T_x$ – ionic liquid interfaces and emphasize the importance of ion–surface interactions in optimizing MXene-based supercapacitors and electrochemical devices that utilize ionic liquid electrolytes.

[1] J. He, L. Cao, J. Cui, G. Fu, R. Jiang, X. Xu, C. Guan, Flexible energy storage devices to power the future, Adv. Mater. 36(4) (2024) 2306090.
[2] B.-H. Xiao, K. Xiao, J.-X. Li, C.-F. Xiao, S. Cao, Z.-Q. Liu, Flexible electrochemical energy storage devices and related applications: recent progress and challenges, Chem. Sci. 15(29) (2024) 11229-11266.
[3] X. Fan, C. Zhong, J. Liu, J. Ding, Y. Deng, X. Han, L. Zhang, W. Hu, D.P. Wilkinson, J. Zhang, Opportunities of flexible and portable electrochemical devices for energy storage: expanding the spotlight onto semi-solid/solid electrolytes, Chem. Rev. 122(23) (2022) 17155-17239.
[4] Y. Gogotsi and B. Anasori, The rise of MXenes, ACS Nano 13, 8491 (2019).
[5] H. Li, A. Li, D. Zhang, Q. Wu, P. Mao, Y. Qiu, Z. Zhao, P. Yu, X. Su, and M. Bai, First-principles study on the structural, electronic, and lithium storage properties of Ti3C2T2 (T= O, F, H, OH) MXene, ACS omega 7, 40578 (2022).
[5] J. Xia, F. Chen, J. Li, and N. Tao, Measurement of the quantum capacitance of graphene, Nature Nanotechnology 4, 505 (2009).

P71

Investigating the effect of metal and non-metal dual doping on the electrocatalytic performance of VSe_2 for water splitting

Riya Mudoi[1,2], Lakshi Saikia[*1,2]

[1]*Materials Sciences Group, Coal, Energy and Materials Sciences Division, CSIR-North East Institute of Science and Technology, Jorhat-785006, Assam, India*

[2]*Academy of Scientific and Innovative Research, Ghaziabad-201002, Uttar Pradesh, India*

Transition metal dichalcogenides have emerged as promising alternatives to noble-metal based catalysts due to their earth-abundance, low-cost and tunable electronic structure. Among them, vanadium diselenide (VSe_2) has attracted significant attention in the field of heterogeneous catalysis due to its metallic conductivity, layered structure and ferromagnetic nature [1]. However, the large value of hydrogen adsorption energies and limited number of active sites limit its intrinsic catalytic activity which requires further strategic modifications to enhance the performance [2]. To address these limitations, heteroatom doping has emerged as an effective way to boost the catalytic activity by modulating the electronic structure, activating inert basal planes and improve adsorption energies [3]. In this work, we have employed a metal-non-metal dual-doping strategy to engineer the catalytic properties of VSe_2 for electrocatalytic water splitting. Preliminary crystallographic, structural and spectroscopic analyses indicate successful dopant incorporation and modulation of the local coordination environment. The incorporation of dopants also induced noticeable morphological changes that led to a reduction in the thickness of the VSe_2 nanosheets. Initial electrochemical studies show a noticeable improvement in catalytic performance upon dual doping. Cyclic voltammetry exhibits clear oxidation and reduction peaks which reflects the activation of redox-active sites. Density functional theory (DFT) calculations reveal noticeable lattice modifications when dopants are introduced which further supports the structural changes observed experimentally. The calculations also identified the catalytically active sites responsible for the enhanced HER performance. These results collectively underline the synergistic influence of metal and non-metal dual doping on tuning the catalytic behavior of VSe_2 which highlights its promise for sustainable energy applications.

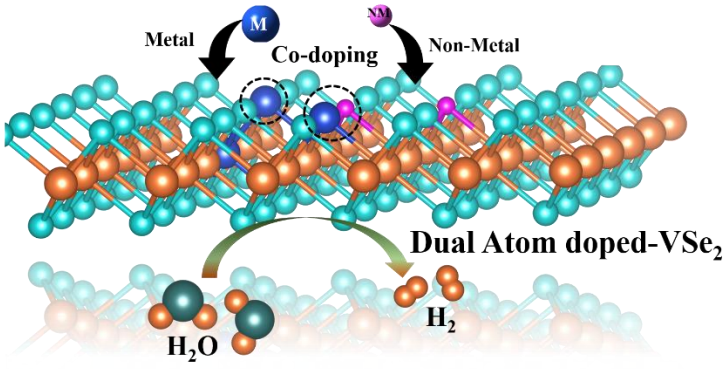

[1] F. Ming, H. Liang, Y. Lei, W. Zhang, and H. N. Alshareef, Nano Energy **53**, 11 (2018).

[2] Q. Zhu, M. Shao, S. H. Yu, X. Wang, Z. Tang, B. Chen, H. Cheng, Z. Lu, D. Chua, and H. Pan, ACS Appl. Energy Mater. **2**, 644 (2018).

[3] Z. Li, X. Li, Y. Gu, X. Hu, L. Wang, and P. Li, Appl. Surf. Sci. **646**, 158959 (2024).

P72

Bi_2WO_6-ZnO heterostructures for photocatalytic degradation of organic dyes

Deependra Das Mulmi[1], Sudhan Koirala[1,2], Damodar Neupane [1,2], Rishi Ram Ghimire[2]

[1]Nanomaterials Research Laboratory, Nepal Academy of Science and Technology, Khumaltar, Lalitpur 4470, Nepal

[2]Department of Physics, Patan Multiple Campus, Tribhuvan University, Lalitpur 44700, Nepal

Heterostructured Bi_2WO_6–ZnO nanocomposite was successfully synthesized via a hydrothermal route and systematically characterized using X-ray diffraction (XRD), UV–visible spectroscopy, and Fourier-transform infrared (FTIR) analysis. The Bi_2WO_6–ZnO heterojunction exhibited outstanding photocatalytic performance toward methylene blue (MB) degradation, achieving approximately 94% removal within 90 min of irradiation. The markedly enhanced photocatalytic activity is attributed to the formation of an efficient heterojunction interface between Bi_2WO_6 and ZnO, which promotes effective separation and migration of photogenerated charge carriers while suppressing electron–hole recombination. Furthermore, the synergistic band alignment facilitates enhanced light absorption and accelerates the generation of reactive oxygen species (•OH and $•O_2^-$), which play a dominant role in the oxidative degradation of MB.

P73

Design and Analysis of Gold Nanoparticle-Based PCF for Cancer Cells Detections

Sushmita*, Than Singh Saini
Department of Physics, National Institute of Technology Kurukshetra, Kurukshetra-136119, Haryana, India
**Corresponding email: 62410041@nitkkr.ac.in*

Abstract: Nowadays, cancer is one of the most harmful diseases across the world. Although there are different methods for the detection of cancer but these are costly and time consuming. So, we need an advance method for the early cancer detection which is accurate and more efficient [1]. This work presents a design of gold nanoparticle based Photonics Crystal Fiber (PCF) for the detection of different cancer cells at early stages. This PCF sensor operates when there is a change in refractive index of normal and cancer cells [2]. Presented work reports the performance of PCF biosensor on the basis of confinment loss. The cross-section view of the PCF containig silica as base material with gold nanoparticle is shown in fig1(a). The main purpose of this biosensor is to analyse the RI changes of normal and cancerous cell in the analyte channel. Here it was observed that the peak varies for all cancer cells with their respective normal cell and the value of the confinment loss (CL) for normal cells was shorter than cancerous cells as shown in fig 1(b) [3].

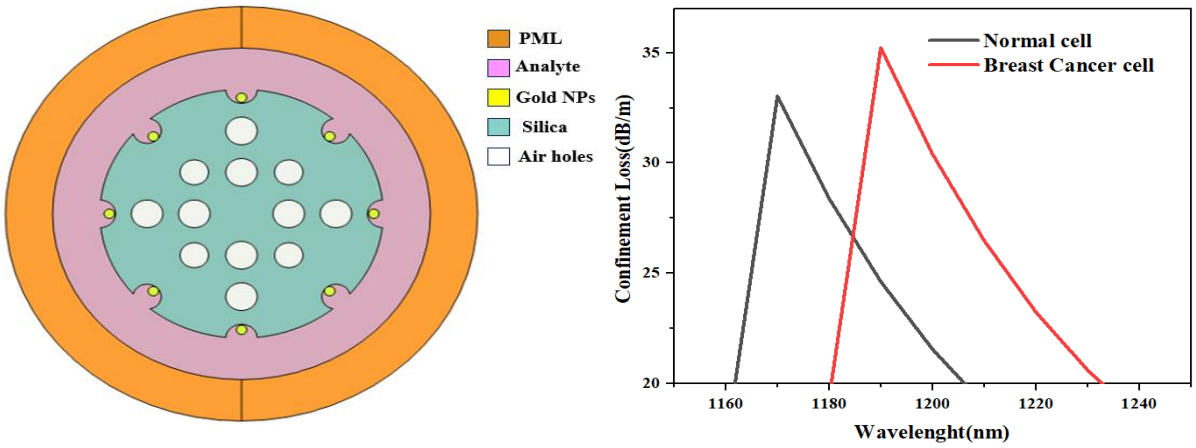

Fig. 1: (a) Cross sectional view of the reported PCF; (b) Spectral variation of CL for normal and cancer cells.

This variation in the peak of CL is observed due to the change in the RI of cancerous cells and normal cells. After evaluating the change in CL graph for both the cells the sensitivity was found to be around 1428.5 dB/m/RIU and detection limit is 0.053 nm RIU per unit loss for breast cancer cells.

References:

[1] M. Y. Azab, M. F. O. Hameed, and S. S. A. Obayya, "Overview of Optical Biosensors for Early Cancer Detection: Fundamentals, Applications and Future Perspectives," Feb. 01, 2023, *MDPI*. doi: 10.3390/biology12020232.

[2] A. Bansal, N. Jaggi, T. S. Saini, "Design and Numerical Analysis of On-chip Leaky Waveguide Structure for Cancer Cell Detection" Cell Biochemistry and Biophysics https://doi.org/10.1007/s12013-025-01864-6.

[3] C. Yang, S. Xiao, Q. Wang, H. Zhang, H. Yu and D. Jia "Nanoparticle-Based FM-MCF LSPR biosensor with open air-hole" doi: 10.3389/fsens.2021.751952.

P74

Probing Spectral and Dynamical Aspects of Photoluminescence–Plasmon Coupling in PPV–Silver Systems

Yadav Rohit Umashankar, Parinda Vasa

Indian Institute of Technology Bombay, India

We investigate the interaction between the photoluminescence (PL) of the organic semiconductor polymer poly(para-phenylene vinylene) (PPV) [1] and propagating surface plasmon polaritons (SPPs) supported by a thin silver film. PPV was optically excited at 400 nm, corresponding to its absorption band, and the resulting PL was coupled to SPP modes at the PPV–Ag interface [2]. Angle-resolved measurements reveal both weakly and strongly outcoupled PL components transmitted through the metal film, with distinct spectral signatures of strong PL–SPP coupling [3-5] observed across the characteristic PPV emission bands at 556 nm, 595 nm, and 669 nm. To probe the dynamical aspects of this coupling, time-correlated single photon counting (TCSPC) [6] measurements were performed on the outcoupled PL as a function of emission wavelength and angle, and compared with the direct PL from PPV. While pronounced strong-coupling features are evident in the outcoupled PL spectra, no measurable modification of the PL lifetime was observed within the temporal resolution of TCSPC. The findings point toward the necessity of employing complementary ultrafast time-resolved techniques to access coupling-induced lifetime dynamics not resolved within the TCSPC time window.

[1] C. A. Gedelian, K. C. Rajanna, B. Premerlani, and T. M. Lu, *J. Lumin.* 145, 473 (2014).
[2] T. U. Tumkur, G. Zhu, and M. A. Noginov, *Opt. Express* 24, 3921 (2016).
[3] P. Vasa and C. Lienau, *ACS Photonics* 5, 2 (2018).
[4] R. J. Holmes and S. R. Forrest, *Org. Electron.* 8, 77 (2007).
[5] P. Törmä and W. L. Barnes, *Rep. Prog. Phys.* 78, 013901 (2015).
[6] W. Becker, *Springer Ser. Fluoresc.* 5, 1 (2005).

P75

Integrating Diffuse Optics and Laser-Induced Spectrochemical Techniques for Reliable Biological Tissue Screening, Classification, and Characterization

Omnia Hamdy

Cairo University, National Institute of Laser Enhanced Sciences, 12613, Giza, Egypt

Optical diagnosis methods are gaining high impact because they are safe, minimally invasive, and non-destructive. Diffuse optical techniques are employed to estimate the absorption and scattering properties of biological tissues using light in the red and near-infrared range (~600-900 nm). Photons could travel deep in tissue in that spectral window due to the relatively small absorption of water and hemoglobin [1]. Light is recorded after passing through thick tissue and the optical properties are spatially reconstructed using mathematical models [2]. The transmitted and/or reflected signal can be reasonably modeled as a diffusive process. Diffuse reflectance and transmittance values are the key data in the tissue's optical parameters estimation process [3]. Tissue optical properties are wavelength dependent and are considered important indicators for tissue health as they are related to tissue's histopathology, hence, they can be utilized in cancer screening and diagnostic tools [4]. The absorption of light in tissues provides quantitative identification of the present molecules, their concentration, and their local environment, while the scattering of light provides information about micrometric-size objects (e.g., molecular weight) that cause light scattering [5]. Moreover, laser-induced fluorescence and laser-induced breakdown spectroscopy are promising spectrochemical techniques that are widely utilized for tissue classification via molecular and elemental analysis of the examined samples [6]. In this work, diffuse optics and spectrochemical techniques combined with different statistical evaluation methods are proposed for non-invasive tissue screening, characterization, and classification.

[1] S. Mahdy, O. Hamdy, M. A. Hassan, and M. A. A. Eldosoky, Lasers Med. Sci. **37**(3), 1855–1864 (2022).

[2] V. V. Tuchin, J. Biomed. Photonics Eng. **1**(2), 98–134 (2015).

[3] T. Durduran, R. Choe, W. . Baker, and A. G. Yodh, Rep Prog Phys. **73**(7), (2010).

[4] Y. Hoshi, Y. Tanikawa, E. Okada, H. Kawaguchi, and M. Nemoto, Sci. Rep. **9**(9165), 1–7 (2019).

[5] M. Eisel, S. Ströbl, T. Pongratz, H. Stepp, A. Rühm, and R. Sroka, J. Biomed. Opt. **23**(9), 091418-1–9 (2018).

[6] R. Gaudiuso, N. Melikechi, Z. A. Abdel-Salam, M. A. Harith, V. Palleschi, V. Motto-Ros, and B. Busser, Spectrochim. Acta - Part B At. Spectrosc. **152**, 123–148 (2019).

P76

Data-Driven Discovery of the Origins of UV Absorption in Alpha-3C Protein

Germaine Neza Hozana[1,2], **Gonzalo Díaz Mirón**[1], **and Ali Hassanali**[1]

[1] *International Centre for Theoretical Physics (ICTP)*
[2] *Dipartimento di Fisica, Universitá degli Studi di Trieste*

Over the last decade, there has been a growing body of experimental work showing that proteins devoid of aromatic and conjugated groups can absorb light in the near-UV beyond 300 nm and emit visible light. Understanding the origins of this phenomena offers the possibility of designing non-invasive spectroscopic probes for local interactions in biological systems. It was recently found that the synthetic protein α_3C displays UV-vis absorption between 250-800 nm which was shown to arise from charge-transfer excitations between charged amino acids. In this work, we use data-driven approach to re-examine the origins of these features using a combination of molecular dynamics and excited-state simulations. Specifically, an unsupervised learning approach beginning with encoding protein environments with local atomic descriptors, is employed to automatically detect relevant structural motifs. We identify three main motifs corresponding to different hydrogen-bonding patterns that are subsequently used to perform QM/MM simulations including the entire protein and solvent bath with the density-functional tight-binding (DFTB) approach. Hydrogen-bonding structures involving arginine and carboxylate groups appear to be the most prone to near-UV absorption. We show that magnitude of the UV-vis absorption predicted from the simulations is rather sensitive to the size of the QM region employed as well as to the inclusion of explicit solvation.

P77

TCAD-Based Performance Analysis of MFMIS FeFET for Energy Efficient Electronics

Nitika [1], **Kolla Lakshmi Ganapathi** [1,2]

[1] *Department of Physics, National Institute of Technology, Kurukshetra 136119, India*
[2] *Department of Physics, Indian Institute of Technology, Madras 600036, India*

Ferroelectric field-effect transistors (FeFETs) have gained significant attention for low-power and non-volatile memory applications. However, FeFET technology is still in its early stages, ongoing research aims to overcome challenges such as reducing leakage current and improving device reliability. In this work, a MFMIS FeFET is systematically analysed and simulated using Silvaco Atlas TCAD. The impact of metal gate work function engineering and interfacial layer material selection on electrical characteristics is analysed in detail. Three different metal gate work functions, 4 eV, 4.65 eV, 5 eV and two interfacial dielectrics, SiO_2 and HfO_2 are considered to study their impact on the device electrical behaviour. Key performance metrics such as drain current (I_D), transconductance (g_m) and output conductance (g_d) are evaluated to understand the device's performance under different design conditions. The optimized device exhibits high ON-current ($I_{ON}=10^{-3}$A) and low OFF-current ($I_{OFF}=10^{-13}$A). The simulation study also shows that optimized gate work function and appropriate interfacial layer choice significantly enhance the device performance. These results highlight the potential of engineered MFMIS FeFET for low-power electronic and memory applications.

[1] M. Singh, T. Chaudhary, and B. Raj, Int. J. Numerical Modelling: Electronic Networks, Devices and Fields **38**, e70055 (2025).
[2] S. Yadav, S. Rewari, and R. Pandey, Silicon **14**, 7245 (2022).

P78

First Principles Study of Structural and Electronic Properties of Cubic $Ca_{3-x}Mg_xPN$ Anti-Perovskites: Promising Lead-Free Photovoltaic Materials

Adhithya Pramod[1], Sushree Sangita Nanda[1], Vineetha P.[1], Lokanath Patra[2,*]

[1]Department of Physics, Mahatma Education Society's Pillai HOC College of Arts, Science, and Commerce (Autonomous), Rasayani, Maharashtra, India – 410207
[2]George W. Woodruff School of Mechanical Engineering, Georgia Institute of Technology, Atlanta, GA 30332, USA.

Photovoltaic technologies are in high demand due to the environmental impact of fossil fuels. Among emerging materials, perovskite and anti-perovskite materials stand out as candidates for next–generation solar cells due to their exceptional optoelectronic properties. This study employs density functional theory (DFT) to systematically investigate the structural and electronic properties of the ternary nitrophosphide series, $Ca_{3-x}Mg_xPN$ (x = 0 – 3), in its cubic phase. Structural optimisation reveals a monotonic decrease in lattice parameters with increasing Mg substitution, attributed to the smaller ionic radius of Mg^{2+} compared to Ca^{2+}. Electronic structure analysis of Ca_3PN indicates that the valence band maximum is primarily composed of N-2p and P-2p states, with minor contributions from Ca-3d orbitals, whereas the conduction band minimum is dominated by Ca-3d states. Progressive Mg incorporation gradually enhances the contribution of Mg-2p/3s states to the conduction band, becoming predominant in Mg3PN. All compositions exhibit direct band gaps at the Γ point, with values suitable for single-junction photovoltaic applications. Furthermore, the calculated electron and hole effective masses are notably low across the series, suggesting excellent charge-carrier transport properties. These findings highlight the potential of $Ca_{3-x}Mg_xPN$ anti-perovskites as efficient, tunable absorber materials for future thin-film solar cells.

*Corresponding author e-mail: lokanath.patra@me.gatech.edu

[1] Han, J., Park, K., Tan, S. *et al.,* Nat. *Rev. Methods Primers* **5**, 3 (2025).
[2] Li, Z., Klein, T., Kim, D. *et al.,* Nat. *Rev. Mater.* **3**, 18017 (2018)
[3] Dhiman Kalita *et al., J. Phys. D: Appl. Phys.* **57**, 343002 (2024)
[4] Sreedevi, P. D., Vidya, R., and Ravindran, P., *Solar Energy **190**, 350* (2019).
[5] Iqbal, S., Murtaza, G., Khenata, R. *et al. J. Electron. Mater.* **45**, 4188 (2016).
[6] K. Haddadi, A. Bouhemadou, L. Louail, S. Maabed, D. Maouche, *Phys. Lett. A*, **373**, 1777 (2009)
[7] Paolo Giannozzi *et al*., *J. Phys.: Condens. Matter* **21** 395502 (2009)
[8] Perdew, John P., Burke, Kieron and Ernzerhof, Matthias, *Phys. Rev. Lett.*, **78**, 1396 (1997)
[9] H. J. Monkhorst and J. D. Pack, *Phys. Rev. B*, **13**, 5188 (1976)
[10] Heyd, J., Scuseria, G. E., & Ernzerhof, M., *J. Chem. Phys.*, **124**, 214103 (2006

P79

Solvation-Driven Dual-Mode Fluorescence Response of Aminoquinoline Derivative for Water Detection

Nupur Pandey [1], Nisha Fatma [1], and Sanjay Pant [1]

[1]Photophysics Laboratory, Department of Physics, Centre of Advanced Study, DSB Campus, Kumaun University, Nainital, Uttarakhand, India.

Solvatochromism has emerged as a versatile phenomenon for probing microenvironmental changes, offering a powerful direction to detect trace water in organic solvents. Water content, even at micromolar levels, can drastically influence chemical reactivity, making its detection vital in environmental, industrial, and biomedical domains [1,2]. In this study, an aminoquinoline derivative was employed as a probe to investigate preferential solvation in the binary mixture of 1,4-dioxane and water using fluorescence spectroscopy. UV-Vis absorption spectra exhibited a hypsochromic shift from 354 nm to 340 nm with increasing water content (0-100% v/v). A hump near 420 nm, weak in pure water, became strongly pronounced at 60% water in dioxane and then gradually diminished beyond this point, approaching the profile of neat water. Fluorescence emission, initially centered at 414 nm in pure dioxane, shifted progressively to 460 nm in water-rich environment, while the 540 nm band characteristic of water was modulated in intensity, being strongest at 60% water. The emission intensity increased up to ~10% water, but beyond this level it steadily decreased, reflecting fluorescence quenching. Importantly, sensing is achieved not only through intensity modulation but also via distinct wavelength shifts, providing a dual-mode detection strategy. These spectral transformations are attributed to preferential solvation, wherein water molecules selectively stabilize the excited states of the probe through polarity and hydrogen-bonding interactions. The study demonstrates the good sensitivity and low limit of detection (LOD), establishing it as fluorescence sensor for trace water detection in organic solvent, with broad relevance to industrial, environmental, and biomedical applications.

[1] K.C. Behera, B.N. Patra, B. Bag, Sens. Actuators B Chem. 338, 129861 (2021).
[2] P. Kumar, A. Ghosh, D.A. Jose, Chem. Select 6, 820 (2021).

P80

Layer-Dependent Study of Exfoliated MoS_2 for Photodetector Operation

Satish Pandey and Pramod Kumar

Department of Physics, Indian Institute of Technology Bombay, Mumbai 400076, India
Email ID - 23d1074@iitb.ac.in

Abstract:

Two-dimensional molybdenum disulfide (MoS_2) exhibits a strong light–matter interaction arising from its reduced dimensionality, layer-dependent electronic structure, and robust excitonic effects. This makes it an attractive material for photodetectors and optoelectronic devices. In this work, we investigate the layer-dependent optical characteristics of mechanically exfoliated MoS_2 flakes using Atomic Force Microscopy (AFM), Raman Spectroscopy, and Photoluminescence (PL) Spectroscopy to elucidate their light–matter interaction behaviour. AFM analysis confirms the successful exfoliation of MoS_2 with well-defined thickness and smooth surface morphology, enabling controlled optical absorption and minimising surface-induced scattering. Raman spectroscopy reveals the characteristic E^1_{2g} and A_{1g} phonon modes, with their frequency separation providing insight into layer number, interlayer coupling, and lattice dynamics. Photoluminescence measurements exhibit pronounced excitonic emission features, with thickness-dependent variations in PL intensity that reflect changes in exciton recombination and nonradiative relaxation pathways. The evolution of excitonic emission from thinner to thicker MoS_2 flakes highlights the interplay between dimensionality and light–matter interaction, where strong excitonic effects dominate in few-layer regimes, while reduced PL in thicker layers suggests enhanced exciton dissociation and prolonged carrier lifetimes. These observations are directly relevant to photodetector operation, where efficient light absorption and photocarrier generation are critical. The combined Raman, PL, and AFM study provides a fundamental understanding of structure-dependent light–matter interactions in mechanically exfoliated MoS_2, also offering a platform for the design and optimization of MoS_2-based photodetectors.

References

[1] G. Munkhbayar *et al.*, *A Study of Exfoliated Molybdenum Disulfide (MoS_2) Based on Raman and Photoluminescence Spectroscopy*, *Solid State Phenomena*, Vol. 271 (2018).
[2] Nalwa, Hari Singh. "*A review of molybdenum disulfide (MoS 2) based photodetectors: from ultra-broadband, self-powered to flexible devices*." *RSC advances* 10, no. 51 (2020): 30529-30602.
[3] Chen, Xia-Yao, et al. "*Multilayer MoS2 photodetector with broad spectral range and multiband response*." *Advanced Devices & Instrumentation* 5 (2024): 0042.

P81

HARNESSING ARTIFICIAL INTELLIGENCE FOR ENHANCED PHOTOPHYSICAL AND PHOTOCHEMICAL SYSTEMS: PATHWAYS TO SOLAR ENERGY CONVERSION AND PHOTOELECTROCHEMICAL CO_2 REDUCTION

Dr. Parveen Singh[1]

[1]*Department of Computer Science, GDC Udhampur, University of Jammu, Jammu*

This poster presents an interdisciplinary approach that leverages advanced artificial intelligence and machine learning techniques to accelerate innovation in photophysical and photochemical research, focusing on applications such as solar energy conversion and photoelectrochemical CO_2 reduction. Building on two decades of experience in computer science and AI-driven data mining across healthcare, environmental, and scientific domains, the work proposes AI-enabled predictive modeling, generative design of photocatalytic materials, and autonomous experimentation platforms. Deep learning architectures are shown to predict and optimize light-matter interactions, guide synthesis of efficient photovoltaic molecules, and interpret complex spectroscopic datasets to foster rapid discovery. The poster highlights workflow examples including inverse design for photoactive materials and ML-assisted catalyst screening for environmentally critical applications. Overall, this research demonstrates how integrating AI/ML with photophysical/photochemical systems accelerates discovery, fosters sustainable energy breakthroughs, and exemplifies cross-disciplinary collaboration within computational and physical sciences.

References

1) J. M. Cole, "Artificial Intelligence and Machine Learning in Photochemistry and Photophysics: Opportunities and Challenges," *Chemical Society Reviews*, 52(4), 1596-1612 (2023).
2) S. Kitchin et al., "Machine Learning for Solar Energy Materials Discovery," *Advanced Energy Materials*, 12(21), 2203724 (2022).
3) L. Yuan, M. S. Kim et al., "AI-Assisted Catalyst Screening for Photoelectrochemical CO_2 Reduction," *Nature Catalysis*, 5, 88-97 (2022).
4) M. Tsai and C. Li, "Deep Learning for Photophysical Property Prediction in Organic Materials," *Journal of Physical Chemistry C*, 127, 6742–6751 (2023).

P82

Unlocking Vanadium Dichalcogenide Monolayers (V_2Se_2 and V_2Te_2) for High-Performing Sodium-Ion Batteries: From Experiment to First-Principles

Mousumi Parvin[1], Beena Mol Babu[2, ¥], Tata Sanjay Kanna Sharma[2, ¥], Jayasmita Jana[2, ¥], Somnath Chowdhury[2, *], Seung Hyun Hur[2], Won Mook Choi, Sung Gu Kang[2, *], Bikash Chandra Gupta[1, *]

[1] *Department of Physics, Visva-Bharati, Santiniketan, India, 731235.*
[2] *School of Chemical Engineering, University of Ulsan, 93 Daehakro, Nam-Gu, Ulsan 44610, South Korea.*

Developing an efficient anode material is always beneficial for advancing sodium-ion battery (SIB) technology. Experimental studies on vanadium-based dichalcogenides have demonstrated the feasibility of synthesizing two-dimensional (2D) materials such as V_2Se_2 and V_2Te_2. These 2D monolayers were successfully synthesized using thermal treatment and characterized using X-ray diffraction (XRD), Raman spectroscopy, X-ray photoelectron spectroscopy (XPS), and field emission scanning electron microscopy (FESEM). Furthermore, Density functional theory calculations were performed to explore the potential of V_2Se_2 and V_2Te_2 monolayers as anode materials. The results confirmed their overall stability, supporting structural robustness during battery operation. Both monolayers exhibit low Na^+ diffusion barriers (0.24-0.28 eV), enabling rapid ion transport, along with a maximum theoretical capacity of 619.17 mAh/g and low open-circuit voltages, highlighting their strong potential as next-generation anode materials for sodium-ion batteries.

¥ Author contributed equally
Authors to whom the correspondence is to be addressed: *somnath89@ulsan.ac.kr (S Chowdhury), *sgkang@ulsan.ac.kr (SG Kang), and *bikashc.gupta@visva-bharati.ac.in (BC Gupta)

P83

Z scheme charge transfer study using $BiVO_4$/boron doped g-C_3N_4 for photoelectrocatalytic (PEC) water splitting

Kanchan J. Pawar [1] , **Archana S. Kalekar** [1]

Institute of Chemical Technology Mumbai, India [1]

The utilization of light-responsive semiconductor materials in photoelectrocatalytic water splitting stands as a promising way for green hydrogen production. To achieve this, artificial photosynthesis involving Z scheme comprising different semiconductor combinations is beneficial. In our current work, a Z scheme, involving bismuth vanadate ($BiVO_4$) and graphitic carbon nitride (g-C_3N_4), was synthesized and studied; notably due to their suitable bandgap, cost-effectiveness, high surface area, ease of synthesis, and stability. $BiVO_4$ in its stable monoclinic phase, with a bandgap of 2.42 eV, was obtained [1]. Thermal polymerization was employed for synthesizing pristine g-C_3N_4 and boron doped g-C_3N_4. The Z-scheme $BiVO_4$/boron doped g-C_3N_4 enhances charge transfer efficiency, and reducing electron-hole recombination, leading to improved photoelectrochemical (PEC) performance. Phase purity and structural composition confirmation were achieved through X-ray diffraction (XRD), Raman spectroscopy, and Fourier-transform infrared (FT-IR) spectroscopy analyses. Morphological characterization was conducted via scanning electron microscopy (SEM). The X-ray photoelectron spectroscopy (XPS) specifically done to know insights about boron doping in g-C_3N_4 framework [2]. PEC measurements provided insights into the material's nature, photocurrent density, and transient behaviour during solar water splitting. The observed substantial increase in PEC response of $BiVO_4$/boron doped g-C_3N_4 over their bare materials; highlights its potential for sustainable hydrogen generation. Thus, the current research can contribute to advancement of efficient and sustainable technologies for hydrogen production thorough understanding of underlying mechanisms of charge transfer, bandgap tunability; electrode/electrolyte interfacial processes in PEC studies.

1. Dai, J. *et al.* Regulating the electronic structure to construct root-soil-like S-scheme BiVO4/Nd-TiO2 heterojunction for visible degradation and hydrogen evolution. *Sep. Purif. Technol.* **354**, 129037 (2025).
2. Wei, B. *et al.* Insight into the effect of boron doping on electronic structure, photocatalytic and adsorption performance of g-C3N4 by first-principles study. *Appl. Surf. Sci.* **511**, 145549 (2020).

P84

Band Alignment and Optical Response in BN- and BP-Based MX_2 (M = Mo, W; X = S, Se) Heterostructures Toward Photocatalytic Water Splitting

Anandavadivel Annamalai[1], **Rajesh A. Prashanth**[1], **Baskar G.**[2] **and Bharathy G.**[3]

[1]*Department of Computer Applications, Dr. Rajalakshmi College of Arts and Science, Palavedu, Avadi-600 055, India.*
[2]*Department of Applied Chemistry, Sri Venkateswara College of Engineering, Sriperumbudur-602 117, India.*
[3]*Department of Applied Physics, Sri Venkateswara College of Engineering, Sriperumbudur-602 117, India.*

Two-dimensional (2D) van der Waals heterostructures have emerged as promising platforms for photocatalytic water splitting owing to their tunable electronic structure and efficient interfacial charge separation. In this study, we investigate the water-splitting potential of 2D/2D heterostructures formed by hexagonal boron nitride (BN) and boron phosphide (BP) combined with transition metal dichalcogenides MX_2 (M = Mo, W; X = S, Se), including BN/MoS_2, BN/$MoSe_2$, BN/WS_2, BN/WSe_2, and the corresponding BP-based systems.

First-principles density functional theory calculations are employed to construct lattice-matched heterostructures and to examine their structural stability using van der Waals corrected exchange correlation functionals. The electronic structure is analyzed through band structure and density of states calculations, with band edge positions referenced to the vacuum level to evaluate thermodynamic alignment with water redox potentials. Interfacial charge redistribution and electrostatic potential profiles are examined to assess charge separation characteristics and to identify favorable type-II or Z-scheme band alignment. Optical properties are investigated via dielectric function calculations to evaluate visible-light absorption. This study aims to provide fundamental insights into interface-driven electronic and optical properties governing photocatalytic water splitting in BN- and BP-based MX_2 heterostructures.

[1] M. Harb and L. Cavallo, ACS Omega **3**, 18117 (2018).
[2] J. Su, J. He, J. Zhang, Z. Lin, J. Chang, J. Zhang, and Y. Hao, Sci. Rep. **9**, 3518 (2019).

P85

Accelerating Photocatalyst Discovery in Halide Double Perovskites via Machine Learning Driven High-Throughput Screening

Zarna D. Ponkiya [1] and Prafulla K. Jha [1]

[1]Department of Physics, Faculty of Science, The Maharaja Sayajirao University of Baroda, Vadodara, Gujarat, India-390002

Halide double perovskites have attracted significant attention for photovoltaic and photocatalytic applications due to their tunable optoelectronic properties [1]. However, identifying suitable compositions for photocatalytic water splitting remains challenging because of the vast chemical space and the high computational cost of first-principles (FP) calculations. In this work, we develop a machine learning (ML) based framework to accelerate the discovery of stable halide double perovskites (HDPs) for water splitting applications. Using a dataset of approximately 800 $A_2BB'X_6$ compounds obtained from the Materials Project [2], ML models were trained to predict formation energy (E_f), energy above hull (E_h) as a measure of thermodynamic stability, band gap class (CL1: 0.5–4.0 eV; CL2: outside this range), and direct band gap values for CL1 compounds. The optimized models achieved strong predictive performance, with R^2 values of 0.97, 0.85, and 0.91 for E_f, E_h, and direct band gap prediction, respectively, and a classification accuracy of 90% for band gap class.

The trained models were employed to screen a large hypothetical compositional space of 1,183,612 HDPs. Based on geometric stability criteria, 33,874 compositions were identified as geometrically stable. Among these, 12,260 compounds with negative formation energies and $E_h < 0.05$ eV/atom were further selected as thermodynamically stable candidates. Band gap classification reduced this set to 7,791 compounds with band gaps in the light-harvesting range (0.5-4.0 eV), for which direct band gap values were subsequently predicted. Band edge positions were then estimated empirically to assess suitability for photocatalytic water splitting by satisfying the redox potential requirements [3]. This multistage screening yielded 722 HDPs as promising photocatalysts for water splitting. Solar-to-hydrogen efficiencies were further evaluated, and approximately ten of the most promising candidates were validated using detailed FP calculations. Overall, this study demonstrates a robust data-driven strategy for the rapid discovery of halide double perovskites for photocatalytic water splitting and provides practical guidance for future experimental realization.

[1] E. Meyer, D. Mutukwa, N. Zingwe, and R. Taziwa, Metals **8**, 667 (2018).

[2] A. Jain, S. P. Ong, G. Hautier, W. Chen, W. D. Richards, S. Dacek, and K. A. Persson, APL Mater. **1**, 011002 (2013).

[3] I. E. Castelli, D. D. Landis, K. S. Thygesen, S. Dahl, I. Chorkendorff, T. F. Jaramillo, and K. W. Jacobsen, Energy Environ. Sci. **5**, 9034 (2012).

P86

From Hydrothermal Crystals to Thin-Film-Compatible Growth of $Cs_2(Na/Ag)FeCl_6$ Double Perovskites

Vijayalakshmi.P[+] and Amrita Dey*

Department of Physics, School of Advance Sciences, Vellore Institute of Technology, Vellore, India-632014

E-Mail correspondence to: amritadey@vit.ac.in

Effective harvesting of solar energy is essential in meeting the ever-increasing energy demand and addressing the environment sustainability issues.[1] Lead-free, non-toxic halide double perovskite (HDP) have emerged in this regard, as a next generation sustainable semiconductor. However, the major challenge with HDP is their wide bandgap, limiting their full potential as efficient solar energy harvester. In recent years, HDPs based on earth abundant iron have been reported to exhibit low bandgap ~1.06 eV, showing its potential as solar energy harvester [2]. Nevertheless, studies on Fe-HDP are found to be limited, possibly due to challenges in their fabrication and thin film processing. In fact, all most every study reported till date on Fe- based HDP relied on growing the crystal using hydrothermal method which requires long waiting hours (18-24 hours) to prepare the HDP crystals. On the other side, ligand assisted reprecipitation (LARP) method has worked wonderfully as an easy and direct thin-film compatible technique for HDP in recent past [3]. Here, we reported that how these two processes differ in growing the $Cs_2(Na/Ag)FeCl_6$ HDP. While the hydrothermally grown-$Cs_2(Na/Ag)FeCl_6$ HDP reflects a sharp rise in the absorption band-edge at 600nm, LARP shows an extended absorption tail in the visible region, without clear signature of HDP phase formation. We analyse the structure-function relationship between LARP *vs* Hydrothermally grown $Cs_2(Na/Ag)FeCl_6$ HDP. Finally, we show a successful path to achieve smooth $Cs_2(Na/Ag)FeCl_6$ HDP thin films, for their potential application in energy harvesting devices.

References:

1. Review on recent Progress of leadfree halide perovskites in Optoelectronics, Nano energy, **2021**, 80, 105526.
2. Band-Gap Engineering of Lead-Free Iron-Based Halide Double Perovskite Single Crystals and Nanocrystals by an Alloying or Doping Strategy, J. Phys. Chem. C **2021**,125,11743−11749.
3. Lead-Free, Luminescent Perovskite Nanocrystals Obtained through Ambient Condition Synthesis, Small, **2023**, 19, 2300525.1

P87

Explainable Machine Learning for Data-Driven Discovery of Single Perovskites for Photovoltaic Applications

Towhidur Rahaman [1], Neelam Gupta [1], and Soumya Jyoti Ray [1]

[1]Department of Physics, Indian Institute of Technology Patna, Bihta 801106, India

Single perovskites (ABX_3) represent a structurally versatile and compositionally rich class of materials with strong potential for photovoltaic and optoelectronic technologies. Their broad chemical tunability enables wide variation in electronic properties, yet systematic exploration of this design space remains challenging without efficient predictive methodologies. In this work, we present an interpretable machine-learning (ML) framework aimed at accelerating the discovery and screening of ABX_3 perovskites. A curated dataset of 4,560 compounds from the Materials Project, encompassing structural, compositional, and electronic information, is used to construct an extensive descriptor set that incorporates elemental characteristics, structural features, and perovskite-specific metrics such as tolerance and octahedral factors.

Using AutoML-guided model selection, the framework achieves a band-gap prediction performance of $R^2 = 0.85$. SHAP-based interpretability further highlights the most influential chemical and structural descriptors governing electronic trends across the ABX_3 chemical space. Overall, the proposed framework offers a scalable and transparent pathway for identifying promising perovskite compositions and provides a robust foundation for guiding subsequent DFT-based validation and experimental investigation.

[1] Anjana Talapatra, Blas P. Uberuaga, Christopher R. Stanek, and Ghanshyam Pilania, *Chemistry of Materials*. ***33*** **(3), 845-858** (2021).
[2] Shiyan Wang, Chaopeng Liu, Weiyao Hao, Yanling Zhuang, Xianjun Zhu, Longlu Wang, Xianghong Niu, Shujuan Liu, Bing Chen, and Qiang Zhao, *ACS Nano*, *19* (32), 29049-29072 (2025).

P88

Enhanced nonlinear optical and photothermal properties of Sr/Bi-doped $LaMnO_3$ and $LaCoO_3$ nano-perovskites: Towards optoelectronic and biomedical applications

P89

A First-Principles Study of Rashba-Driven Hydrogen Evolution Activity in 2D BiSb and BiAs Monolayers

Abhay Rawat[1], Sudip Chakraborty[1]

[1]*(Harish Chandra Research Institute (HRI), Prayagraj, India)*

Two-dimensional (2D) materials with strong spin–orbit coupling (SOC) and broken inversion symmetry provide an attractive platform for manipulating electronic and catalytic properties. In this work, we perform first-principles density functional theory [1] calculations to investigate the electronic structure, Rashba spin splitting, and hydrogen evolution reaction (HER) activity of hexagonal BiSb and BiAs monolayers. Both systems adopt a buckled honeycomb structure and exhibit direct band gaps with pronounced Rashba-type spin splitting at the conduction band minimum near the Γ point, arising from strong SOC associated with the heavy Bi atom. The pristine BiSb and BiAs monolayers exhibit Rashba parameters of 2.26 eVÅ and 1.97 eVÅ, respectively. Biaxial strain is employed as an external tuning parameter to systematically modulate the Rashba spin splitting without compromising the structural stability of the monolayers. Tensile strain significantly enhances the Rashba parameter, whereas compressive strain suppresses it. Spin texture analysis confirms a robust Rashba-type chiral spin configuration across all strain values, indicating a pure Rashba mechanism. To evaluate HER activity, we compute the Gibbs free energy of hydrogen adsorption (ΔG^*_H) on strained BiSb and BiAs surfaces. We find that ΔG^*_H decreases as the Rashba splitting increases, leading to an enhancement in HER efficiency. Enhanced Rashba splitting suppresses electron–hole recombination by lifting spin degeneracy and introducing spin-split intermediate states near the band edges. As a result, carrier lifetimes are prolonged, increasing the availability of electrons for participation in the HER process [2]. Bader charge analysis further reveals enhanced charge transfer to the adsorbed hydrogen atom and strengthened H–substrate bonding in regimes of stronger Rashba splitting. Our results establish the possibility that Rashba spin–orbit coupling acts as a key driving factor for enhanced HER activity, with strain serving as an effective control parameter. This study highlights Rashba engineering as a promising strategy for the design of efficient 2D electrocatalysts.

[1] P. Hohenberg and W. Kohn, Phys. Rev. 136, B864 (1964).

[2] D. Kumar and S. Chakraborty, J. Mater. Chem. A 12, 10287 (2024).

P90

Fluorescence enhancement in hexagonal boron nitride quantum dots coupled microcavity

Debojyoti Ray Chawdhury[1], Shruti Narayanan[1], Prem Ballabh Bisht[1, 2]
[1]*Department of Physics, Indian Institute of Technology Madras, Chennai, India*
[2]*Centre of Excellence in Biochemical Sensing and Imaging Technologies (CenBioSIm), IIT Madras, Chennai, India*

Quantum dots (QDs) are excellent candidates in quantum imaging, sensing and single photon emission [1]. In this work, QDs of hexagonal boron nitride (hBN) have been synthesized by using bottom-up approach [1]. The QDs have been incorporated in dielectric microcavities to study the effect of nano-microcavity interaction. Photoluminescence (PL) spectra were recorded for QDs coupled polystyrene (PST) microspheres of different sizes (Fig. 1(A)). The number of whispering gallery modes (WGMs) increases with the size of the microspheres. PL enhancement (~4 times) was observed for QDs coupled microcavity (Fig. 1(A)). Inset of Fig. 1(A) shows the patches on smooth surface of PST microsphere due to the presence of QDs.

According to Mie theory, the scattering efficiency (Q_{sc}) can be written as [2]

$$Q_{sc} = \frac{2}{(kr)^2}\sum_{n=1}^{\infty}(2n+1)(|a_n|^2 + |b_n|^2) \quad (1)$$

where k is the wave vector, r is the radius of the microsphere, a_n and b_n are the scattering coefficients corresponding to transverse magnetic (TM) and transverse electric (TE) modes, respectively. Using Eqn. (1), the modes can be fitted with a microsphere of radius ~3.3845 μm and refractive index 1.595 (Fig. 1(B)). The broadness of WGMs in the experimental spectrum is due to the absorption and scattering losses by the QDs. These sharp resonant modes (WGMs) find applications in sensing, bioimaging, microlasing and cavity quantum electrodynamics.

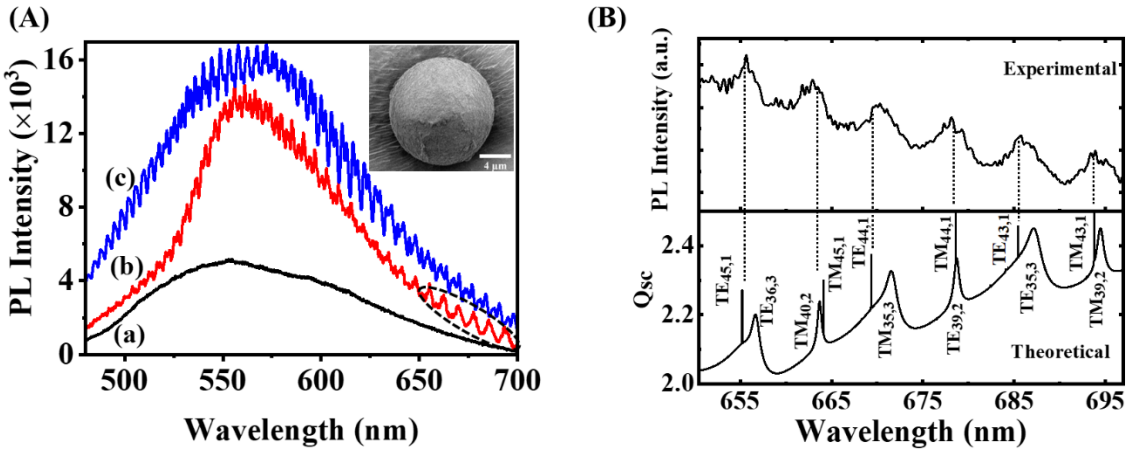

Figure 1. (A) PL of (a) hBN QDs, and hBN QDs coupled PST microspheres of radii (b) ~3 μm, and (c) ~7 μm. Inset shows the scanning electron microscope image of QDs coupled PST microsphere, and (B) theoretical fitting (bottom panel) of WGMs for a part of PST microsphere (encircled portion in Panel A). From the fitting, the radius (r) of the PST microsphere is determined as ~3.3845 μm. The dotted lines are guide to the eye.

[1] Yongliang Chen, Xiaoxue Xu, Chi Li, Avi Bendavid, Mika T. Westerhausen, Carlo Bradac, Milos Toth, Igor Aharonovich, and Toan Trong Tran, "Bottom-Up Synthesis of Hexagonal Boron Nitride Nanoparticles with Intensity-Stabilized Quantum Emitters," Small **17**, 2008062 (2021).
[2] G. Mie, Beitr¨age zur Optik trüber Medien, speziell kolloidaler Metall¨osungen, Ann. Phys. **330**, 377 (1908).

P91

Chirality-Driven Second Harmonic Generation and Distinctive Modal Raman Optical Activity in SiC−GeC Quantum Nanodots

Anirban Roy [1], Deep Mondal [2], Supriya Ghosal [3] and Debnarayan Jana [1]

[1]*Department of Physics, University of Calcutta, 92 A.P.C. Road, Kolkata 700009, India*
[2]*Department of Physics, Indian Institute of Technology Bombay, Mumbai-400076, India*
[3]*Theoretical Sciences Unit, Jawaharlal Nehru Centre for Advanced Scientific Research, Bangalore, Karnataka 560064, India*

Quantum confinement in heterojunction configuration enables customizable electronic features and effective interfacial charge separation, providing a solid foundation for future generation optoelectronics. However, the nuanced connection between structural asymmetry, Raman optical activity (ROA) and nonlinear optical (NLO) signals, particularly while performing selective solvent adaptation remains largely unexplored. Motivated by the newly synthesized honeycomb monolayer of SiC [1], we present the comprehensive analysis of modal Raman optical activity, with solvent and chirality-driven hyper-Rayleigh scattering (HRS) in 18 distinct quantum dots of SiC, GeC and isostructural SiC−GeC, ranging from 1 to 3 nm [2]. By examining diverse point group symmetries within this material family, we identify a distinct chiral SiC−GeC configuration and conduct an extensive ROA analysis over all pertinent scattering geometries and feasible experimental circumstances. The detection of a low-frequency chiral phonon mode, circular intensity difference signatures, and optical tensor-dependent handedness descriptors confirm the vibrational basis of chiral response. Employing NLO phenomena in such engineered nanostructures are crucial for next-generation photonic platforms, including quantum information processing and integrated light control. In addition to dynamic higher-order hyperpolarizability profiling, we have further investigated the second harmonic generation (SHG) using HRS, indicating strongly polarized and symmetry-governed signals with a high depolarization ratio and multipolarity factor. Additionally, when these designed enantiomers are placed in chiral environments, a significant enhancement in chiral-specific HRS is observed [3]. This elevation of chiral-specific HRS in these enantiomers demonstrates their promise for real-world applications such as enantioselective biosensing, drug purity monitoring, and improved circularly polarized display technology.

[1] C. M. Polley et. al. Phys. Rev. Lett. 130, 076203 (2023)
[2] A. Roy et. al. ACS Appl. Nano Mater. **8**, 1852-1864 (2025)
[3] A. Roy et. al. J. Phys. Chem. C 129, 15825−15842 (2025)

P92

Engineering Ce-MOF/$CoFeO_3$ Heterostructures for Enhanced Piezo-Photocatalytic Chromium Reduction and Nitrogen Fixation

Vahid Safarifard*, Negin Khosroshahi, Nooshin Gholhovallahi Ardakan, and Parsa Azaddehghan

Department of Chemistry, Iran University of Science and Technology, Tehran 16846-13114, Iran

Metal–organic framework (MOF) composites are emerging as promising platforms for light-driven redox reactions due to their structural tunability, high surface area, and ability to interface with functional inorganic phases. In this work, we developed a series of Ce-based MOF/$CoFeO_3$ heterostructures and evaluated their performance as hybrid piezo-photocatalysts under simultaneous visible-light irradiation and ultrasonic mechanical excitation. Structural analysis confirmed successful integration of MOF frameworks (Ce-UiO-66, Ce-MOF-808, Ce-MOF-801) with MOF-derived $CoFeO_3$ nanoparticles without altering the crystalline integrity of the parent MOFs. The resulting heterojunctions exhibited broadened optical absorption (200–550 nm), reduced band gaps, improved charge-carrier separation, and lowered recombination rates, as demonstrated by UV–vis DRS, PL, EIS, and photocurrent measurements.

Among the prepared materials, the $CoFeO_3$/Ce-MOF-801 composite showed the most efficient dual-mode catalytic behavior, achieving 100% Cr(VI) reduction within 30 minutes at pH = 1 and an ammonia production rate of 292.13 μmol g^{-1} h^{-1} L^{-1} in N_2 fixation. Mott–Schottky analysis revealed p–n semiconductor coupling between $CoFeO_3$ and Ce-MOF-801, enabling directional interfacial charge transfer. The synergy between piezoelectric polarization and photoexcitation substantially enhanced electron–hole separation and boosted overall redox efficiency.

These results demonstrate that Ce-MOF/$CoFeO_3$ heterostructures constitute a robust and low-cost class of piezo-photocatalysts with strong potential for applications in environmental remediation and solar-to-chemical energy conversion.

[1] S. Tu, et al., Adv. Funct. Mater. **30**, 2005158 (2020).
[2] B. Dai, et al., Chem. Soc. Rev. **50**, 13646 (2021).
[3] J. He, et al., Crystals **13**, 1382 (2023).
[4] L. Pan, et al., Adv. Energy Mater. **10**, 2000214 (2020).
[5] Y. Li, et al., Chem. Commun. **58**, 11488 (2022).

P93

Convoluted nested square split ring resonator for multiband and chiral response in THz range

Bhavya Sanghavi[1], Parinda Vasa*

[1], Department of Physics, IIT Bombay, Mumbai, India*

[1]bhavyasnghavi18@gmail.com, *parinda@iitb.ac.in

Terahertz radiation (0.1–10 THz; 0.03–3 mm) bridges the microwave and infrared domains, enabling non-ionizing, high-resolution imaging and spectroscopy. Its applications span biomedical diagnostics (e.g., tumour margin mapping), pharmaceutical quality control (polymorph detection), and non-destructive testing of composites. Emerging THz wireless links promise multi-gigabit to terabit-per-second data rates for future 6G networks. Metastructures artificially engineered subwavelength arrays of resonators tailor terahertz wavefronts through precise control of amplitude, phase, and polarization. In the THz range, metasurfaces enable ultra-compact devices for beam steering, flat-lens imaging, and dynamic modulation. They serve as highly sensitive sensors for molecular fingerprinting and environmental monitoring via enhanced field confinement. The split ring resonator is quite commonly used metastructure design, which can provide tailoring of optical response in desired frequency range. Using convolution, we can expand the usage of any structure by making it multiband, and making it strongly interacting with EM wave. In this work, we have explored modifying the split ring resonator structure by changing the slot position and making it double L shaped structure. The change slot position making it double L shaped provides asymmetry and gives chirality to the structure, as a result, it behaves differently for RCP and LCP lights. Along with that the convolution of two such structure provides multiple band response form conventional single band response, and the interaction between structure also modifies chiral response of the structure. Below figure shows comparison of the designed simple double L shaped square split ring structure's response to circular polarization and circular polarization response of the convoluted double L shaped square split ring structure.

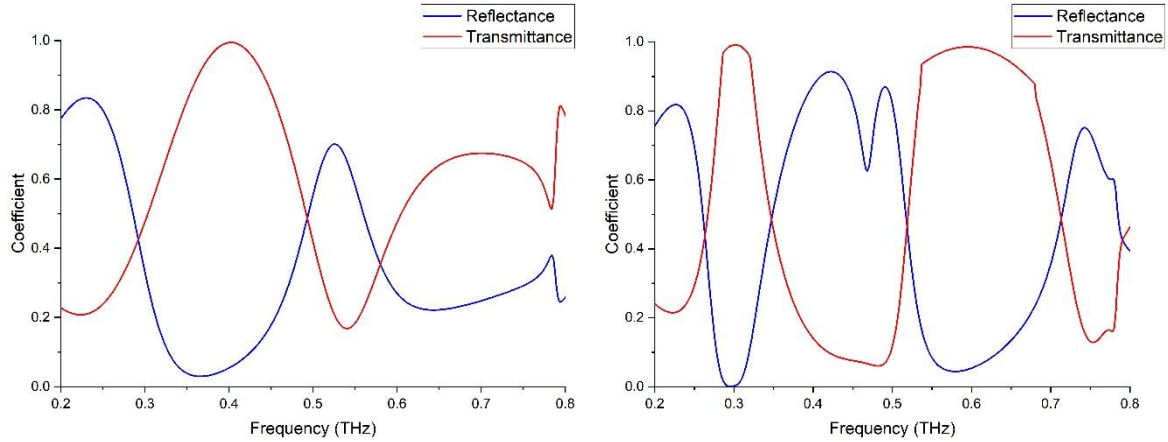

Fig.1: (a) LCP transmittance and reflectance spectra for single ring structure, (b) LCP transmittance reflectance spectra for convoluted double ring structure.

As we can see, by using the convolution, the number of bands increased in the same frequency range. This kind of structure can be helpful in shielding the communication system for particular frequency range, which can be selected by carefully engineering the design parameters.

P94

Spin-Orbit Driven Dark Excitons in Low Dimensional Systems from First Principles Calculations

Akram Hossain Sarkar[1] and Indra Dasgupta[1]

[1]*School of Physical Sciences, Indian Association for the Cultivation of Science,*

2A & 2B Raja S.C. Mallick Road, Kolkata-700032, West Bengal, India

Abstract

Excitonic effects in two-dimensional (2D) systems, due to reduced screening, play an important role in determining the optical response. Excitons in 2D systems are broadly classified into bright (optically allowed) and dark (optically suppressed) species, where dark excitons may arise from spin-forbidden or momentum-forbidden transitions. The spectral ordering of bright and dark excitons is governed by band splitting in the presence of SOC. Since dark excitons typically exhibit longer lifetimes, systems with dark exciton states can be useful for optoelectronic applications. We have studied a 2D buckled honeycomb system, capable of hosting dark excitons. We performed a detailed first-principles study of the electronic and optical properties considering the electron–hole interaction of monolayer using the GW approximation and the Bethe–Salpeter equation (BSE). Based on our calculations, we characterized the excitons as Wannier–Mott-type excitons with binding energies ranging from 110 to 310 meV without SOC and 155 to 258 meV in the presence of SOC, showing their spatially delocalized nature. Through the analysis of exciton envelope functions, we identify both bright and dark excitons as 1s type. By evaluating the oscillator strengths, we have identified the dark states, which, despite being optically allowed, remain dark due to suppressed dipole-matrix elements. A group-theoretical framework is employed to understand the origins of these excitonic states.

P95

CO_2 Activation in B- and N-doped C_{20} Fullerene-supported Single-Atom Catalysts – A DFT Study

Ranjini Sarkar [1, 2] and Tarun Kumar Kundu [2]

[1] Department of Physics "E. Pancini", University of Naples Federico II, 80126 Napoli, Italy
[2] Department of Metallurgical and Materials Engineering, Indian Institute of Technology Kharagpur, 721302 West Bengal, India

Over the past decade, transition metal single-atom catalysts (TM-SACs) have attracted significant attention owing to their promising performance in water splitting, and CO_2 and nitrogen reduction reactions. Carbon-based materials, particularly pristine and heteroatom-doped graphene or carbon nanotubes, are well-recognized supports for TM-SACs. [1] In this work, we propose the C_{20} fullerene nanocage as a novel molecular support for TM-SACs and investigate its potential for CO_2 activation and reduction. TM single-atoms (Ni, Pd, and Pt; denoted as 'M') are anchored on C_{20} (MC_{19}), B- and N-doped C_{20} (MB_2C_{17} and MN_2C_{17}), and B/N-codoped C_{20} ($MBNC_{17}$) to construct a series of SAC models.

Fullerenes are polyhedral carbon cages with the general formula C_{20+2n} ($n \geq 0$, $n \neq 1$) composed of sp^2-hybridized carbon networks. The C_{20} dodecahedral nanocage is the smallest fullerene and, despite being less stable than C_{60}, has been successfully synthesized experimentally by Paquette group et al.[2] Motivated by the reported electrocatalytic performances of fullerene-based systems,[3, 4] we systematically investigate CO_2 adsorption, activation, dissociation to CO* and O*, and the initial pathways of CO_2 reduction reaction (CO_2RR) on pristine and doped C_{20} fullerene-supported TM-SACs.

Density functional theory (DFT) calculations are performed implementing localized orbital basis sets within Gaussian16 package. Structural optimizations of the TM-SACs, with and without adsorbed CO_2 molecules, are carried out using PBE0-D3, B3LYP-D3, ωB97XD, M06-2X, and HSE06 functionals. LanL2DZ effective core potentials are employed for the transition metal atoms, while the 6-311+G(d,p) basis set is used for the lighter elements. Dynamic stability of the optimized geometries is confirmed by the absence of imaginary vibrational frequencies, and thermodynamic stability is further validated through ab-initio Born-Oppenheimer molecular dynamics (BOMD) simulations. Metal-support interactions are characterized using Bader's quantum theory of atoms in molecules (QTAIM), bond orders, and electronic charge transfer analyses.

For all SACs, only physisorption of CO_2 is observed, as evidenced by the nearly linear geometries of the adsorbed CO_2 molecules. Formation energies, HOMO-LUMO gaps, CO_2 adsorption energies, and structural parameters of the adsobed CO_2 molecules show good consistency across the employed functionals, and B3LYP-D3 is therefore adopted for detailed electronic structure and catalytic analyses. The thermodynamics and kinetics of CO_2 dissociation (CO_2* → CO* + O*) are evaluated, revealing that B-doped systems exhibit the most favorable energetics and lowest activation barriers. Furthermore, the initial steps of the formate and carboxyl pathways are further examined in competition with the hydrogen evolution reaction (HER), providing insights into CO_2RR selectivity toward CO or HCOOH formation. Overall, this study highlights the potential of C_{20}-based nanocages as molecular supports for TM-SACs in electrocatalytic CO_2RR.

[1] W. Song, C. Xiao, et al., Adv. Mater. **36**, 2301477 (2023)
[2] L. A. Paquette, R. J. Ternansky, et al., J. Am. Chem. Soc. **105**, 5441-5446 (1983)
[3] R. Zhang, Y. Li, et al., Nat. Commun. **14**, 2460 (2023)
[4] C-X. Li, S-L. Tong, et al. Molecules **30**, 4494 (2025)

P96

Polarons additive enhanced saturable absorption in MoS_2/PANI nanocomposite films

Anjali Sharma, B. Karthikeyan [1]

[1]Nano-photonics Laboratory, Department of Physics, National Institute of Technology, Tiruchirappalli – 620015, India.

Significant research has been conducted to investigate polarons in two-dimensional systems as a solid-state medium for observing enhanced nonlinear optical responses.[1] As quasiparticles that result from a strong interaction between electrons and a material's lattice vibrations, polarons have made it possible to modify material properties in a variety of ways. In this context, exploring MoS_2/PANI nanocomposites becomes particularly significant for elucidating the influence of polaronic and bipolaronic states on their nonlinear optical (NLO) responses, thereby providing deeper insight into the charge–lattice interactions governing their nonlinear optical behaviour. Advancements in materials exhibiting significant nonlinear optical responses, characterised by rapid response times and pronounced two-photon absorption (2PA) and three-photon absorption (3PA), hold considerable promise in fields such as photodynamic treatment (PDT), lasing, optical limiting, and bioimaging.[2] Nanomaterials demonstrating two-photon absorption (2PA) and three-photon absorption (3PA) are employed in applications such as fluorescence imaging, three-dimensional imaging, and lithography, as their spatial resolution may be modulated by light intensity due to their capacity to localise excitation inside a confined spatial region.[3]

In this study, we have prepared MoS_2 nanorods/PANI nanocomposite films and analysed it for their third-order nonlinear optical properties using open-aperture (OA) z-scan measurement with 532 nm nanosecond pulsed laser excitation. Our z-scan data revealed that both MoS_2 and PANI exhibit SA behaviour, originating from Pauli blocking near the conduction band edge in MoS_2 and intragap polaron transitions in doped PANI (emeraldine salt form). Incorporation of MoS_2 into the PANI matrix significantly improves the nonlinear absorption coefficient (β) and saturation intensity (I_S) of nanocomposite films, signifying strong interfacial charge transfer from PANI's polaron bands to the MoS_2 conduction band. This charge-transfer process enables faster carrier extraction, reduces recombination, and enhances the overall SA response of the nanocomposites. Our material shows significant saturable absorption, which makes it promising for ultrafast photonic uses such as Q-switching, mode-locking, optical modulation, photonic switching, pulse shaping, optical signal processing, and laser protection devices.

[1] A. Author, B. Coauthor, J. Sci. Res. **13**, 1357 (2012).
[2] Y. Chen, Y. Jin, H. Zhu, H. Zhang, L. Wei, Y. Tang, R. Wang, D. Zhou and J. Gu, *npj Clean Water* **8**, 1–14 (2025).
[3] L. Tang, L. Chen, Y. Luo, Y. Li, Y. Zhang, J. Zhao and W. Shen*ACS Appl. Opt. Mater.* 2025, **3**, 212–222 (2025).

P97

Visible-Light-Driven CO_2 Conversion on Group-10 Metal–Supported Janus Sc_2COS MXene with Enhanced Solar-to-Hydrogen Efficiency

Swati Shaw[1], **and Subhradip Ghosh**[1]

[1]*Department of Physics, Indian Institute of Technology Guwahati, Guwahati-781039, Assam, India.*

Water splitting and CO_2 conversion through photocatalysis offer sustainable routes to generate green energy and valuable hydrocarbons. Our previous DFT studies [1, 2] identified Janus-functionalized MXenes M_2COT (M = Sc, Zr, Hf; T = S/Se) as promising photocatalysts, with Sc_2COS showing visible-light activity. Its asymmetric charge distribution creates an intrinsic electric field that optimizes band alignment for water splitting, achieving up to 4% solar-to-hydrogen efficiency under strain. Sc_2COS can drive both hydrogen evolution and CO_2 reduction to CH_4, with analyses of its electronic and catalytic properties confirming spontaneous CO_2 reduction under photoexcitation [3].

Despite its promising photocatalytic behavior, Sc_2COS faces challenges such as a large band gap, low STH efficiency, and poor CO_2 activation, leading only to weak physisorption and requiring impractically high pressures for full conversion. To address this, we introduced group-10 transition metal adatoms (Ni, Pd, Pt) on the Sc_2COS surface, creating active sites to enhance its catalytic reactivity.

These group-10 transition metals act as single-atom catalysts (SACs) when anchored on the Sc_2COS surface, serving as electron-trapping centers that promote charge transfer from photogenerated carriers. The presence of Ni, Pd, or Pt enables strong CO_2 adsorption and activation by inducing bending in the otherwise linear CO_2 molecule. The incorporation of these atoms also introduces defect states above the Fermi level, effectively forming a new conduction band while maintaining the semiconducting nature of the system. As a result, the band gap of pristine Sc_2COS (2.57 eV) is significantly reduced to 1.89 eV for Ni@Sc_2COS, 1.77 eV for Pd@Sc_2COS, and 1.25 eV for Pt@Sc_2COS, thereby enhancing visible-light absorption and photocatalytic performance.

Importantly, the intrinsic internal electric field between the two asymmetrical surfaces of Sc_2COS remains unaffected by the metal decoration. This field continues to facilitate favorable band-edge alignment with respect to the oxidation potential (1.23 eV vs. NHE), hydrogen reduction potential (0 eV vs. NHE), and CO_2 reduction potentials at pH = 5. The reduced band gaps contribute to a marked increase in STH efficiency across all systems. Moreover, the introduction of transition metal adatoms renders the CO_2 reduction reaction (CO_2RR) more exothermic along all feasible reaction pathways, significantly lowering the limiting potential. Under moderate conditions (1 atm and elevated temperature), CO_2 adsorption and CH_4 desorption occur readily. All three systems exhibit strong CO_2RR selectivity over the competing hydrogen evolution reaction (HER). The low limiting potentials and overpotentials observed indicate that Ni-, Pd-, and Pt-decorated Sc_2COS surfaces possess high catalytic efficiency and hold great promise for enhanced CO_2 conversion and renewable fuel generation.

[1] Swati Shaw and Subhradip Ghosh. *J. Mater. Chem. C*, 12:9146–9157, 2024.
[2] Swati Shaw and Subhradip Ghosh. *Phys. Chem. Chem. Phys.*, 26:25105–25117, 2024.
[3] Swati Shaw and Subhradip Ghosh. *J. Phys. Chem. C.*, 129:16796–16810, 2025.

P98

QUANTUM EMITTERS IN TWO-DIMENSIONAL MATERIALS VIA ION IMPLANTATION

Ikshvaku Shyam[1], Amrita Majumder[1], Kousik Bera[1], Janhavi Jayawant Khunte[1], Ekta[1], A. M. Sonawane[2], Akash Khaire[2], S. S. Dahiwale[2], and Anshuman Kumar[1]

[1] *Laboratory of Optics of Quantum Materials, Department of Physics, IIT Bombay, Mumbai 400076, India*

[2] *Low Energy Ion Beam Laboratory, Department of Physics, Savitribai Phule Pune University, Pune 411007, India*

Controlling defect formation in hexagonal boron nitride (hBN) is essential for scalable quantum photonic platforms, yet ion-induced defect pathways remain insufficiently understood. We demonstrate that Krypton ion implantation provides a chemically inert and tunable route to engineer optically active defects in hBN by modulating implantation energy and fluence[1, 2]. The resulting photoluminescence (PL) spans two dominant bands: a near-infrared emission at ∼820 nm associated with negatively charged boron vacancies (V_B^-), and a visible band near ∼620 nm linked to carbon complex defect[4]. These optical signatures coincide with characteristic Raman features, including a V_B^--related mode at ∼1290 cm^{-1} and a broader defect-complex band near ∼1580 cm^{-1}[3]. Temperature-dependent PL, analysed using Arrhenius and Mott–Seitz models, reveals distinct activation energies for nonradiative quenching of the two defect families, indicating fundamentally different thermal stabilities and recombination pathways. Together, these results establish Krypton implantation as an effective strategy for deterministic generation of stable, wavelength-selective luminescent defects in hBN, offering a controllable platform for integrating defect-based quantum photonics.

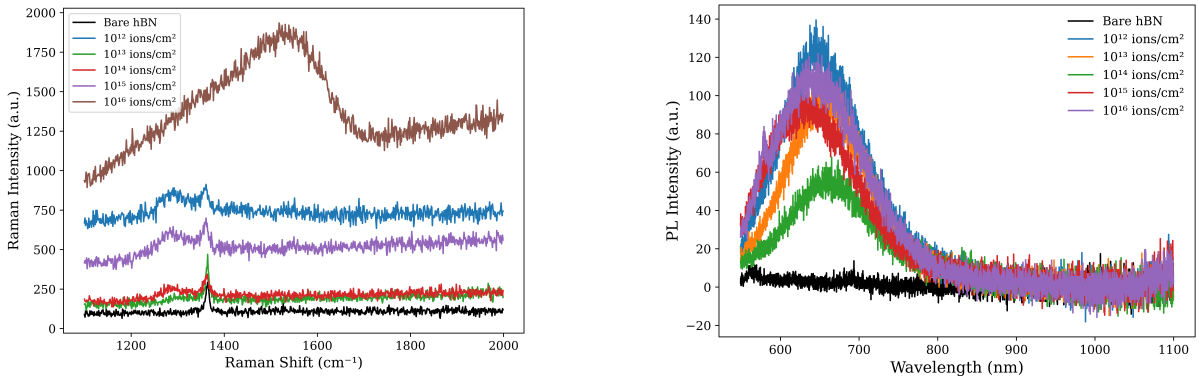

(a) Raman spectra

(b) PL spectra

Figure 1: **Raman and PL comparison for bare and ion-implanted hBN.**

[1] G. Venturi et al., Laser Photonics Rev. 18, 2300973 (2024).
[2] R. Gu et al., ACS Photonics 8, 2912–2922 (2021).
[3] A. Gottscholl et al., Sci. Adv. 6, eabc8182 (2020).
[4] M. Abdi et al., ACS Photonics 5, 1967–1976 (2018).
[5] J. F. Ziegler et al., Nucl. Instrum. Methods B 268, 1818–1823 (2010).

P99

Solvatochromic Photophysics of Benzanthrone Derivatives for Next-Generation Optoelectronic and Photovoltaic Applications

Emmanuel Karungani[1], Elena Kirilova[2], Titus Ochodo[1], Mildred Airo[3] and Francis Otieno[1]

[1] Department of Physics and Materials Science, Maseno University, Kisumu 333-40105, Kenya.
[2] Department of Applied Chemistry, Institute of Life Sciences and Technology, Daugavpils University, LV-5401 Daugavpils, Latvia.
[3] Department of Chemistry, Maseno University, Kisumu 333-40105, Kenya.

Harnessing the intricate interplay between molecular structure and light–matter interactions, benzanthrone derivatives have emerged as promising candidates for advanced organic optoelectronic systems due to their strong photostability, extended π-conjugation, and highly tunable luminescence [1,2]. In this study, a series of benzanthrone-based fluorophores were synthesized through multi-step routes and comprehensively characterized to investigate their photophysical and photochemical responses in solvents of varying polarity. The derivatives exhibited pronounced solvatochromism arising from intramolecular charge transfer (ICT) processes between donor–π–acceptor (D–π–A) moieties embedded within the molecular framework [3]. Optical analyses revealed significant bathochromic shifts exceeding 110 nm in fluorescence emission as solvent polarity increased, accompanied by large Stokes shifts (up to 4800 cm^{-1}) and solvent-dependent modulation of optical band gaps from 2.20 eV to 1.96 eV. Quantum yield measurements indicated high emission efficiency in non-polar solvents, while polar environments promoted twisted intramolecular charge transfer (TICT) states that quenched fluorescence. The combined effects of charge redistribution, solvent-induced stabilization, and bandgap modulation highlight the sensitivity of these fluorophores to their microenvironment. This work underscores the ability to molecularly engineer benzanthrone systems to achieve tunable optical and electronic properties suitable for next-generation optoelectronic devices. The robust photophysical response, large dipole moment variation, and excellent chemical stability of these compounds make them sustainable, metal-free alternatives for color-tunable organic light-emitting diodes (OLEDs), organic solar cells, and photonic sensors. Such structure–property insights provide a foundation for designing new emissive materials with enhanced energy conversion and light-harvesting capabilities.

[1] A. Maļeckis, E. Romanovska-Dzalbe, Chemical Papers **79**, 3463 (2025).

[2] M.B. Patel, V.A. Trivedi, R.C. Dabhi, J.J. Maru, Z.M. Patel, Mini Rev Org Chem. **22**, 685, (2024).

[3] E.M. Kirilova, A.I. Puckins, E. Romanovska, M. Fleisher, S.V. Belyakov, Spectrochim Acta A Mol Biomol Spectrosc. **202**, 41 (2018).

P100

Composition-Driven Luminescence Tuning in Silicate Nanophosphors

P101

PEO Based Solid Polymer Electrolyte for Dye Sensitized Solar Cell

Kumari Pooja*[1] , Mridula Tripathi[1], Priyanka Chawla[1] and Anshu Maurya[1]
[1]Department of Chemistry C.M.P. Degree College, University of Allahabad, Prayagraj
*E-mail- p.mishra011094@gmail.com

Introduction

A dye-sensitized solar cell (DSSC) comprises a photoanode, electrolyte, sensitizer, and photocathode—each essential for efficiency and stability. In this work, a chitosan-based biopolymer electrolyte with graphite filler is employed to overcome leakage and sealing issues of liquid electrolytes. Chitosan's polycationic β(1-4) glucopyranose structure enables strong anionic interactions and polyelectrolyte formation, while its biodegradability and non-toxicity enhance sustainability. The TiO_2 photoanode is modified with CuO nanopowder to reduce interfacial energy barriers. A 1:1 cocktail dye from beetroot and spinach replaces synthetic dyes, further boosting eco-friendliness. The fabricated DSSC achieves an efficiency of ~2.3% with a 54% fill factor under 100 mW/cm² illumination.

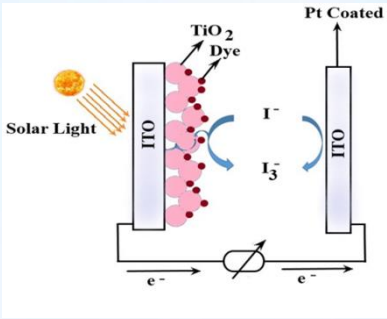

Major Components Of Dye Sensitized Solar Cell

Experimental

Extraction of natural Dye

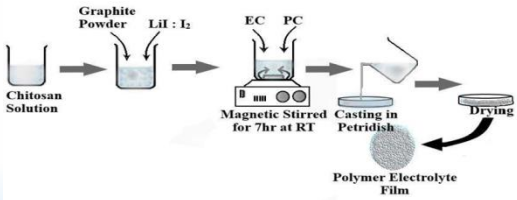

Preparation of Polymer electrolyte via solution cast technique

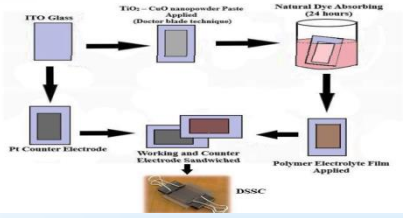

Fabrication Of DSSC

Result and Discussion

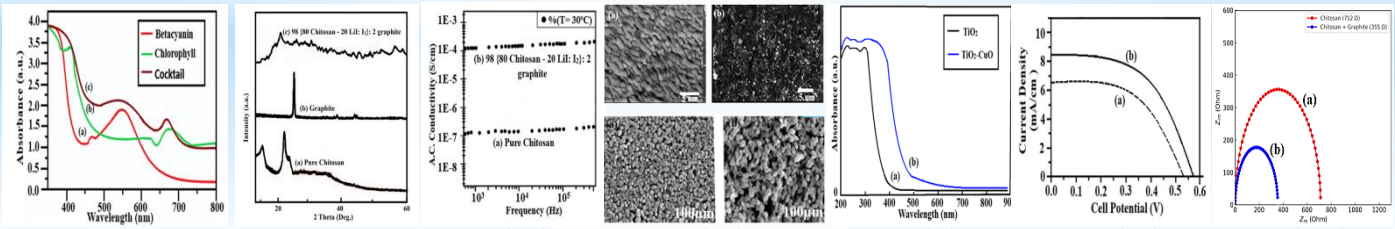

(I) (II) (III) (IV) (V) (VI) (VII)

I. The absorption spectra of spinach and beetroot is low when compared to the cocktail dye.
II. From the comparative study of the XRD patterns it is clear that the addition of filler (Graphite) in the polymer reduces the intensity of the main peak followed by broadening of the peak area, which is an indication of increase in the degree of amorphousity, which provides conductive interfacial layer with polymer which aids in better conductivity.
III. Figure shows that the ac conductivity of the chitosan based polymer electrolyte rises from ~10^{-7} to ~10^{-4} S/cm, due to addition of graphite filler.
IV. The SEM images of polymer electrolyte show uniform graphite dispersion in chitosan, with dark regions indicating particles, confirming good filler–polymer compatibility and increased amorphous content, consistent with XRD results.
The SEM image of the prepared TiO_2–CuO nanomaterial reveals its nanocrystalline structure with an average grain size of 25–35 nm.
V. The absorption spectra of cocktail dye-coated TiO_2–CuO composite photoelectrodes on ITO glass show enhanced absorption compared to pure TiO_2.
VI. The DSSC with 2 wt% graphite-filled chitosan electrolyte shows higher efficiency (2.3%) and fill factor (54%) than pure chitosan (0.50%, 45%), with improved J–V characteristics confirming its enhanced performance.
VII. The total resistance decreased from 712 Ω in pure chitosan to 355 Ω in the chitosan–graphite system, indicating enhanced ion mobility with filler incorporation.

P102

G0W0 Many-Body Perturbation Theory for Ground and Excited States in CsSrF3 Perovskite First-Principles Study with Yambo

P103

Electron-phonon coupling induced renormalization of electronic properties in a ternary chalcogenide, $FeBi_4S_7$

Pradhi Srivastava, and Sudip Chakraborty

Materials Theory for Energy Scavenging Laboratory, Condensed Matter Physics, Harish-Chandra Research Institute, A.C.I. of Homi Bhabha National Institute, Chhatnag Road, Jhunsi, Prayagraj 211019, India

We use first-principles simulations to investigate band-gap renormalization in $FeBi_4S_7$, a transition metal bismuth ternary chalcogenide, under uniaxial strain. Our study emphasizes the role of electron-phonon coupling in determining the electronic properties of this quasi-one-dimensional antiferromagnet, which consists of chains of edge-sharing iron-sulphide (FeS_6) octahedra [1–4]. We examine the ground state magnetic structure and the influence of spin-orbit coupling (SOC) on the electronic properties. The ground-state magnetic structure is found to be antiferromagnetic and is in agreement with the experimental observations. While SOC modifies the magnitude of the band-gap, it does not alter the nature of the band-dispersion curves. The application of hydrostatic pressure as well as uniaxial strain induces a structural transition and significantly reduces the band-gap. We compare the band-gap values from ground-state calculations with those obtained from the simulated optical absorption spectrum, confirming the indirect band-gap nature of the material.

The presence of electron-phonon coupling shows a substantial impact on the band structure, leading to band-gap renormalization at different temperatures and strain levels. The strength of this coupling is quantified using the Huang-Rhys factor [5], and the resulting photoluminescence spectra are computed as a function of uniaxial strain. We observe a direct correlation between the electronic band-gaps and the electron-phonon coupling strength, with both quantities varying oppositely under strain. This coupling significantly influences the excited-state properties, particularly in systems where electronic states are strongly coupled with phonon modes. Strong electron-phonon coupling may lead to non-radiative decay processes and reduce exciton lifetimes [6]. These findings highlight the importance of tailoring electron-phonon interactions to optimize photovoltaic efficiency and device performance.

[1] I. Campbell, V. O. Garlea, Q. Zhang, Y. Adhikari, P. Xiong, N. J. Yutronkie, A. Rogalev, and M. Shatruk, Chem. Mater., **36**, 3417 (2024).
[2] Z. Luo, C. Lin, W. Cheng, W. Zhang, Y. Li, Y. Yang, H. Zhang, and Z. He, Cryst. Growth Des., **13**, 4118 (2013).
[3] J. Labégorre, A. Virfeu, A. Bourhim, H. Willeman, T. Barbier, F. Appert, J. Juraszek, B. Malaman, A. Huguenot, R. Gautier, V. Nassif, P. Lemoine, C. Prestipino, E. Elkaim, L. Pautrot-d'Alençon, T. Le Mercier, A. Maignan, R. A. R. A. Orabi, and E. Guilmeau, Adv. Funct. Mater., **29**, 1904112 (2019).
[4] S. Azam, S. A. Khan, S. Goumri-Said, and M. B. Kanoun, J. Electron. Mater., **46**, 23 (2017).
[5] S. A. Tawfik, and S. P. Russo, Comput. Phys. Commun., **273**, 108222, 2022.
[6] R. Kentsch, M. Scholz, J. Horn, D. Schlettwein, K. Oum, and T. Lenzer, J. Phys. Chem. C, **122**, 25940 (2018).

P104

Up/down conversion luminescence properties of $Ca_2Ga_2GeO_7$: Er, Yb for versatile applications.

Reshmi Thekke Parayil [1,2], Arsha P[3]. Santosh K.Gupta [1,2*] Boddu S. Naidu[3*] and M.Mohapatra [2]

[1]Radiochemistry Division, Bhabha Atomic Research Centre, Mumbai, 400085, India.
[2] Homi Bhabha National Institute, DAE, Anushaktinagar, Mumbai, 400094, India.
[3] Energy and Environment Unit, Institute of Nano Science and Technology (INST), Mohali, Punjab 140306, India.

Lanthanide-activated phosphors have gained widespread attention due to their applications in non-contact optical thermometry, solid-state lighting, anticounterfeiting, fingerprint detection, and biomedical fields [1-2]. Traditional temperature measurement techniques suffer limitations in harsh or biological environments, leading to the development of fluorescence intensity ratio (FIR)-based non-invasive thermal sensors that offer high spatial resolution, sensitivity, and fast response [1]. Here the Er and Yb co-doped $Ca_2Ga_2GeO_7$ (CGGO) phosphor was synthesized via a conventional solid-state method, exhibiting both down-conversion and up-conversion emissions under visible and near-infrared excitation. This study focused on the temperature-dependent fluorescence intensity ratio of (FIR) of Er^{3+} ions in CGGO under 980 nm excitation. The luminescence-based temperature sensing demonstrated high relative sensitivity value of 0.65% K^{-1} at 400 K, underscoring the material's potential for sensitive non-contact temperature sensing. Additionally, the work highlights the importance of developing luminescent materials with strong contrast and minimal background interference, which is crucial for applications like latent fingerprint visualization in forensic science and anticounterfeiting studies.

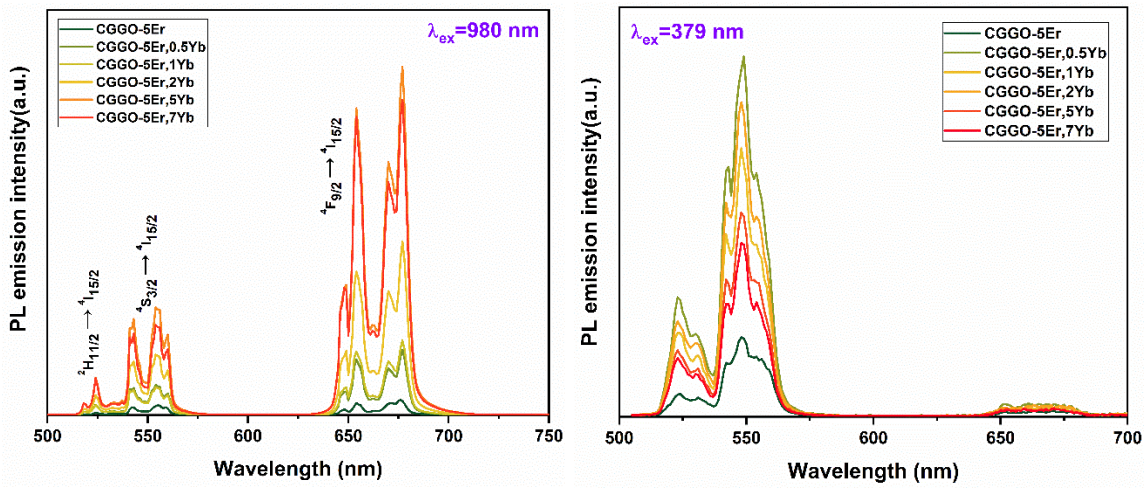

Figure A: (a) Upconversion (b) downconversion of CGGO-5Er, x%Yb

[1] J. Periša, Z, Ristić, W. Piotrowski, Ž. Antić, L.Marciniak and M.D. Dramićanin, RSC Adv. **11**, 5933-15942 (2021).
[2] M. Pokhrel, G. A. Kumar and D. K. Sardar, J. Mater. Chem. A, **1**, 11595-11606 (2013).

P105

Cationic Interplay for the Halide Ion Migration: Implication to Neuromorphic Computing

Ayushi Tripathi[1], Sudip Chakraborty[1*], Tisita Das[1*]

[1]*Materials Theory for Energy Scavenging (MATES) Lab, Harish-Chandra Research Institute (HRI), A C.I. of Homi Bhabha National Institute (HBNI), Chhatnag Road, Jhunsi, Prayagraj, 211019, India*

Presenting Author's E-mail: tripathiaayushi488@gmail.com
Corresponding Author's E-mail: tisitadas@hri.res.in sudipchakraborty@hri.res.in

Abstract:
Halide perovskites are emerging as attractive materials for neuromorphic computing because their mixed ionic–electronic transport naturally enables gradual and history-dependent changes in conductance, similar to biological synapses. Among them, the one-dimensional copper–iodide perovskite CsCu2I3 exhibits good structural stability and semiconducting behaviour, but its relatively sluggish ion migration can limit the speed and adaptability of neuromorphic switching. In this work, we explore how replacing Cs+ with the smaller Rb+ cation modifies the structure, electronic properties, and ionic mobility in the alloy series RbxCs1−xCu2I3. Using first-principles calculations, we find that while the overall electronic character remains semiconducting across all compositions, the ease of halide-ion migration is strongly influenced by the Cs/Rb ratio. Rb incorporation leads to noticeable changes in the local lattice environment, which in turn reshapes the energy landscape for ion transport and allows smoother tuning between more volatile and more stable switching behaviours. These results show that A-site cation engineering provides a powerful degree of control over ionic dynamics in Cu–I perovskites, offering a clear pathway for optimizing their performance in next-generation, low-power neuromorphic devices.
Keywords: Neuromorphic computing, halide perovskites, ion migration, cationic interplay, NEB, memristive devices.

References:
(1) K. Sakhatskyi, R. A. John, A. Guerrero, S. Tsarev, S. Sabisch, T. Das, G. J. Matt, S. Yakunin, I. Cherniukh, M. Kotyrba, Y. Berezovska, M. I. Bodnarchuk, S. Chakraborty, J. Bisquert, M. V Kovalenko, "Assessing the Drawbacks and Benefits of Ion Migration in Lead Halide Perovskites", ***ACS Energy Letters***, 7 (2022) 3401.
(2) S. K. Vishwanath, B. Febriansyah, S. Ng, T. Das, J. Acharya, R. A. John, D. Sharma, P. A. Dananjaya, M. Jagadeeswararao, N. Tiwari, M. R. C. Kulkarni, W. S. Lew, S. Chakraborty, A. Basuf and N. Mathews, High-Performance One-Dimensional Halide Perovskite Crossbar Memristors and Synapses for Neuromorphic Computing, ***Material Horizons***, 11, 2643–2656, 2024.

P106

Improved Power Conversion Efficiency of $RbAX_3$ (A= Ge, Sn; X=Cl, Br) Absorber Based Solar Cell Through the Variation of ETL

Namrata A. Tukadiya [1] and, Prafulla K. Jha[1]

[1]Department of Physics, Faculty of Science, The Maharaja Sayajirao University of Baroda, Vadodara, Gujarat, India-390002

The class of perovskite solar cells (PSCs) based on rubidium $RbAX_3$ (A = Ge, Sn; X = Cl, Br) is gaining attention from researchers because of its outstanding semiconducting properties. Several configurations of $RbAX_3$-based single junction photovoltaic cells have been investigated, here we have included hole transport layers (HTLs) made of V_2O_5 and $MoTe_2$ and their bilayers, as well as electron transport layers (ETLs) made of CdS and SnS2. We investigated the configurations Al/ETL/$RbAX_3$/V_2O_5/$MoTe_2$/Ni with the different ETL layers and studied elements including band alignment, defect density, layer thickness, doping concentration, interface defect density, carrier concentration, generation, recombination, open circuit voltage (V_{OC}), short circuit current (J_{SC}), fill factor (FF), and power conversion efficiency (PCE) through DFT and extensive numerical analysis using SCAPS-1D simulation software. According to the results, Al/FTO/CdS/$RbSnBr_3$/V_2O_5/$MoTe_2$/Ni shows V_{OC} of 1.14 V, J_{SC} of 35.84 mA/cm^2, and an FF of 82.97 %, achieving the highest PCE of 36.32 %. In contrast, the configuration Al/FTO/SnS_2/$RbGeBr_3$/V_2O_5/$MoTe_2$/Ni shows the lowest efficiency among the six studied configurations, with PCE of 27.44 %, V_{OC} of 1.26 V, J_{SC} of 26.21 mA/cm^2, and an FF of 82.55 % The remaining four device configurations exhibit performance values that fall within this range. These results provide insightful information and a workable strategy for creating $RbAX_3$-based, reasonably priced thin-film solar cells.

[1] Ghosh, Avijit, et al. Journal of Physics and Chemistry of Solids 193 (2024): 112179.
[2] Reza, Md Selim, et al. Materials Today Communications 39 (2024): 108714.

P107

Quantized spin Hall effect in bottom-up designed synthetic 2D materials

Rahul Verma[1] and Bahadur Singh[1]

[1]Department of Condensed Matter Physics and Materials Science,
Tata Institute of Fundamental Research, Homi Bhabha Road, Colaba, Mumbai-400005, India

Two-dimensional topological insulators protected by time-reversal symmetry exhibit spin-polarized helical edge states and are promising candidates for dissipation less spintronic devices. In materials, however, the S_z spin Hall conductivity (SHC) is often not quantized because of breaking of spin U(1) symmetry by spin mixing arising from strong spin-orbit coupling or other material-specific effects. In this work, we develop a theoretical bottom-up materials-design method for realizing synthetic 2D layered materials that lack parent 3D bulk analogues. We show that by systematically reducing the symmetries in monolayers of 1H-MA_2Z_4 (M = Mo/W; A= Si/Ge; Z = Pnictogen) compounds, a structural distortion in the 1H phase leads to the 1T′ phases, exhibiting a QSH insulator state with large inverted band gap; however, the SHC values deviates from the quantized limit of $2e^2/h$. By extending this design principle, we identify a new family of QSH insulators featuring nearly quantized SHC and high-order van Hove singularities (VHSs) in monolayers MA_2Z_4 compounds with a square-octagonal geometry. Our spin-resolved topology and symmetry analysis shows that these systems are non-trivial with a spin Chern number C_s=1 and host S_z spin polarized edge states. The QSH phases exhibit an emergent spin U(1) quasi-symmetry, leading to nearly quantized SHC of $2e^2/h$. Among these materials, WSi_2Sb_4 displays quasi flat-band-like dispersions and high-order VHSs near the Fermi level. The coexistence of high-order VHSs and QSH topology in these materials offers a unique platform to explore correlation-driven phenomena.

1 R. Verma, Y. Vardhan, H. Lin, and B. Singh, *Emergent spin Hall quantization and high-order van Hove singularities in square-octagonal MA_2Z_4*, arXiv:2510.12935 (2025).

2 R. Islam, R. Verma, B. Ghosh, Z. Muhammad, A. Bansil, C. Autieri, and B. Singh, *Switchable large-gap quantum spin Hall state in the two-dimensional MSi_2Z_4 class of materials,* Phys. Rev. B **106**, 245149 (2022).

3 R. Islam, B. Ghosh, C. Autieri, S. Chowdhury, A. Bansil, A. Agarwal, and B. Singh, *Tunable spin polarization and electronic structure of bottom-up synthesized $MoSi_2N_4$ materials,* Phys. Rev. B **104** L201112 (2021).

P108

Atomic-Scale Insights into Passivation and Halide Mixing in 3D and 2D Halide Perovskites

Vikram [1], **M. Saiful Islam** [1]

[1] *Department of Materials, University of Oxford, UK*

Some of the key factors for achieving high efficiency and long-term operational stability in metal-halide perovskite optoelectronic devices require precise control over film growth and effective defect passivation strategies. Recently, amino-silane-treated perovskite solar cells have demonstrated exceptional stability.[1] However, the atomic-scale interactions of these silane molecules at perovskite surfaces remain poorly understood. Separately, to enhance efficiency in quasi-2D perovskites, a recent study achieved vertical crystallization by using methylammonium chloride (MACl) additives during precursor processing.[2] However, the absence of detectable I/Cl halide mixing in 3D perovskites raise fundamental questions about such halide mixing in 2D perovskites.

Our density functional theory and ab initio molecular dynamics simulations reveal atomic-scale insights into these performance improvements, shedding light on the mechanisms of silane passivation in 3D perovskites and halide mixing in 2D perovskites. These findings align with the experimental results and offer a deeper structural and mechanistic understanding at the atomic level.

[1] Lin, Y.-H. et al. Bandgap-universal passivation enables stable perovskite solar cells with low photovoltage loss. Science 384, 767–775 (2024).

[2] Zanetta, A. et al. Vertically oriented low-dimensional perovskites for high-efficiency wide band gap perovskite solar cells. Nat. Commun. 15, 9069 (2024).

P109

Prediction of the Thermoelectric Properties of Lead Telluride under Applied Strain Using Advanced Computational Methods

H. S. Patel, V. A. Dabhi and A. M. Vora*

Department of Physics, University School of Sciences, Gujarat University, Navrangpura, Ahmedabad 380 009, Gujarat, India
**Corresponding Author Email: voraam@gmail.com*

The energy age has seen a shift towards an emphasis on energy reuse. One promising aspect of this shift is thermoelectric energy, which has attracted the attention of researchers due to its potential in various thermoelectric applications. Lead telluride in particular is increasingly used in endeavors ranging from deep-sea exploration to space missions, and evaluation of its performance under pressure conditions is essential. This study focuses on evaluating the power generation capabilities of lead telluride (PbTe) under applied strain from -5% to +5%. Advanced computational methods, such as HSE hybrid functional combined with Wannier interpolation, have been used to improve the accuracy of the results. Our findings have attempted to yield accurate predictions for both electrical and thermoelectric properties. During this study we observed significant change in thermoelectric power generation under compression strain. The results obtained in this study can be a valuable reference point for future researchers in this field.

[1] Hiren S. Patel, Vishnu A. Dabhi, and Aditya M. Vora, ACS Omega **8**, 43008 (2023).
[2] Hiren S. Patel, Vishnu A. Dabhi and Aditya M. Vora, Phys. Scr. **98**, 125930 (2023).
[3] Hiren S. Patel, Vishnu A. Dabhi and Aditya M. Vora, Sci. Rep. **14**, 20700 (2024).
[4] Hiren S. Patel, Vishnu A. Dabhi and Aditya M. Vora, Mater. Adv. **6**, 5777 (2025).

P110

Solvent Driven Crystallisation in $CsPbBr_3$ Perovskites for High Structural Quality and Luminescence Stability

Veena V.P.[a], Khaleelu Rahman[b], M. Aslam[a]*

[a]Department of Physics, Indian Institute of Technology Bombay, Mumbai, India

[b]Department of Physics, Central University of Karnataka, Karnataka, India

[*]Corresponding author: E-mail ID: m.aslam@iitb.ac.in

Abstract

In recent years, tremendous efforts have been made to stabilise and enhance the efficiency of lead-based all-inorganic perovskite, typically $CsPbBr_3$. Due to their humidity and thermal stability, long-term shelf life, defect tolerance, and wider bandgap, these materials have achieved a power conversion efficiency of 11.08%, progressing towards the Shockley-Queisser limit of 16.37% while remaining open to further refinement. Among the various material leverage approaches used for $CsPbBr_3$, solution engineering can offer improved performance, enhanced flexibility, and cost-effectiveness. As a novel procedure, various solvents were tested during the sample nucleation stage and growth stage, yielding a coherent correlation between solvent composition and product characteristics. This dominant influence of solvent engineering is utilised to enhance the stability and boost the efficiency of $CsPbBr_3$ perovskites. The present work proposes a detailed study on the role of various demulsifier solvents in easing the synthesis protocol, the equipped quality of prepared perovskites, and the even photoluminescence performance, as well as phase and size-dependent optical properties of $CsPbBr_3$.

Keywords: Perovskite, Lead halide, Solution engineering, Optoelectronic devices

Reference

1. Chen, C., Lu, X., Hu, X., Liang, G. and Fang, G., 2024. Solution fabrication methods and optimization strategies of CsPbBr3 perovskite solar cells. *Journal of Materials Chemistry C*, *12*(1), pp.16-28.
2. Wang, F., Bai, R., Sun, Q., Liu, X., Cheng, Y., Xi, S., Zhang, B., Zhu, M., Jiang, S., Jie, W. and Xu, Y., 2022. Precursor engineering for solution method-grown spectroscopy-grade CsPbBr3 crystals with high energy resolution. *Chemistry of Materials*, *34*(9), pp.3993-4000.
3. Zhang, Q., Diao, F. and Wang, Y., 2024. The Role of Antisolvents with Different Functional Groups in the Formation of Cs4PbBr6 and CsPbBr3 Particles. *Inorganic Chemistry*, *63*(3), pp.1562-1574.

4. Yuan, L., Patterson, R., Wen, X., Zhang, Z., Conibeer, G. and Huang, S., 2017. Investigation of anti-solvent induced optical properties change of cesium lead bromide iodide mixed perovskite (CsPbBr3-xIx) quantum dots. *Journal of colloid and interface science*, *504*, pp.586-592.
5. Nair, G.B., Tamboli, S., Kroon, R.E., Dhoble, S.J. and Swart, H.C., 2022. Facile room-temperature colloidal synthesis of CsPbBr3 perovskite nanocrystals by the emulsion-based ligand-assisted reprecipitation approach: tuning the color-emission by the demulsification process. *Journal of Alloys and Compounds*, *928*, p.167249.

P111

Rational Design of Electron-Deficient Tricyanofuran HTMs for Stable Perovskite Solar Cells: A DFT-Based Approach

Mainak Mukherjee, V N Ravi Kishore Vutukuri*

Dept. of Chemistry, Sri Sathya Sai Institute of Higher Learning, Puttaparthi,

Sathya Sai Dt., Andhra Pradesh – 515134.

Email: vnrkishorevutukuri@sssihl.edu.in

Two novel tricyanofuran-based hole-transport materials (HTMs), RK7 and RK8—featuring D_1–D_2–A_1 and A_1–D_1–D_2–A_1 molecular architectures, respectively—were designed and computationally investigated. These designs incorporate phenothiazine–triphenylamine (PTZ–TPA, D_1), benzodithiophene (BDT, D_2), and the electron-deficient tricyanofuran (TCF, A_1) units. Their geometric, electronic, and photophysical properties were analyzed using DFT and TD-DFT calculations at the B3LYP/6-31+G(d,p) level. Clear structure-dependent electronic differences between RK7 and RK8 were revealed through comparisons of HOMO–LUMO distributions, fragment-based energy-level alignments, excited-state electron–hole separation, intramolecular charge-transfer (ICT) character, and ground & excited-state dipole moments. Corresponding trends in their spectroscopic signatures are discussed, with particular emphasis on the influence of introducing a second A_1 moiety in RK8. Finally, the computational findings are correlated with preliminary experimental observations from ongoing collaborative studies, providing comprehensive insight into the structure–property relationships that govern the performance and stability of TCF-based HTMs in perovskite solar cells.

P112

Photophysical Optimization of CdS/CdSe Co-sensitized Quantum Dots for Enhanced Quantum Dot Sensitized Solar Cells

Arshiya Wadhwa[1], Iqbal Singh[1], Aman Mahajan[1]

[1]Department of Physics, Guru Nanak Dev University, Amritsar-143005
Corresponding author e-mail: aman.phy@gndu.ac.in

The dependence on fossil fuels for global energy raises serious concerns, such as their finite availability and role in climate change, leading to a shift towards renewable sources, particularly solar energy, however, enhancing the efficiency of solar cells continues to be a significant hurdle. To this, quantum dot-sensitized solar cells (QDSSCs) have garnered considerable attention due to the unique photophysical properties of semiconductor quantum dots (QDs), including size-tunable band gaps and high optical absorption coefficients. In this work, the performance of QDSSCs was enhanced through controlled deposition and co-sensitization of CdS and CdSe quantum dots. The effect of successive ionic layer adsorption and reaction (SILAR) cycles on QD loading was systematically optimized to improve light harvesting, while simultaneously suppressing aggregation induced recombination losses. Furthermore, CdS/CdSe co-sensitization effectively broadened the absorption spectrum and facilitated interfacial electron transfer, leading to enhanced photoconversion properties. The optimized QDSSC device achieved a power conversion efficiency of 3.10 %, highlighting the importance of optimized QD deposition and co-sensitization as viable strategies for enhancing the efficiency of next generation QDSSC devices.

P113

COMPARATIVE INVESTIGATION OF FULLERENE AND NON-FULLERENE ACCEPTORS BLENDED WITH POLYMER DONOR P3HT FOR SOLAR CELL APPLICATIONS

Franklyne Wekesa Wakoli[1], **Isaac T. Motochi**[1,2], **and Francis Otieno**[2]

[1]*Maasai Mara University, Narok, Kenya*
[2]*Maseno University, Kisumu, Kenya*

Polymer Solar Cells (PSCs) based on the bulk heterojunction (BHJ) structure have recorded remarkable improvements in their performance over the past few years. They have elicited considerable research interest in recent years because they have a higher potential to promote low-cost, environmentally friendly, non-complex, and flexible large-area devices compared to their inorganic counterparts. In this study, different films of the organic polymer P3HT(Poly-(3-hexylthiophene-2,5-diyl)) mixed with fullerene acceptors $PC_{71}BM$([6,6]-Phenyl C_{71} butyric acid methyl ester, mixture of isomers), and non-fullerene acceptors IEICO-4F(2,2'-[[4,4,9,9-Tetrakis(4-hexylphenyl)-4,9-dihydro-s-indaceno[1,2-b:5,6-b']dithiophene-2,7-diyl]bis[[4-[(2-ethylhexyl)oxy]-5,2-thiophenediyl]methylidyne(5,6-difluoro-3-oxo-1H-indene-2,1(3H)-diylidene)]]bis[propanedinitrile]), and COi8DFIC(2,2-[[4,4,11,11-tetrakis(4-hexylphenyl)-4,11-dihydrothieno [2,3:4,5]thieno [2,3d] thieno[2,3:4,5]-thieno[2,3:4,5] pyrano[2,3:4,5]thieno[2,3:4,5] thieno[3,2- b]pyran-2,9-diyl]bis[methylidyne(5,6-difluoro)) were fabricated on glass substrates. ultra-violet-visible-near-infrared(UV-VIS-NIR), and Photoluminescence(PL) characterizations were performed to determine the Optical properties and eventual analysis of the structural (H- and J-aggregation) differences in the blends, while atomic force microscopy(AFM) was used to analyse the surface morphologies of the polymer blends. The results of ultraviolet-visible-near Infrared(UV-VIS-NIR) spectroscopy depicted better light harvesting capabilities in non-fullerene acceptor(NFA) based polymer blends of P3HT: COi8DFIC and P3HT: IEICO-4F, which had wider absorption spectra, indicating a larger absorption window and higher absorption intensities extending from NIR(near Infrared) to the Ultra-violet(UV) region compared to P3HT: $PC_{71}BM$ blends, which had narrower absorption windows and lower absorption intensities. P3HT-Fullerene-based blends depicted a blue-shifted spectra, a characteristic of H-aggregates, while the NFA-based blends depicted Red-shifted vibronic structures, a characteristic of J-aggregates. There was lower photoluminescence(PL) intensities of the non-fullerene based blends compared to the fullerene-based polymer blends, depicting more charge carrier recombination in fullerene-based polymer blends. These implied that the fullerene-based blend had lower power conversion efficiency compared to non-fullerene-based blends.

P114

Mechanical, Dynamical, Thermal, Electronic, Magnetic, and Optical Properties of Ti_2InC and Ta_2InC MAX Phases: Potential for Thermoelectric and Optoelectronic Applications

Sukrit Kumar Yadav[1], Ganesh Poudel[1], Om Shree Rijal[1], Hari Krishna Neupane[1], and Rajendra Parajuli[1]

[1](Presenting author underlined) Amrit Campus, Institute of Science and Technology, Tribhuvan University, Kathmandu Nepal

MAX phase materials possess unique and tunable physical properties which make them a preferred candidate for applications in various fields such as spintronics, optoelectronics, and energy storage devices. In present work, the physical properties of Ta_2InC and Ti_2InC MAX phase materials have been investigated by using first principles calculations in a comparative way for potential device application selectivity. The calculations were performed using VASP computational software by employing two exchange correlations functions namely GGA: PBE and GGA: PBE+U. The calculation of structural parameters, stiffness tensor, and phonon dispersion curves indicated that the considered materials exhibit structural, mechanical, and dynamical stability respectively. The calculated bond length, bond angles, lattice parameters, formation energy, and volume of unit cell suggested the structural stability of the material. Stiffness tensor elements have been calculated to investigate mechanical properties. Young's modulus, shear modulus, bulk modulus, Poisson's ratio, Pugh's ratio, linear compressibility, and Vicker's Hardness have been calculated using Voigt-Reuss-Hill approximations. Thorough analysis of anisotropic properties was done by calculating various anisotropy indices along with directional dependent 3D plots of strength of various mechanical properties in real space with their minimum and maximum values. The value of Poisson's ratio and Pugh's ratio revealed brittle nature, while Cauchy pressure shows the materials' ionic bonding. Similarly, we have calculated the free energy, Specific heat capacity, Entropy, and Debye temperature of Ta_2InC and Ti_2InC materials from phonon density of state. Furthermore, electronic band structure revealed the metallic behavior and density of state (DOS), and projected density of state (PDOS) showed the non-magnetic for PBE and magnetic for PBE+U functional. The optical parameters of the considered MAX Phases have been investigated by studying its dielectric function, reflectivity, absorptivity, refractive index, extinction coefficient, and energy loss function for all regions of electromagnetic spectrum. Both materials showed noticeable dielectric responses in infrared regions. Both materials showed distinctive reflectance for in-plane and out-plane light orientation for different spectral regions. However, a higher reflectance in infrared and extreme UV regions and comparatively decreased reflectance for visible and low UV regions have been noted. Both the materials showed a fluctuating but increasing trend of absorptivity and energy loss for increasing photon energies. Refractive index within the infrared region is found to be five to twenty-five times greater than other regions of the spectrum, and a similar trend is observed for extinction coefficient too. These properties can be selectively harnessed for infrared devices, optoelectronic devices, coating, and energy storing purposes.

P115

Visible-light Active Metal Nanoparticles@Carbon Nitride for Photocatalytic Degradation of Organic Water Pollutants and Photoelectrochemical Properties

Mostafa Zedan [1,2] , **Abdallah F. Zedan** [1] , **and Xu LI** [2,3]

[1] *National Institute of Laser Enhanced Sciences, Cairo University, Giza 12613, Egypt.*
[2] *Institute of Materials Research and Engineering, Agency for Science, Technology, and Research (A*STAR), Singapore 138634, Singapore.*
[3] *Institute of Sustainability for Chemicals, Energy and Environment, Agency for Science, Technology and Research (A*STAR), Singapore 138634, Singapore.*

Water is a valuable reserve that shall be efficiently treated for sustainable growth and development. Graphitic carbon nitride (g-C_3N_4 or gCN) has drawn great attention recently because of its visible light response, suitable energy band gap, good redox ability, and metal-free nature. gCN can absorb visible light directly, therefore has a better photocatalytic ability under solar irradiation and is more energy-efficient than other semiconductors. However, pure gCN still has the drawbacks of insufficient light absorption, small surface area and fast recombination of photogenerated electron and hole pairs. In this work, the visible light harvesting and photoelectrochemical properties of bulk gCN were expanded by hybridization with noble metals including gold (Au) and silver (Ag) nanoparticles (NPs) using different approaches. Firstly, we developed a practicable method by in-situ reduction-deposition with the assistance of reducing agents to fabricate a series of x% Au@gCN and x% Ag@gCN nanohybrid photocatalysts by varying the ratio of Au and Ag NPs in the final nanohybrids as 2, 5, and 10 wt.%. Secondly, a sequential approach combining sonodispersion followed by in-situ photoreduction and deposition for the synthesis of MNPs/gCN. Two different types of noble metals (Au and Ag NPs) with different loading ratios were photodeposited onto gCN. The morphological, structural, optical and surface properties of obtained photocatalysts were well-characterized using several techniques including the HR-TEM, FE-SEM, XRD, FTIR, XPS, BET surface area, PL, UV-vis DRS and zeta potential. The characterization results confirmed the successful deposition and well-distribution of the metal nanoparticles over the bulk gCN surface. The adsorption and photocatalytic performances of the plasmonic gCN-based nanohybrids were examined using organic water pollutants including MB, MO, CIP and RB in darkness and under light irradiation. The obtained results revealed that the MNPs/gCN materials could serve as efficient visible-light-sensitive catalysts for photocatalytic water treatment. Interestingly, this work paves a feasible, eco-friendly, large-scale production possibility and cost-effective pathways to fabricate a highly stable, effective and visible-light active of plasmonic gCN-based nanohybrids. Additionally, the successful outcomes of this work can be beneficial and further extended for numerous expected applications in environmental remediation, water splitting and health concerns.

[1] Zedan, Mostafa, *et al*. "Visible-light active metal nanoparticles@ carbon nitride for enhanced removal of water organic pollutants." Journal of Environmental Chemical Engineering, 10 (3), 107780, (2022).

[2] Zedan, Mostafa, *et al*. "Photodeposited Silver versus Gold over g-C_3N_4 toward Photocatalytic Oxidation of Organic Water Pollutants." Egyptian Journal of Chemistry 65 (132): 119-136, (2022).